

AD671079

FAA-ADS-86

EVALUATION OF THE CALLAIR A-9
AGRICULTURAL AIRCRAFT

TECHNICAL REPORT



November 1966

By
Michael R. Smith, John D. Patrick

The Aerophysics Department
Mississippi State University
State College, Mississippi

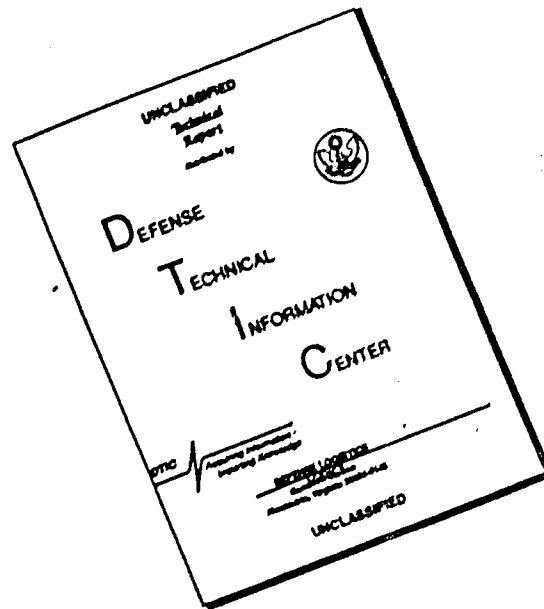
Under Contract FA-65WA-1027

For
FEDERAL AVIATION AGENCY
AIRCRAFT DEVELOPMENT SERVICE

Reproduced by the
CLEARINGHOUSE
for Federal Scientific & Technical
Information Springfield Va 22151

JUL 2 1968

DISCLAIMER NOTICE



THIS DOCUMENT IS BEST QUALITY AVAILABLE. THE COPY FURNISHED TO DTIC CONTAINED A SIGNIFICANT NUMBER OF PAGES WHICH DO NOT REPRODUCE LEGIBLY.

EVALUATION OF THE CALLAIR A-9
AGRICULTURAL AIRCRAFT

TECHNICAL REPORT

ADS-86

Contract FA-65WA-1027

by

Michael R. Smith
John D. Patrick

November 1966

Prepared For
THE FEDERAL AVIATION AGENCY
Under Contract No. FA-65WA-1027

by

The Aerophysics Department
Mississippi State University
State College, Mississippi

The contents of this report reflect the views of the contractor, who is responsible for the facts and the accuracy of the data presented herein, and do not necessarily reflect the official views or policy of the FAA. This report does not constitute a standard, specification, or regulation.

ABSTRACT

This report presents the results of the performance evaluation of the CallAir A-9 agricultural aircraft. The aircraft was evaluated in three configurations: (1) clean or basic aircraft, (2) basic aircraft with solid material distributor attached, and (3) basic aircraft with spray dispersal equipment attached.

Level flight power required tests and climb performance tests indicate that the dispersal systems greatly reduce the economy and safety of the aircraft in agricultural operations. The results of this investigation indicate that the aerodynamic efficiency of the dispersal systems must be increased before improvement in the aerodynamic design of the basic aircraft will significantly increase the economy and safety of operation.

A qualitative evaluation of the stability and control characteristics of the CallAir A-9 revealed that the aircraft had adequate lateral-directional stability, but that the static longitudinal stability was marginal. The inflight handling qualities at normal operating speeds were very good and the rudder forces were especially light. The large leading edge radius of the wing resulted in very low stall speeds and mild stall characteristics in unaccelerated flight. In accelerated climbing turns, the aircraft exhibited a tendency to roll unusually rapidly toward the outside wing even though it was shown that the air-flow was attached over the ailerons.

Aerodynamic measurements were made to determine the chordwise wing pressure distributions, the spanwise wing loading, the profile wing drag, the skin friction drag, the wing stall patterns, and the nature of the wing-tip vortex field behind the aircraft.

Chemical distribution tests were conducted to determine the distribution characteristics of the solid material distributor. The swath distribution patterns are presented graphically to illustrate the effect of airspeed, altitude, and rate of application on the distribution characteristics. An operations analysis shows the effect of ferry distance, application rate, loading time, swath width, and field size on the productivity of the CallAir A-9 in various types of agricultural operations.

The effect of proposed modifications on the performance of the aircraft is discussed.

CONTENTS

	<u>Page</u>
ABSTRACT -----	111
LIST OF ILLUSTRATIONS -----	vii
LIST OF SYMBOLS -----	ix
CHAPTER	
1. INTRODUCTION -----	1
2. DESCRIPTION OF AIRCRAFT -----	2
3. INSTRUMENTATION OF AIRPLANE FOR FLIGHT PERFORMANCE TESTS -----	3
4. RESULTS OF PERFORMANCE TESTS -----	4
A. Static Thrust and Takeoff Performance -----	4
B. Climb Performance -----	5
C. Level Flight Performance -----	6
D. Glide Tests -----	7
E. Analysis of Power Requirements of the Dispersal Equipment -----	7
F. Stalls -----	8
G. Approach and Landing -----	9
H. Stability and Control -----	9
5. AERODYNAMIC MEASUREMENTS AND FLOW VISUALIZATION INVESTIGATIONS -----	11
6. QUALITATIVE EVALUATION OF THE AIRCRAFT -----	15
A. Cockpit Evaluation -----	15
B. Ground Handling Evaluation -----	16
7. MODIFICATIONS -----	17
8. CHEMICAL DISTRIBUTION TESTS -----	18
9. OPERATIONAL ANALYSIS FOR THE CALLAIR A-9 IN AGRICULTURAL OPERATIONS -----	19
A. Flight Characteristics and Assumptions -----	19
B. Analysis of Results -----	20
10. GENERAL CONCLUDING REMARKS -----	22

	<u>Page</u>
ILLUSTRATIONS -----	24
REFERENCES -----	57
APPENDIX -----	58

ILLUSTRATIONS

<u>Figure</u>		<u>Page</u>
1	Aircraft Airspeed Correction Chart -----	24
2	Static Thrust Curves -----	25
3	Takeoff Trajectories - Clean Configuration -----	26
4	Climb Performance Curves -----	27
5	Excess Horsepower Available for Climb -----	27
6	Level Flight Performance Curves -----	28
7	Effect of Flaps and Propeller Pitch on Power Required - $W_s = 2100$ Pounds -----	29
8	Effect of Flaps on Lift-Slope Curves - $W_s = 2100$ Pounds -----	30
9	Glide Test Data -----	31
10	Linearized Drag Polars for CallAir A-9 in Gliding Flight -----	32
11	Aircraft Profile Drag Coefficient in Gliding Flight -----	33
12	Power Requirements of Dispersal Systems -----	33
13	Wing Stall Pattern in a Right Climbing Turn -----	34
14	Propulsive Efficiency -----	35
15	Power Required for Engine Cooling -----	36
16	Wing Pressure Distributions -----	37
17	Spanwise Lift Distributions -----	39
18	Analysis of Wing Drag -----	40
19	Aerodynamic Wing Data -----	41
20	Boundary Layer Parameters -----	42
21	Skin Friction Distribution -----	44

<u>Figure</u>		<u>Page</u>
22	Visualization of Airflow Over the Wing and Fuselage ----	45
23	Visualization of Wing Tip Vortices -----	47
24	Path of Motion of Wing Tip Vortices for Several Heights of Operation - $C_L = 1.15$, $W_s = 2100$ Pounds -----	48
25	Hopper Calibration Curve -----	50
26	Granular Swath Distributions -----	51
27	Operation Analysis for Granular Materials -----	53
28	Operation Analysis for Spray Materials -----	55

ILLUSTRATIONS IN APPENDIX

I	Front Quarter View of Test Vehicle in Clean Configuration -----	58
II	Side View of Test Vehicle in Clean Configuration -----	58
III	Rear Quarter View of Test Vehicle in Spray Configuration -----	59
IV	Front Quarter View of Test Vehicle in Spray Configuration -----	59
V	Rear Quarter View of Test Vehicle in Distributor Configuration -----	60
VI	Side View of Test Vehicle in Distributor Configuration -----	60
VII	Controls Operated With the Left Hand -----	61
VIII	Cockpit Arrangement - Flight Test Instrument Panel Installed -----	62
IX	Distribution Equipment -----	63
X	Boundary Layer Profiles -----	64

SYMBOLS

V_c	calibrated airspeed - miles per hour
V_{ew}	equivalent airspeed - miles per hour
W_t	aircraft test weight - pounds
W_s	aircraft standard weight - pounds
THP	thrust horsepower (gliding flight)
BHP	engine brake horsepower
C_l	wing section lift coefficient - $C_l = \int C_p d(x/c)$
C_L	aircraft lift coefficient
C_D	aircraft drag coefficient
C_f	skin friction coefficient
C_{D_0}	wing profile drag coefficient
C_{D_i}	induced drag coefficient
AR	geometric aspect ratio
AR_e	effective aspect ratio
e	wing efficiency factor
L/D	lift-to-drag ratio
u	local velocity in airstream - miles per hour
U_L	local velocity in the boundary layer - miles per hour
U_τ	local friction velocity - feet per second
U_∞	free-stream velocity - feet per second or miles per hour
η_p	propulsive efficiency - level flight
η_{pc}	propulsive efficiency - climb
z	wing semi-span - inches
x/c	percent of wing chord

C_p wing pressure coefficient
 δ boundary layer thickness - inches
 δ^* displacement thickness - inches
 θ momentum loss thickness - inches
 H boundary layer shape factor $H = \delta^*/\theta$
 τ_o local shear force - pounds per foot squared
 ν kinematic viscosity of air

1. INTRODUCTION

This report presents the results of safety and performance investigations on the CallAir A-9 agricultural aircraft. This aircraft was manufactured by the Intermountain Manufacturing Company of Afton, Wyoming and was loaned to Mississippi State University for this research program. The program was conducted as one phase in the investigation of the capabilities and limitations of existing agricultural aircraft. These studies also show the performance of this aircraft in aerial application operations. It is anticipated that these investigations will define areas where aerodynamic modifications and the development of improved aerial application techniques and equipment will substantially increase the safety and utility of aerial application systems.

The program consisted of the measurement of the flight performance of the test aircraft in the clean configuration and in both spray and granular distributor configurations. A qualitative evaluation of the aircraft's flight characteristics and productivity in aerial application operations was conducted. Distribution tests were conducted using granular materials to determine the effect of various operating techniques on swath width and the material distribution pattern. Special techniques and instrumentation were used to investigate the airflow about the aircraft, the power requirements of the dispersal systems, and other aerodynamic characteristics.

The evaluation program was conducted at the Raspet Flight Research Laboratory, Starkville Municipal Airport, Starkville, Mississippi, from April 1965 to February 1966.

2. DESCRIPTION OF AIRCRAFT

The CallAir A-9 is a specialized aircraft built exclusively for the aerial application industry. It is a single-place, low-wing monoplane with a strut-braced wing and is powered by a Lycoming model O-540-B, opposed piston, naturally aspirated engine which develops 235 horsepower at 2575 r.p.m. at sea level. The 84-inch-diameter propeller is a McCauley two-piston type having a pitch of 14 degrees at the low stop and a pitch of 17 degrees at the high stop. The modified airfoil has a drooped leading edge and the wing incorporates a 25-degree flap system and ailerons that deflect 10 degrees upon extension of the flaps. The distribution equipment is furnished by Transland Manufacturing Company. The aircraft was manufactured in October 1964 and had 52 hours on the airframe and the engine when delivered to the project.

List of Aircraft Specifications

Span	-----	34 feet, 8 inches
Wing Area	-----	182 square feet
Wing Chord	-----	63.375 inches
Airfoil	-----	Modified Clark-Y
Length	-----	24 feet, 0.75 inch
Height (Level Flight)	-----	10 feet, 1 inch
Passenger & Crew Capacity	-----	1
Empty Weight (Wet)	-----	1823 pounds
Gross Weight (FAR Part 3)	-----	3000 pounds
Useful Load (Full Fuel & Pilot)	-----	956 pounds-spray 934 pounds-distributor
Placarded Maximum Hopper Capacity	-----	1250 pounds
Fuel Capacity	-----	40 gallons
Oil Capacity	-----	12 quarts

3. INSTRUMENTATION OF AIRPLANE FOR FLIGHT PERFORMANCE TESTS

Upon receipt of the aircraft, all regular flight and power instruments were removed and calibrated. In addition to the aircraft airspeed system, another airspeed system was installed using a Kiel tube total head and a neutral static source on the side of the fuselage. This system was dynamically balanced and calibrated using a trailing sonde and a third airspeed indicator. The airspeed correction chart for the original airspeed system is shown in Figure 1. In addition, the aircraft was equipped with a calibrated manifold pressure gauge and an electric outside air temperature gauge. Special instrumentation which was required for detailed investigation of aerodynamic characteristics and evaluation of the dispersal systems is described in the appropriate sections of the report.

4. RESULTS OF PERFORMANCE TESTS

Standard weights of the aircraft used in the performance tests were 2100 pounds and 3400 pounds for the empty and loaded configurations, respectively. These gross weights included full fuel, oil, and pilot. Although the certificated gross weight under FAR Part 3 was 3000 pounds, the hopper was placarded at 1250 pounds, which brought the takeoff weight with full fuel to 3450 pounds. It was felt that the applicator would be inclined to load the hopper to the maximum limit under favorable atmospheric and runway conditions and that 3400 pounds would be more representative of the loaded condition than 3000 pounds.

A. Static Thrust and Takeoff Performance

The static thrust developed by the engine-propeller system is presented in Figure 2. A maximum of 50 pounds difference was noted in the static thrust produced by the system in the high and low pitch propeller positions. These curves show that the low pitch (high r.p.m.) position gives a thrust increase of 6.5 percent over the high pitch setting at the start of the takeoff run. This is a small increase for a system which was designed to add appreciably to the takeoff performance.

Takeoff tests were performed to investigate the best pilot technique during takeoff and to evaluate the performance of the flaps. In the clean configuration at a gross weight of 2100 pounds with the flaps up, full elevator travel failed to raise the tail until lift-off speed was nearly attained. This characteristic limited the range of pilot technique in this case. The use of flaps, which brought the tail off the runway at a lower airspeed, enabled the aircraft to leave the ground in 94 percent of the no-flap distance. Initial rate of climb was also slightly improved by use of the flaps so that the aircraft cleared a 50-foot obstacle in 93 percent of the distance required when the flaps were not used. Figure 3a illustrates the takeoff trajectories for these tests.

In the clean configuration at 3400 pounds gross weight, the effect of the flaps is more pronounced. Figure 3b illustrates the takeoff trajectories at the 3400-pound gross weight. It can be seen that with the flaps retracted, the take-off run is 1300 feet, while the use of flaps reduced this distance to 1100 feet. With flaps, the aircraft cleared the 50-foot obstacle at 1550 feet as compared with 1725 feet with the flaps retracted. The CallAir A-9 incorporated drooped ailerons in the flap system so that when flaps are extended, the ailerons deflect downward 10 degrees. This characteristic nearly doubles aileron control forces as compared with those experienced with flaps retracted. This increase in control forces plus the high pressure of the flaps on the flap control lever during retraction tends to distract the pilot. Another disadvantage of the flap system related to the high forces on

the flap control lever is the fact that above 70 miles per hour the forces become so high that the lever cannot be moved out of the detent. This inability to move the lever above 70 miles per hour leaves only 10 miles per hour between stall speed and maximum flap retraction speed in the loaded configuration. This situation is aggravated by the fact that the flap control lever in the flaps-down position is too high and too far aft for easy operation.

B. Climb Performance

Climb tests were conducted at gross weights of 2100 pounds and 3400 pounds in the basic, spray, and distributor configurations. In addition, one flight was made in the basic, empty configuration with the propeller in the high pitch position. These sawtooth climbs were flown at full throttle from 500 feet pressure altitudes to 1500 feet pressure altitudes. The results of these tests have been reduced to standard atmospheric and weight conditions and are summarized in Figure 4. Excess horsepower available for climb at various loads and configurations is presented in Figure 5.

The effect of distribution equipment and load on the performance of the aircraft is shown by the significant reduction in rate of climb (Figure 4) due to the presence of the distribution equipment. This effect illustrates the need for further aerodynamic refinement in equipment design. The addition of the dispersal equipment reduced the best climb speed by 5 to 10 miles per hour at the same gross weight (2100 pounds). Under the same conditions, the maximum rate of climb was reduced by 18 to 22 percent.

It can also be seen that the rate of climb of the clean aircraft at 3400 pounds gross weight and 96.5 miles per hour is the same as that of the aircraft with distributor attached and operating at a gross weight of 2100 pounds. Comparison of the rates of climb of the aircraft in the clean configuration and the spray configuration shows that the rate of climb of the clean aircraft is 1.4 to 6.5 times greater than that of the spray configuration in the normal speed range, depending on gross weight.

Figure 5 illustrates the excess horsepower available for climb in six configurations. These curves show that more horsepower is available in the clean configuration at 3400 pounds gross weight than is available in either agricultural configurations at a gross weight of 2100 pounds at cruising airspeeds. As would be expected, this condition becomes more exaggerated as speed is increased, so that at 100 miles per hour the excess horsepower available for climb with the clean aircraft exceeds twice that of the aircraft with either dispersal system.

The information presented by these curves dramatically illustrates the detrimental effect of the distribution equipment on an important

aspect of aerial application which is the ability of the aircraft to climb rapidly over an obstruction. The effect of externally mounted dispersal equipment is seen to have a more detrimental effect on climb performance in the cruising range than that of a full hopper load. Of further interest is the fact that addition of the dispersal equipment reduces the best rate of climb speed so that less margin is left between the best rate of climb speed and the stall speed.

C. Level Flight Performance

Relationships between engine brake horsepower and equivalent airspeed were determined for three configurations at gross weights of 2100 pounds and 3400 pounds and at pressure altitudes of 2000 feet or less. One flight was flown with the propeller in high pitch and also a flight was flown with the flaps extended. Stabilized altitude and airspeed points were flown for each configuration across the entire speed range of the aircraft, and the data obtained were reduced to standard weight and atmospheric conditions. The results of these tests are presented in Figure 6. Figure 7 compares the power requirements of the aircraft with flaps extended and also with the propeller in high pitch with the flaps up and in the low pitch propeller condition. Figure 8 illustrates the effect of flaps on the lift-slope curve.

The level flight power required data (Figure 6) show that the power required to overcome the drag of the dispersal systems at 100 miles per hour is 19 to 25 percent of that required to operate the clean aircraft. The power required to lift a 1250-pound load (aircraft gross weight of 3400 pounds) is 21 percent of the power requirement of the clean aircraft at 100 miles per hour and 2100 pounds gross weight. At 80 miles per hour, the power requirement of a 1250-pound load plus the dispersal system is 63 to 69 percent of that of the clean aircraft. The reduction of this large power requirement for load and equipment would allow the aircraft to operate at a reduced power setting for a given airspeed, therefore, reducing the operation cost and increasing the engine lift.

The two-position propeller on the aircraft does not appear to be properly adjusted or of the proper design to greatly effect takeoff or cruise performance as is shown in Figure 7. The static thrust of the propeller is approximately the same for each propeller setting with a maximum difference of approximately 50 pounds at full-throttle. The level flight and climb performance indicate that the fine blade setting is more efficient at speeds up to 100 miles per hour, and that the coarse blade setting will increase the maximum speed by about 3 miles per hour.

The power requirements of the aircraft with the flaps extended are also shown in Figure 7. As can be observed, the use of flaps lower the stall speed 3 miles per hour; however, the power requirements

increase rapidly as the airspeed is reduced below 50 miles per hour. At airspeeds above 60 miles per hour, the power requirements with the flaps extended are greater than with the flaps retracted; therefore, if the flaps are retracted slowly as soon as the airspeed reaches 60 miles per hour, the aircraft will accelerate more rapidly to the best climb speed.

D. Glide Tests

The efficiency and aerodynamic characteristics of an aircraft can be more accurately measured in the power-off gliding flight due to the absence of engine-propeller, and engine instrument deterioration. Computing errors are also minimized or eliminated.

In this method, the propeller is removed and ballast substituted to bring the center of gravity to the desired position. The aircraft is then towed to an appropriate altitude, released, and glided at a stabilized airspeed. By measuring the rate of sink and calculating the true airspeed, the thrust horsepower required to fly the aircraft in a given configuration and weight can be computed.

Figure 9a presents the L/D curves for the test aircraft in four configurations, and Figure 9b gives the thrust horsepower required to fly the aircraft at various speeds in the same configurations. The "clean and sealed" curve was obtained by sealing the cowling so as to make it relatively airtight. A comparison of the "clean and sealed" curve with the "clean" curve gives a measurement of the thrust horsepower required to cool the engine. The linearized drag polars obtained from the glide tests are shown in Figure 10. Figure 11 presents the aircraft profile drag coefficients of the clean and empty aircraft at various airspeeds.

E. Analysis of Power Requirements of the Dispersal Equipment

The thrust horsepower required for each system was found from the glide tests, and the brake horsepower requirements were taken from the level-flight-power-required data. Figure 12 gives the power absorbed by the dispersal systems at various airspeeds. A comparison between the brake horsepower required for the dispersal equipment and the total power required in the operating range shows that the spray system absorbs 18 to 22 percent of the total power required while the distributor takes 20 to 22 percent of the total.

Although the power requirements of the distribution equipment are high, both the spray and solid material distributor systems have drag reduction features not found on some other systems. The spray pump is enclosed inside the aircraft (Figure IV) and the spray booms, although not in the best position, are behind the wing trailing edge. Wing profile drag measurements (Figure XI) indicate that the boom is placed too

low to make full use of the low velocity region in the wing wake at normal operating speeds. The distributor differs from most in that the area at the rear approximates the area at the front instead of being much greater (Figure IX). This feature insures minimum drag in comparison to a regular venturi of the same profile area.

Unfortunately, both systems also displayed many of the common equipment disadvantages. The windmills used to drive the spray pump and solid material agitator have been proved to have a working efficiency of about 10 percent. This low efficiency means that to obtain 2-shaft horsepower, about 20-drag horsepower is added to the system. Due to detrimental propeller effects caused by locating the windmills in close proximity to the aircraft propeller, propulsive efficiency will generally be less than 65 percent. This means that approximately 20-brake horsepower are required to produce 2-shaft horsepower at the pump. The location of distributors and spray systems directly behind the propeller and cowling also adds to the total drag due to the superelevations behind the propeller.

In order to reduce the power requirements of the dispersal equipment so that the safety and performance of the aircraft will be increased, careful attention should be given to the design of the dispersal systems. One possible solution would be to suppress the spray boom in the wing wake in such a manner as not to cause interference with the ailerons. Such a modification can reduce the drag of the boom to less than 40 percent of its original value. A more extensive modification would entail installing the boom within the wing structure and driving the spray pump from an auxiliary power pad on the engine. Such a modification could reduce the total power requirement of the spray system to approximately 5-brake horsepower for general operation. The drag of the solid material distributor is very moderate as compared to units on other aircraft; however, it still contributes considerably to the total drag. The design of the distributor on the CallAir A-9 represents an effort to design a minimum drag system; however, the swath width is reduced due to the decrease in venturi effect. Further efforts to decrease the drag of the distributor should be directed toward auxiliary powered systems which would impart energy directly to the particles to give them a lateral acceleration. Such devices should be capable of attaining much wider and more uniform swaths while reducing the power requirements.

F. Stalls

The aerodynamic stall warning on the test aircraft was generally adequate with the exception of stalls during accelerated maneuvers in the 3400-pound configuration. In straight ahead stalls from level flight at 2100 pounds, wing and elevator buffet gave ample warning and recovery with power could be made in 50 to 75 feet. One excellent feature of the CallAir A-9 is the aileron effectiveness throughout the stall (Figure 13). The photographs shown in Figure 13 were taken with

an automatic camera during an accelerated stall in the clean and empty configuration. The orientation of the woolen tufts indicate that the wing is completely stalled, but the airflow is still attached over most of the aileron. Even though the attached flow over the aileron provides considerable aileron power at low airspeeds, the aileron power that is available is not sufficient to prevent the wing from dropping during a complete stall due to the low dynamic pressure at stall speed.

At the 2100-pound gross weight, recovery from a complete stall in an accelerated climbing turn required approximately 150 feet of altitude. At 3400 pounds, recovery from a climbing turn stall required about 275 feet. In both cases, the aircraft rolled very rapidly toward the outside wing, such that a steep nose-down attitude was attained during recovery. At 2100 pounds, aerodynamic stall warning occurred in time for the pilot to initiate corrective action which reduced the severity of the stall. At 3400 pounds the aerodynamic stall warning did not occur in time for the pilot to take the corrective action. The following chart gives the power-on and power-off stall speeds in level flight in various configurations.

CONFIGURATION	WEIGHT (lb)	STALL SPEED V_{sw} (M.P.H.)	
		POWER-OFF	POWER-ON
Clean (25° Flaps)	2100	46.2	41.6
Clean	2100	58.2	43.9
Spray	2100	61.0	47.9
Distributor	2100	61.0	48.5
Clean	3400	70.5	59.5
Spray	3400	74.0	61.5
Distributor	3400	72.0	61.0

G. Approach and Landing

No quantitative data were taken for the approach and landing phase of operation. Qualitative evaluation by several pilots showed that the empty aircraft could be stopped in less than 500 feet on a hard surface from either a power-off or power-on approach. Visibility is adequate for safe operation during either type of approach. Although directional control is easily maintained with tailwheel steering and brakes, the aircraft shows a tendency to wander during the landing roll. Flaps were not used during landing because aileron control forces were increased.

H. Stability and Control

The results of dynamic stability and control tests on the CallAir A-9 will be presented in a separate report. The discussion in this section shall be limited to a qualitative evaluation of the stability and control of the test aircraft.

When the aircraft was delivered to the project, it was rigged as per the manufacturers specifications and according to the requirements of FAR Part 8. At the low gross weight, the aircraft could be trimmed to fly hands-off; however, the aircraft appeared to possess negative longitudinal stability. The direction of divergence was entirely dependent upon the direction of the disturbance. In several stick-free tests, the aircraft entered a right spiraling turn with no tendency to neutralize before reaching the limiting speed. Another unusual characteristic was the requirement for opposite aileron displacement during a steady turn. This characteristic was most noticeable in a left turn and in the loaded configuration.

In the 3400-pound configuration, the aircraft could not be trimmed to fly hands-off in level flight or climbing flight and the static, longitudinal, stick-free stability appeared negative.

Before the dynamic stability and control tests were conducted, the aircraft was rigged to meet the specifications of FAR Part 3. This entailed the removal of a balance spring on the up-elevator cable and placement of a second spring on the down-elevator cable. This simple modification appeared to greatly reduce elevator loads in the vicinity of the neutral stick position and substantially increased the static stability of the aircraft. The dynamic longitudinal stability of the aircraft was increased to the point that the aircraft does not tend to rapidly diverge, but continues a very lightly damped phugoid motion when disturbed from a static condition. In general, the handling qualities of the aircraft were satisfactory below 3000 pounds gross weight. The rudder forces are extremely light and permit long hours of operation with minimum pilot fatigue. The aileron control power was adequate at all working speeds and the control forces were moderate for this type of aircraft. With the flaps extended the aileron forces were substantially higher and lateral control was minimal near the power-on stall speed.

5. AERODYNAMIC MEASUREMENTS AND FLOW VISUALIZATION INVESTIGATIONS

To the aircraft designer and the aerodynamicist, the accurate determination of the aerodynamic characteristics of the aircraft is of paramount importance in that it allows them to determine the aerodynamic qualities of the aircraft and methods by which the performance of the aircraft may be improved. Flow visualization aids in the determination of separated flow and the nature of disturbances caused by various aircraft components. A visualization of the total flow field surrounding the aircraft aids in determining the optimum heights and speeds to fly under various conditions so as to effect the best distribution characteristics of sprays and other materials.

The propulsive efficiency of the engine-propeller system is a basic parameter upon which the performance of the airplane in level flight and in climbing flight is computed. The propulsive efficiency of the engine-propeller system can be computed from information obtained in the glide and level flight tests, and as such it is defined as the thrust power required in gliding flight divided by the level flight power required at the same speed, load, and configuration. Propulsive efficiency curves for the climb and level flight conditions in the various agricultural configurations are presented in Figure 14. Propulsive efficiency includes losses due to cooling, slipstream effects, and propeller efficiency and, therefore, as such, is not a direct measurement of propeller efficiency. It should be noted that propulsive efficiency can be increased by the reduction of interference drag caused by the various aircraft components and the dispersal equipment and also, due to reduction in cooling drag requirements.

The power required for engine cooling in agricultural airplanes is usually much higher than that on utility aircraft due to the strenuous climb requirements under various conditions of speed and engine power. From the glide tests with the engine cowling open and with the cowling sealed, it is possible to estimate the power required for cooling at the various airspeeds. Since the engine was not operating, thermoaerodynamic effects of cooling were ignored; however, this method of presentation gives a measure of the cooling system efficiency which is easily obtained with a minimum error. Figure 15 presents the power required for engine cooling at various airspeeds. It should be remembered that, in this case, the power required represents the energy loss due to the pressure drop through the cowling and is not a measure of the total energy loss due to the cowling design itself. For instance, with a fixed cowl flap it is possible to obtain a negative cooling drag due to the fact that the drag of the cowling system is greater when closed than when opened, which would indicate that aerodynamic cleanup of the basic cowling could possibly reduce the cooling drag requirements even further.

Chordwise wing pressure distributions were measured at several airspeeds in both flap configurations at the empty gross weight. The pressure distributions were obtained through the use of a multitube plastic tape which was attached around the surface of the airfoil. Numerous static taps were drilled in the plastic tape at various chordwise positions and each channel of the tape was connected to a multi-channel photographic water manometer. A trailing static sonde was used as a pressure reference on the manometer and the pressure distributions were recorded at several different airspeeds. The results of these pressure distribution measurements are presented in Figure 16. Pressure distributions were taken at four spanwise stations along the wing to obtain the spanwise loading of the wing. The individual pressure distributions were integrated to obtain the local lift coefficient, and the spanwise loading curves are presented in Figures 17a and 17b. By reference to Figure 19 it can be observed that the droop loading edge modification on the CallAir A-9 provides the aircraft with an excellent high-lift airfoil and that there is very little difference in the maximum lift coefficient between the flapped and unflapped airfoil. The main advantage of the flaps is that they allow the aircraft to attain the same lift coefficient at approximately 6 to 10 degrees lower angle of attack which will permit the pilot a better vision in the forward direction. In addition, the flaps will also greatly reduce the ground run due to the fact that the aircraft can attain a higher lift coefficient while still in a 3-point attitude. The chordwise pressure distributions indicate that due to the effectiveness of the flap system, a considerable portion of the total air loads are carried by the trailing edge portion of the wing when the flaps are extended, particularly at speeds greater than 50 miles per hour. This supports the manufacturer's recommendation that flaps should be used for takeoffs only and should not be applied as a means of decreasing turnaround time. As the spanwise load distributions and the level flight data also indicate, the turnaround time can not be reduced appreciably by the application of flaps due to the fact that the maximum aircraft and section lift coefficients are approximately the same for both flap configurations. If a stall should be inadvertently encountered with the flaps extended, recovery could be complicated by the fact that the loading of the rear section of the wing would cause a positive pitching moment which might delay recovery from the stall.

The wing profile drag was measured by the use of a remotely controlled wake traversing rake which measured the total head and static pressure at various points behind the trailing edge of the wing. The results of these drag tests are presented in Figure 18, and the wake velocity profiles are presented in Figure X. The minimum drag coefficient for the wing occurs at an airspeed of approximately 80 miles per hour in the empty configuration or at an angle of attack of approximately 8.5 to 9 degrees. At airspeeds above 80 miles per hour, there is a substantial increase in the profile drag of the wing which is probably due to excessive camber in the leading edge of the wing caused

by the drooped leading edge modification; however, it should be remembered that the extra camber in the wing leading edge also contributes to the lift increment which is depicted in Figure 19.

Boundary layer velocity profiles were taken at several chordwise positions along the wing by means of a remotely controlled traversing boundary layer probe which measured the total head and static pressure at each position above the wing surface. The velocities in the boundary layer were read directly on a sensitive, helicopter airspeed indicator and the indicated airspeeds were later corrected for instrument error. The corrected boundary layer velocities were plotted against the y -values which were read from the remotely controlled traversing device and are presented in Figure XI. The boundary layer thickness was measured directly from the velocity profiles, and the boundary layer parameters were calculated by integration of the boundary layer velocity profiles. The results of these tests are presented in Figures 20a and 20b. By reference to Figure 20 it can be observed that transition from laminar flow to turbulent flow occurs very near the leading edge of the airfoil under all flight conditions. This early transition to turbulent flow is caused by a geometric imperfection in the surface contour at approximately the 3-percent chord position on the upper leading edge of the wing and can be most easily recognized by the abrupt drop in the pressure curve in the high-lift case as shown in Figure 16b.

The surface shear on the airfoil was determined from the boundary layer velocity profiles using a modified Wall Law technique from turbulent boundary layer theory. The modified Wall Law techniques by Roberts (Reference 4) plots u/U_τ against yu/ν , and for each boundary layer point $u(y)$, a value of u/U_τ and hence U_τ , was obtained. U_τ was plotted against y for each boundary layer profile. In the Wall Law region U_τ should be a constant and hence that constant value of U_τ was the friction velocity for the profile. The values of τ_0 obtained from the values of U_τ were used for the computation of the skin friction values. The distribution of the surface skin friction is presented in Figure 21. By reference to Figure 18 it can be observed that the skin friction comprises approximately 40 percent of the total profile drag of the wing at normal working speeds.

In order to delineate the nature of the airflow over the wing and fuselage of the aircraft, the aircraft was tufted with small woolen tufts and the resulting flow patterns were photographed from a second aircraft. The results of these flow visualization tests are shown in Figure 22. As can be observed from the photographs, the intersection of the lift strut and wing causes considerable interference at all airspeeds and in both flap configurations; however, the use of flaps improves the airflow over the wing. The cowling flaps, the strut intersection at the fuselage, and the wing root-fuselage intersection all cause appreciable interference drag as evidenced by the turbulent nature of the tuft pattern in the photograph. In addition, there is evidence of a strong shed vortex being formed at the base of the windshield. This vortex extends downstream along the side of the fuselage

and causes considerable interference drag on the fuselage and tailplane. It can also be noted that the airflow over the aileron remains attached at all airspeeds which speaks well for the efficient design of the aileron slots. Likewise, modification of the cowling flaps and the windshield could also provide substantial reductions in the overall profile drag coefficient.

The nature of the wing tip vortices is of considerable interest to the aerial applicator due to the fact that the strength and path of motion of the vortices control to a great degree the application of lightweight materials such as sprays and dust. To aid in visualizing the flow field behind and surrounding the aircraft, several techniques have been devised (Reference 1). The most productive of the various techniques for the purpose at hand appears to be that of ejection of inert powder into the wing tip vortices and photographing the movement of the vortices with a remotely controlled camera and intervalometer system. This method utilizes a 135-mm camera positioned along a flight path center line to record the movement of the vortices by photographing the patterns at a set time interval. In this case, the camera was equipped with an intervalometer which was fired at the time that the dust was injected into the vortices and continued on a 3-second interval. Figure 23 presents a series of photographs which show the path of motion behind an aircraft operating at a typical lift coefficient, and Figure 24 presents the path of motion of the wing tip vortices for several various heights and for a typical flight configuration. As will be noticed, the height of operation has considerable influence on the trajectory of the wing tip vortices, and there appears to be an optimum height from which the aircraft should be operated in order to obtain the maximum swath width. Similarly, from field evaluation tests it has been observed that there is also a best height to fly in order to obtain the maximum downwash which will effect greatest penetration of the chemical into the treated crop. As a general rule of thumb, it can be stated, for most cases, that the best height of operation is approximately one half the total wing span of the aircraft, the height for maximum swath width being slightly greater than one half the wingspan height and the height for greatest penetration being slightly less. In the case that this method of application is used where the wing tip vortices are used to help transport the material, it must be remembered that the equipment must be calibrated and adjusted while operating from a specific height in order to effect a uniform swath distribution and that under no conditions should the height of application be altered. Should the wind conditions become high enough that the pilot feels that a change of altitude would be warranted, then all applications should be ceased since any change in height may result in an uneven swath distribution. It has been further demonstrated by field evaluation tests that this mode of operation can result in a substantially wider swath and that the safety of operation is greatly increased due to the fact that the pilot is flying several feet above the treated crop. In all cases, it should be remembered that the height of operation discussed in this section is in reference to the height of the wing tip above the ground and not the height above the treated crop.

6. QUALITATIVE EVALUATION OF THE AIRCRAFT

A. Cockpit Evaluation

The CallAir A-9 is entered by climbing onto the wing and then entering the cockpit by a prescribed method. Entry is awkward, especially for a pilot of above average height. The process is reversed to deplane with care being taken not to step on the flap. Once seated in the cockpit, the pilot of average height can expect reasonable comfort for this class of aircraft. The seat cushions are comfortable, but the slight forward tilt to the seat back is fatiguing over long periods. The seat and rudder pedals are not adjustable but seem to be well placed for the average pilot. The seat belt and shoulder harness are standard and well anchored. There is no floor in the cockpit other than the heel tracks provided for each foot, so care must be taken not to drop loose objects which might cause a hazard in flight. Attached to the right side of the cockpit is a map case.

The location of the flight controls is good with the exception of the full forward position of the stick and flap control lever. With the safety harness adjusted properly, it is difficult to push the stick full forward. This situation could cause a problem in attempting a stall recovery or short run takeoff. The flap control lever is too far aft for easy operation. Also the throttle is too close to the longeron for comfort and should be moved further from the side of the cockpit.

Location of individual dispersal system controls is convenient with the exception of the dispersal control lever; however, their close proximity to each other interferes with their operation (Figure VII in Appendix). Especially is this true of the emergency dump handle and the dispersal control lever in the forward position. The rearward limit of the dispersal control lever is too far aft for operator comfort. Also, some type of scale should be provided for use with solid material so that varying rates of application could be easily set in the cockpit. The pump fan brake control is located too low in the cockpit for easy reach; however, this should not be a problem when operating in the cruising condition.

All instruments are located on the instrument panel directly in front of the pilot (Figure VIII in Appendix). Arrangement is good in that there is definite order to the panel. Flight instruments are located to the left, and engine instruments and the spray pressure gauge are located in the center. The right side of the panel is reserved for radio equipment and the ammeter. The location of the panel itself is too low and too close to the pilot for the quick reference needed in application work. If a radio is used,

the present jack location will cause some inconvenience. The position of the jack in relation to the helmet is such that the cable interferes with head and/or right arm movement.

Ventilation is achieved by means of a scoop on the fuselage forward of the hopper. The aircraft may also be flown with the side doors opened without excessive buffet in the cockpit area; however, this condition greatly increases cockpit noise level and is not recommended when dispensing chemicals. A cabin heater is provided but provision should be made to close the airscoop to get adequate response in cold weather.

The CallAir A-9 fuel system contains two fuel tanks which must be individually selected. This feature in itself is not dangerous if reasonable care is used. A bell type warning device is installed to warn the pilot when the fuel pressure drops below the required level.

Crash protection appeared to be very good in this aircraft. The location of the hopper forward of the cockpit, standard in any well-designed agricultural aircraft, and the obviously well-braced cockpit structure protect the operator from excessive impact forces. The placement of the fuel tanks in the wings reduces the possibility of fire in the event of structural damage.

B. Ground Handling Evaluation

Taxi operation is excellent under all conditions. Although the aircraft is easily displaced from a straight course by a rough surface or crosswind, it can be easily corrected with proper tailwheel steering or differential braking. With the inside brake locked, the aircraft will pivot on the inside wheel in both the loaded and empty condition. Using tailwheel steering alone, the aircraft will turn in a radius of 39.5 feet at a speed of 8.5 miles per hour in the empty condition. When the aircraft is loaded, the turning radius increases to 43.5 feet. Tailwheel steering is very responsive and is adequate for all taxi operations with the exception of sharp turns where brakes must be used. The brakes are the toe-actuated type and are adequate for all ground operations. The parking brake control, located on the instrument panel, is convenient to use. The brakes will hold the aircraft at full throttle whether empty or loaded. Ground visibility is also excellent.

7. MODIFICATIONS

The results of flow visualization tests, performance tests, and aerodynamic measurements indicate that considerable drag reduction could be accomplished by modifying the basic aircraft.

The measurement of the wing profile drag indicates that the drooped leading edge modification causes considerable profile drag at airspeeds greater than 80 miles per hour (Figure 18). It is anticipated that modification of the leading edge by more extensive fairing on the lower surface and/or a reduction of the total leading edge radius would greatly reduce the drag without greatly reducing its lift capability. Similarly, removing the small, geometric imperfection in the upper surface of the wing leading edge would improve its lift capability and result in some small reduction in skin friction drag.

As a result of the flow visualization tests (Figure 22), it is felt that a wing root fairing would greatly reduce the interference drag caused by the wing-fuselage intersection. Also, improved wing strut fairings would effect some small drag reduction and possibly improve the lateral control at low airspeeds. In addition, it was observed in flow visualization tests that the steep windshield angle on the canopy caused considerable separation on the sides of the canopy drag. It is felt that a less acute angle on the windshield would result in lower drag. Similarly, the forward portion of the engine cowling could be modified to effect a lower drag.

8. CHEMICAL DISTRIBUTION TESTS

The solid materials distributor was evaluated using superphosphate fertilizer. The metering system was calibrated over a measured course by checking the ground speed of the aircraft with a stopwatch and measuring the total material dispensed after each run. Hopper loads of 300 and 600 pounds were used during calibration. Figure 25a shows the results of the calibration tests.

After completing the calibration, a series of tests were run at various altitudes, airspeeds, gate openings, and hopper loads to determine the effect of each parameter on the swath characteristics. These tests were made by flying over a sampling station which had sample pans spaced five feet apart along a line perpendicular to the line of flight. The samples obtained were collected in a series of calibrated glass tubes and photographed. From these pictures, rate of application, swath width, and swath irregularities were determined (Figure 26).

The results obtained from these tests indicate a reduction in application rate in the center of the swath except at the 405-pound-per-acre setting. The use of several distributor vane positions failed to correct this characteristic. In Figure 26b, it can be seen that application rate increases as airspeed decreases. This change in application rate occurred because the hopper setting remained constant for all three runs. It can be seen that as airspeed decreases, the characteristic peaks in application rate become more pronounced. Figure 26c indicates that as the height of the aircraft increases, swath width increases and application rate decreases. Variation in hopper load produced only small changes in the distribution pattern as is shown in Figure 26d.

9. OPERATIONAL ANALYSIS FOR THE CALLAIR A-9
IN AGRICULTURAL OPERATIONS

A. Flight Characteristics and Assumptions

The productivity of the CallAir A-9 was carefully investigated with the aid of a computer program. By using the computer, more thorough and accurate analysis could be obtained. The variables of swath width, ferry distance, rate of application, and loading time were investigated in relation to their effect on productivity.

The aerodynamic and flight characteristics of the CallAir A-9 which were used in the analysis were obtained from the experimental data gathered during flight performance investigations and presented in previous sections of this report.

Except when varied to study their effects, the following figures were used throughout the program:

DISTRIBUTOR SYSTEM OPERATIONS:

hopper load = 1200 pounds
swath width = 40 feet
rate of application = 100 pounds per acre
turn around time = 25 seconds
time to load = 5 minutes
ferry distance = 4 miles
ferry speed = 95 miles per hour
swath speed = 90 miles per hour

SPRAY SYSTEM OPERATIONS:

hopper load = 1200 pounds
swath width = 50 feet
rate of application = 20 pounds per acre
turn around time = 25 seconds
time to load = 5 minutes
ferry distance = 4 miles
ferry speed = 95 miles per hour
swath speed = 90 miles per hour

The ferry distance and loading time figures were based on a survey of Mississippi aerial applicators during 1964. Turning time was based on the usual method of executing a 180 degree change of direction to align the aircraft for a swath run adjacent to the previous swath.

It was further assumed that the fields being treated were square in shape and could be worked from all directions. This assumption is not

unreasonable since a particular field will probably be worked from different directions during the season due to wind conditions. Provision was also made for four additional "clean up" swaths around trees on the field border or obstructions in the field.

B. Analysis of Results

The results of this analysis are illustrated in Figures 27 and 28. Productivity associated with the CallAir A-9 was assumed to be mainly dependent on ferry distance, loading time, application rate, and swath width. Figure 27 illustrates the effect of these variables on the fertilizing and seeding operations. The effect of application rate (Figure 27a) indicates the loss in productivity as the rate is increased. Productivity is approximately 5 times greater at the 50-pound per acre rate than at the 400-pound per acre rate.

Figure 27b shows the effect of loading time on productivity. It can be seen that the rate at which productivity falls off as loading time increases is greater at the short loading time interval. Productivity at a field size of 200 acres falls off 21 acres per hour between loading times of 1 and 5 minutes and 14 acres per hour between 5 and 10 minutes.

The drastic effect of ferry distance on productivity is presented in Figure 27c. For the 200 acre field, productivity drops from 64 acres per hour at a ferry distance of 2 miles to 14 acres per hour at a ferry distance of 32 miles; a 78 percent reduction.

Swath width, Figure 27d, is seen to have the least effect on productivity of the four variables investigated. For the case of the 200 acre field, a reduction of 13 acres per hour is seen to exist between swath widths of 20 and 50 feet.

Figure 28 presents the effect of the four variables on productivity in spraying operations. In general a larger effect of the variables on productivity was noted for the spray operation than for granular operations. This larger range of productivity was due to the wider swath width and smaller application rate characteristic of the spraying operation.

Figure 28a shows the effect of rate of application on productivity over a wide range of application rates. The 1 pound per acre curve approximates the ultra low volume case. For a 200 acre field the productivity is seen to increase by 100 acres per hour for the 1 pound per acre rate over the more normal 20 pound per acre rate.

The effect of loading time, Figure 23b, for the spraying operation is seen to be about the same as for the granular operation case from a percentage standpoint. Actual productivity, however, shows a much

larger variation throughout the range of field sizes. Figures 28c and 28d show the same characteristics as Figure 28b. The larger range of productivity due to the effects of swath width and ferry distance for the spray operation as opposed to the granular operation is due mainly to the lower rates of application associated with the spraying operation.

10. GENERAL CONCLUDING REMARKS

The CallAir A-9 is specifically designed for aerial application work and, therefore, is an improvement over the many aircraft that have been modified to perform the aerial application task. The main improvement has been in the structural design and integrity of the vehicle to offer a vehicle which protects the pilot in the event of a crash. The location of the hopper, forward of the cockpit, and of the fuel tanks in the wings, as well as the structural rigidity of the fuselage are obvious results of this attention to crash protection. The placement of the fuel tanks in the wings is an important consideration when it is realized that the latest FAA statistics reveal that chances of surviving a serious aerial application accident are 39 percent better if the aircraft does not burn.

The level flight and climb performance tests indicate that dispersal equipment has an adverse effect on the performance of the aircraft, which reduces the overall safety of operation. It is felt that considerable improvement in the overall performance of the aircraft could be effected by careful attention to the design of the dispersal systems. The drag coefficients of the present systems are so large that improvement in the aerodynamic design of the basic aircraft will not significantly increase the safety or performance of operations. If the drag of future dispersal systems could be reduced to about 20 percent of the present system, improvement in the aerodynamic design of the aircraft would result in notable increases in safety and performance.

The results of the performance tests indicate that the basic drag coefficient of the CallAir A-9 is somewhat higher than one would expect for this type aircraft. It is felt that several modifications could be made to the existing aircraft to improve its performance and safety. The drooped leading edge on the aircraft wing causes unusually high drag at airspeeds above 80 miles per hour. It is felt that a further modification to the leading edge droop or the selection of another airfoil section would greatly improve the performance of the A-9 at higher speeds. In addition, it is felt that a wing root fairing at the junction of the wing and fuselage would also be beneficial.

Distribution tests were conducted to determine the distribution characteristics of the solid materials distributor and the effect of air-speed, altitude of operation and rate of application on these characteristics. The results indicate that the swath pattern is most uniform at rates of application of 175 pounds per acre and that the uniformity decreases as the rate of application is increased. It was further found that the distributor system provided a very uniform swath at 50 pounds per acre and was capable of dispensing material at rates up to 400 pounds per acre. The uniformity of the swath pattern at the higher rate of application is much better than is common for this type of system.

Although aerodynamic stall warning in the empty configuration was considered adequate under most conditions, it was felt that additional stall warning was needed for the loaded configuration and for accelerated maneuvers. Additional stall warning would greatly increase the overall safety of operation since the stall speed varies over a considerable range with variation of load and configuration. The acoustic stall warning device described in FAA-ADS Report No. 51 is one which is unaffected by gross weight, flap configuration, or aircraft attitude.

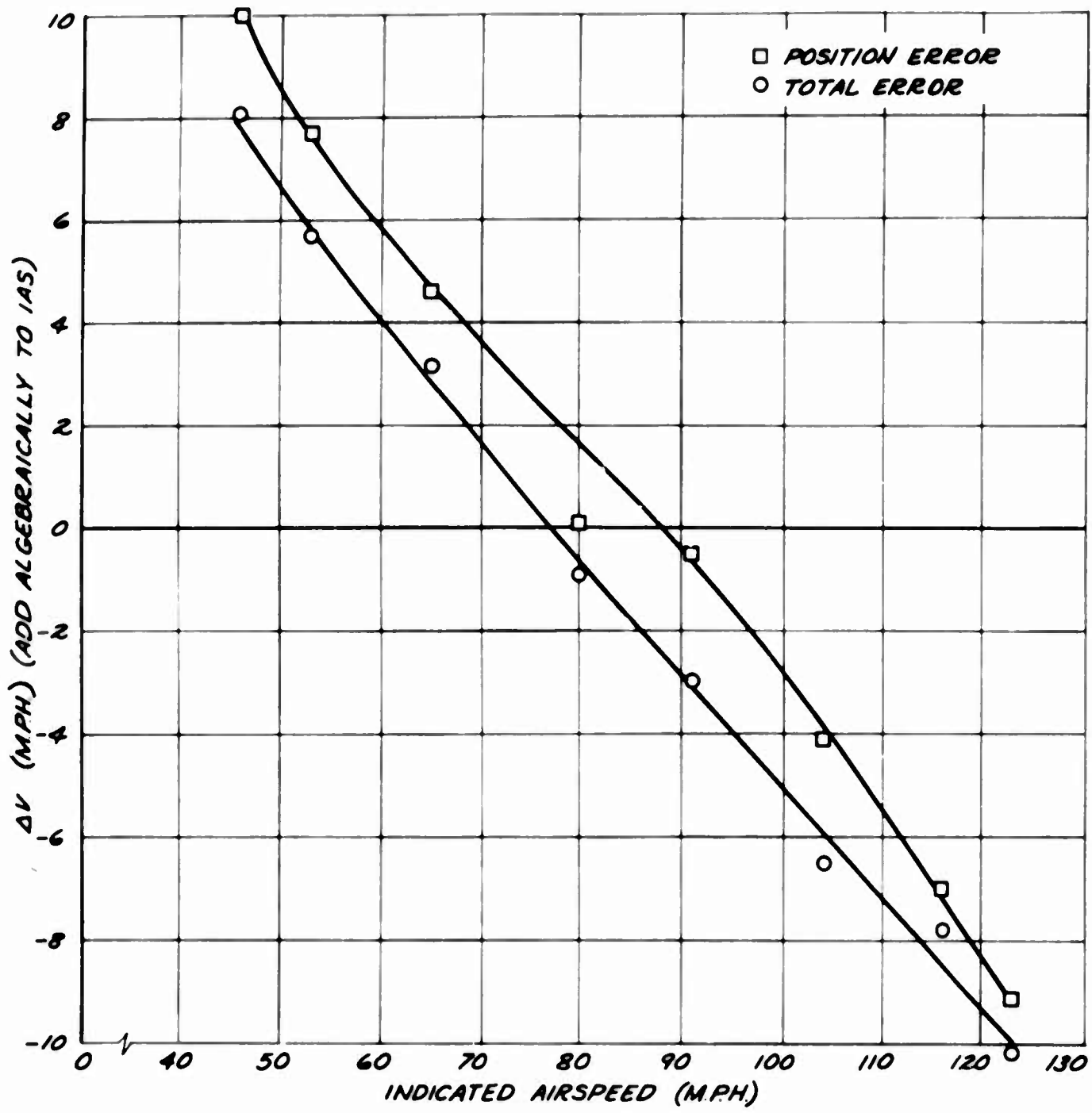


Figure 1. Aircraft Airspeed Correction Chart.

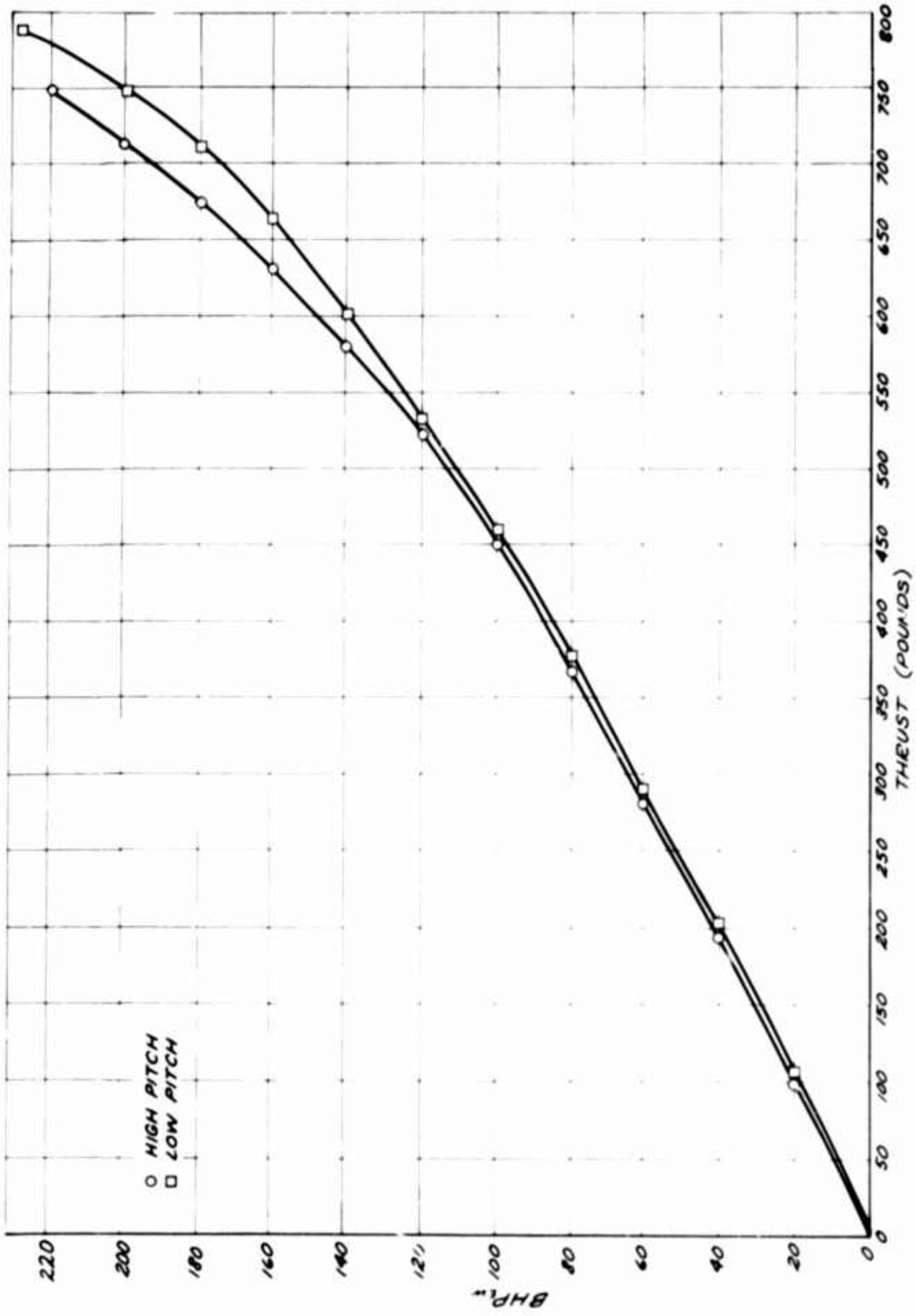
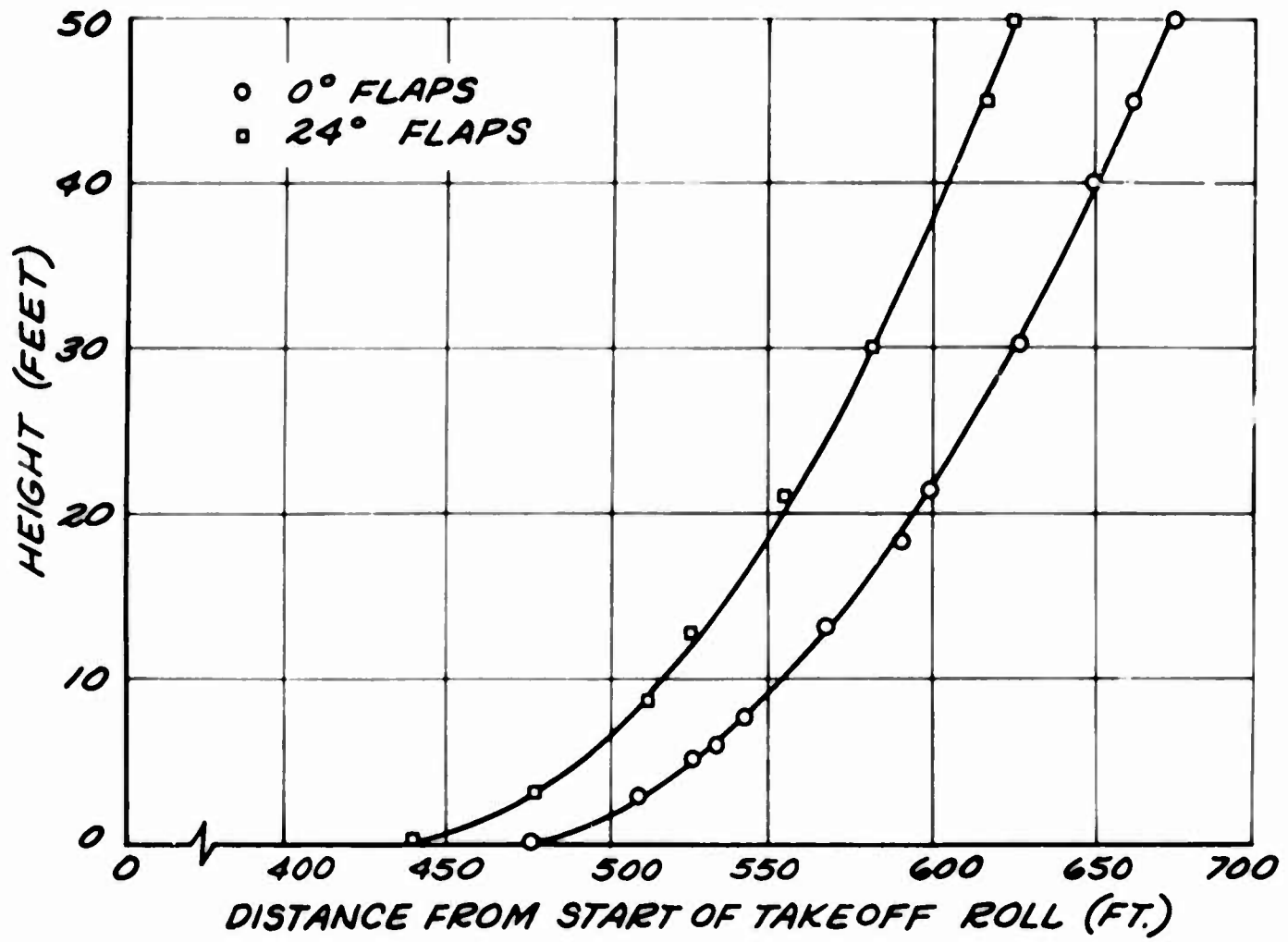
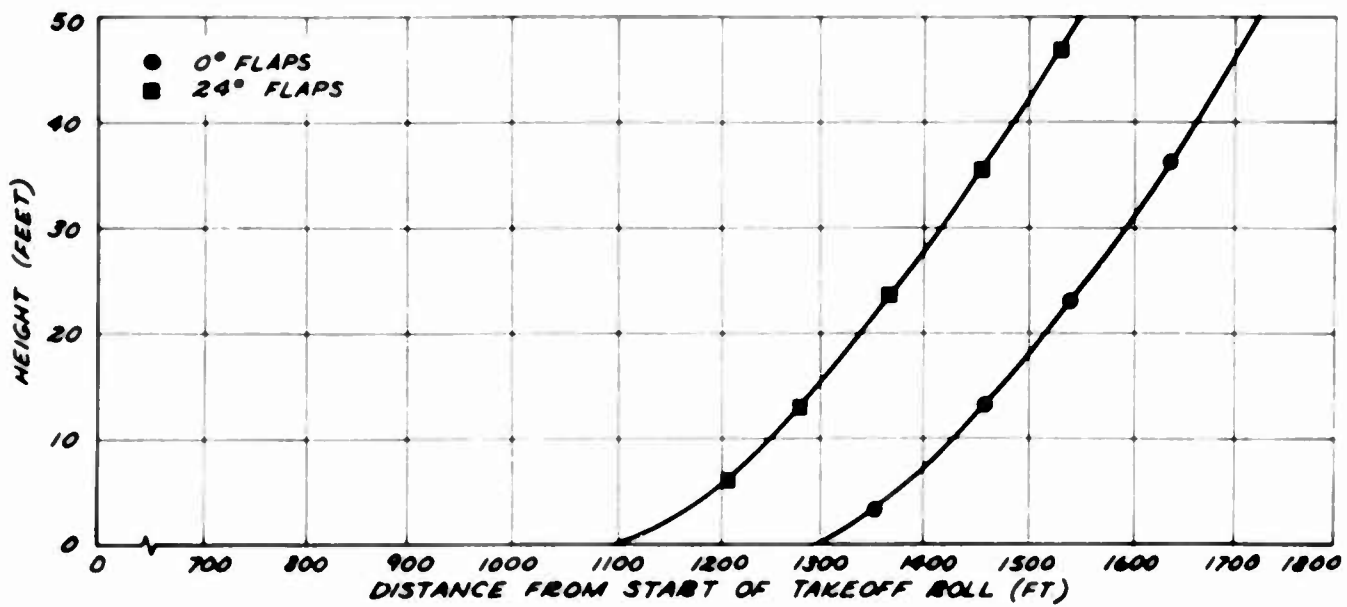


Figure 2. Static Thrust Curves.



(a). $W_s = 2100$ Pounds.



(b). $W_s = 3400$ Pounds.

Figure 3. Takeoff Trajectories - Clean Configuration.

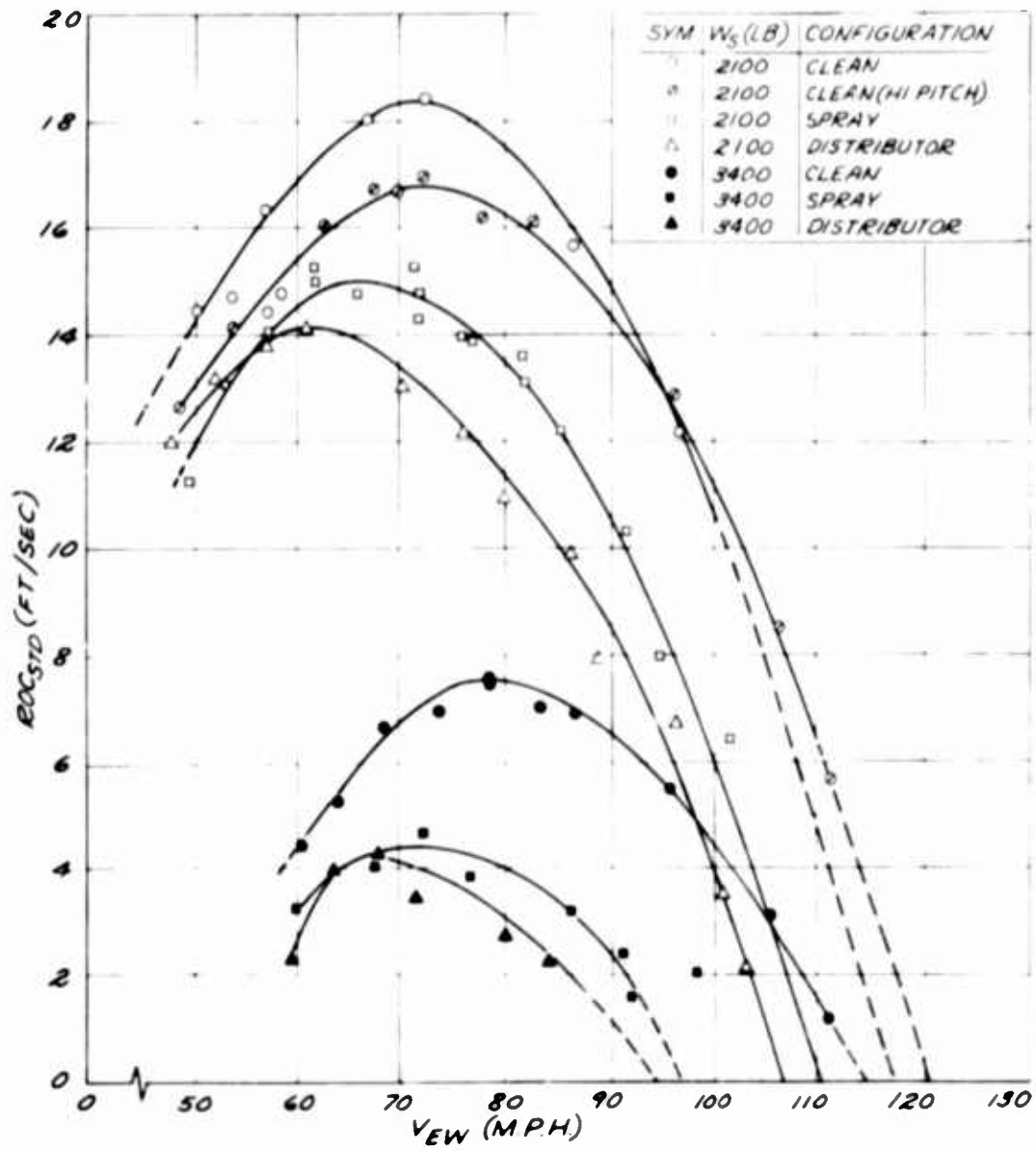


Figure 4. Climb Performance Curves.

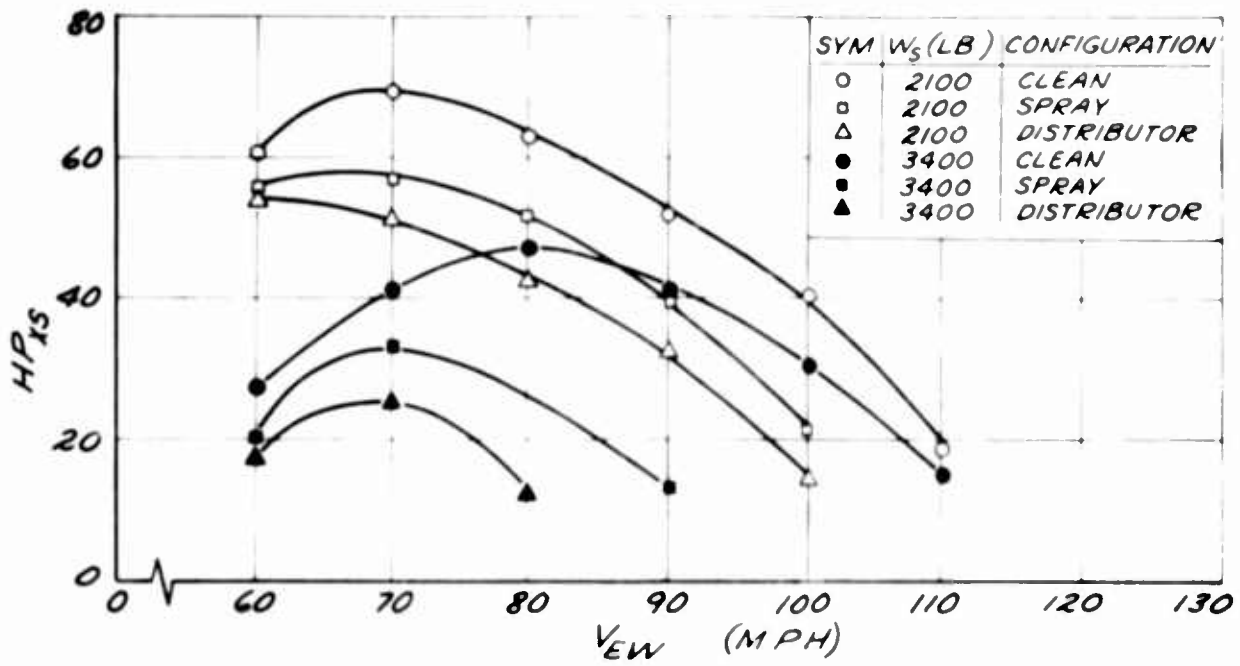


Figure 5. Excess Horsepower Available for Climb.

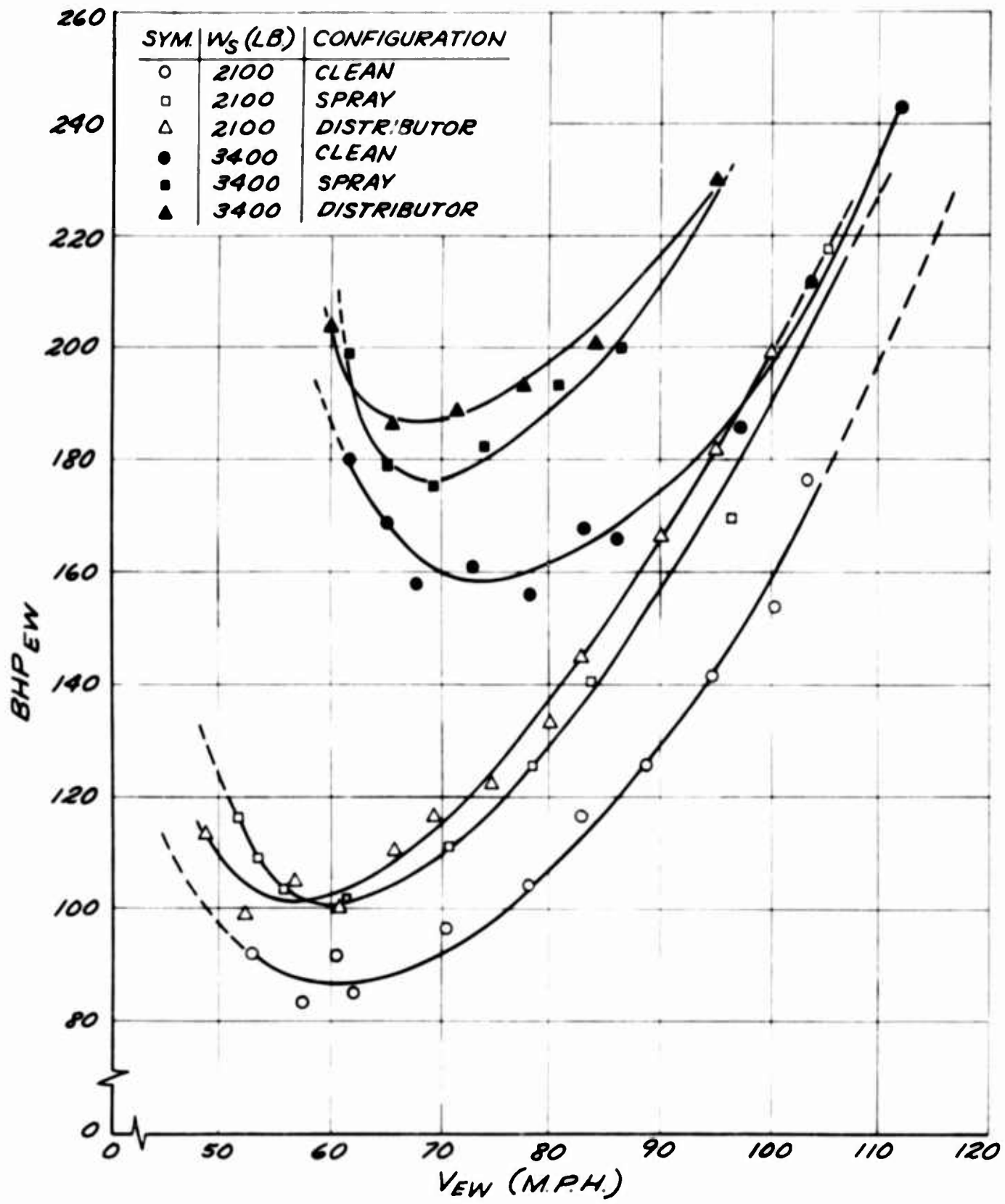


Figure 6. Level Flight Performance Curves.

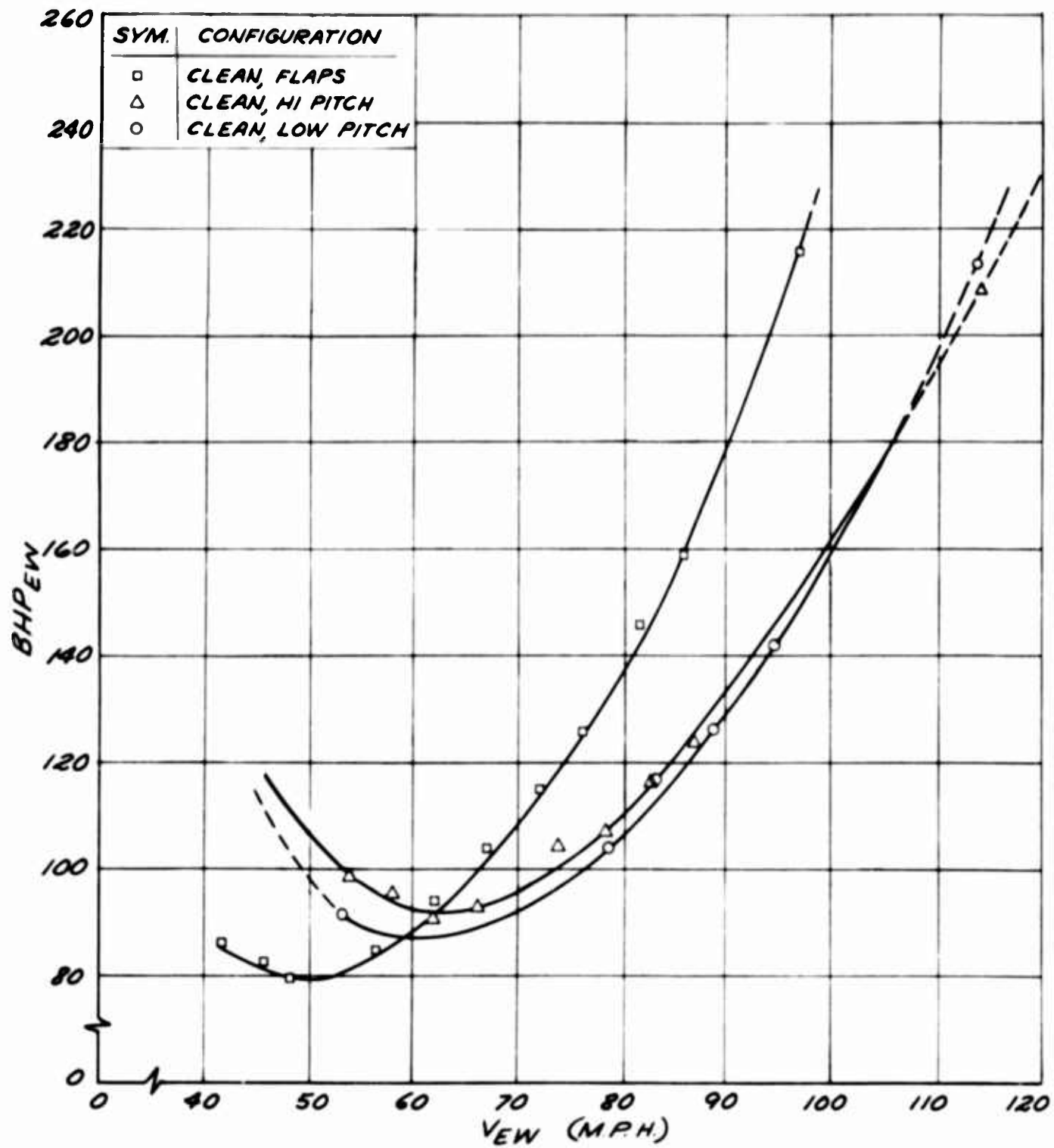


Figure 7. Effect of Flaps and Propeller Pitch on Power Required - $W_s = 2100$ Pounds.

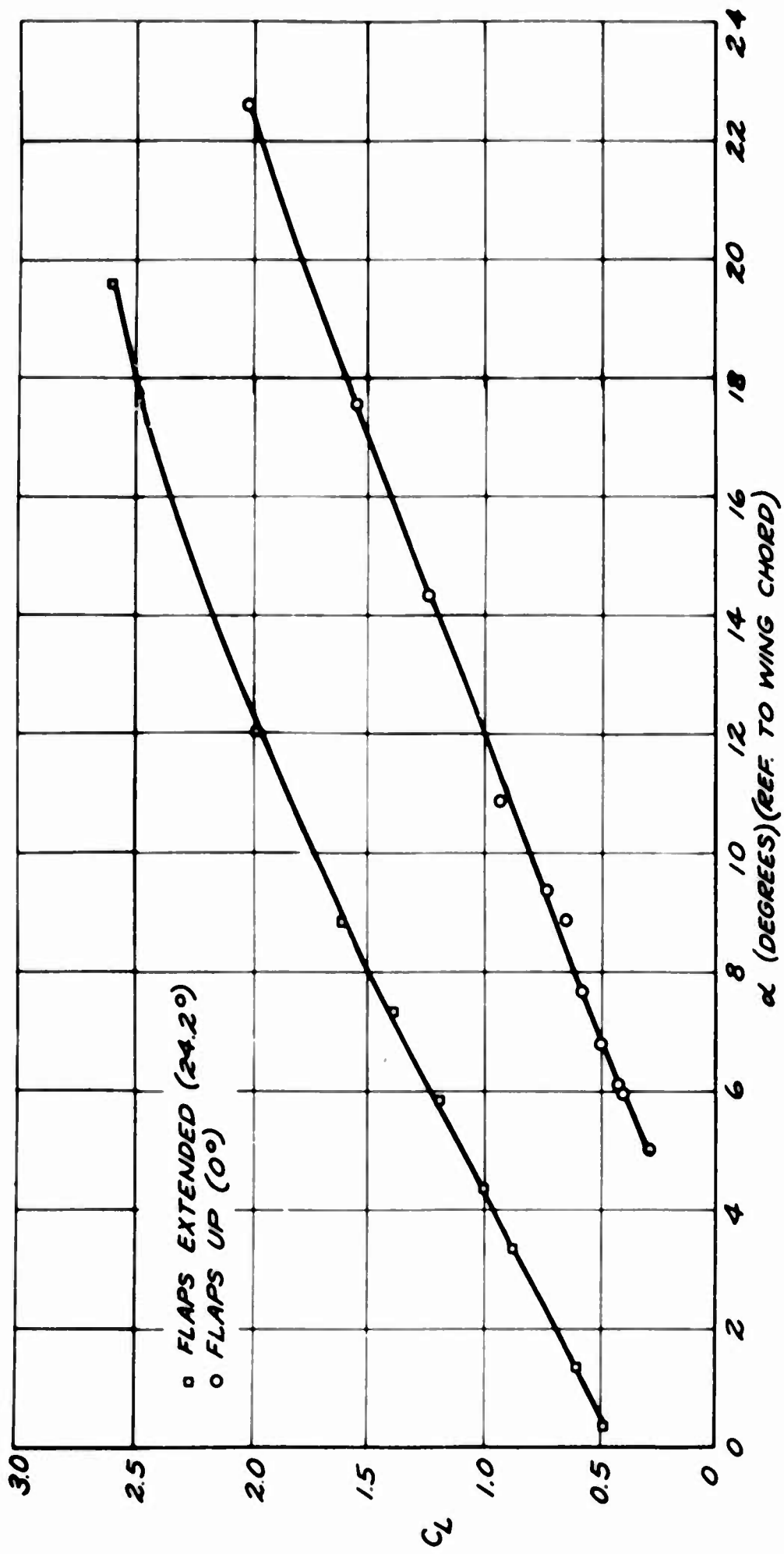
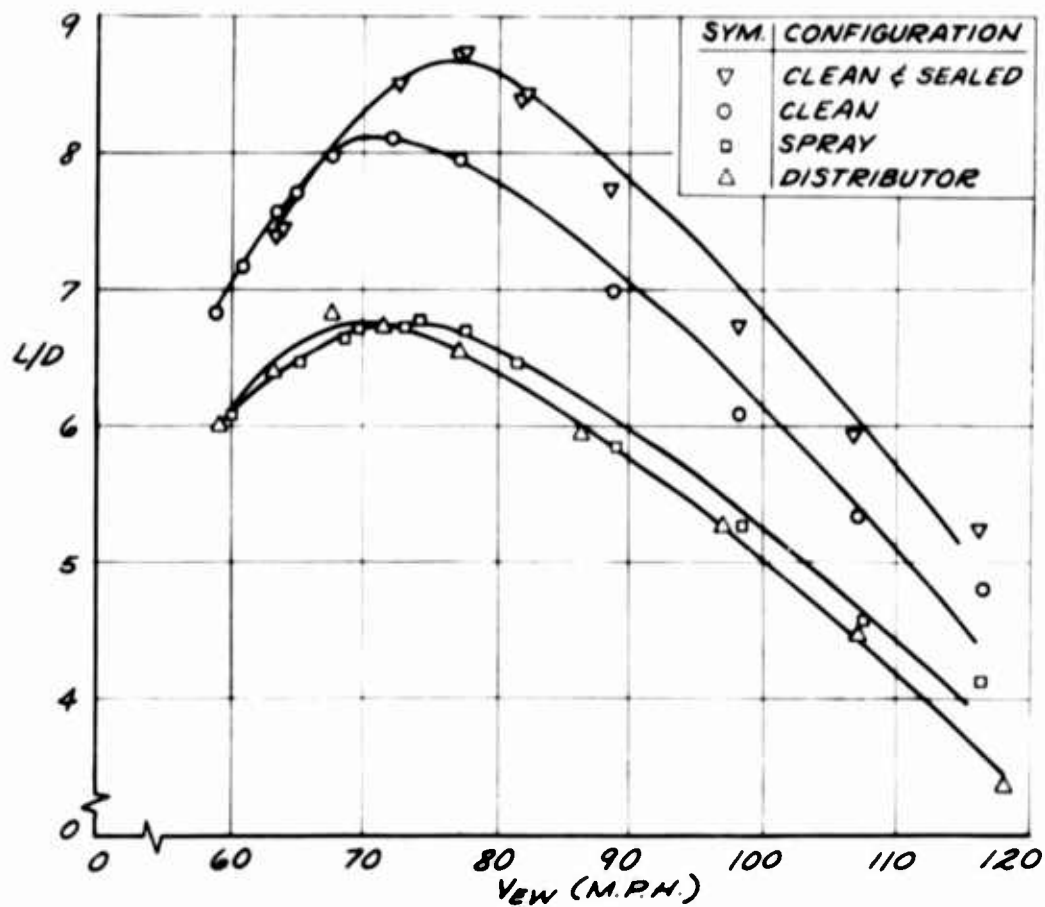
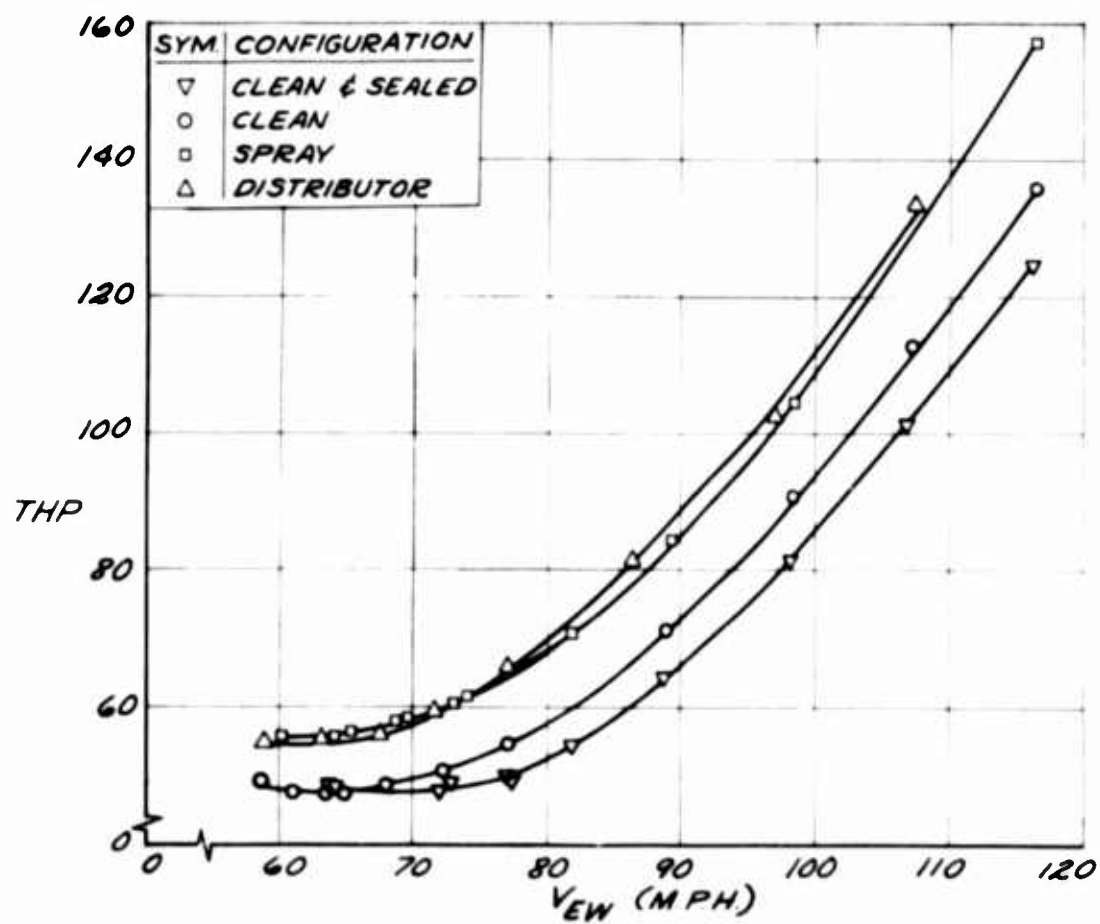


Figure 8. Effect of Flaps on Lift-Slope Curves - $W_s = 2100$ Pounds.



(a). Lift-Drag Polars for CallAir A-9 in Gliding Flight.



(b). Thrust Horsepower Required in Gliding Flight.

Figure 9. Glide Test Data.

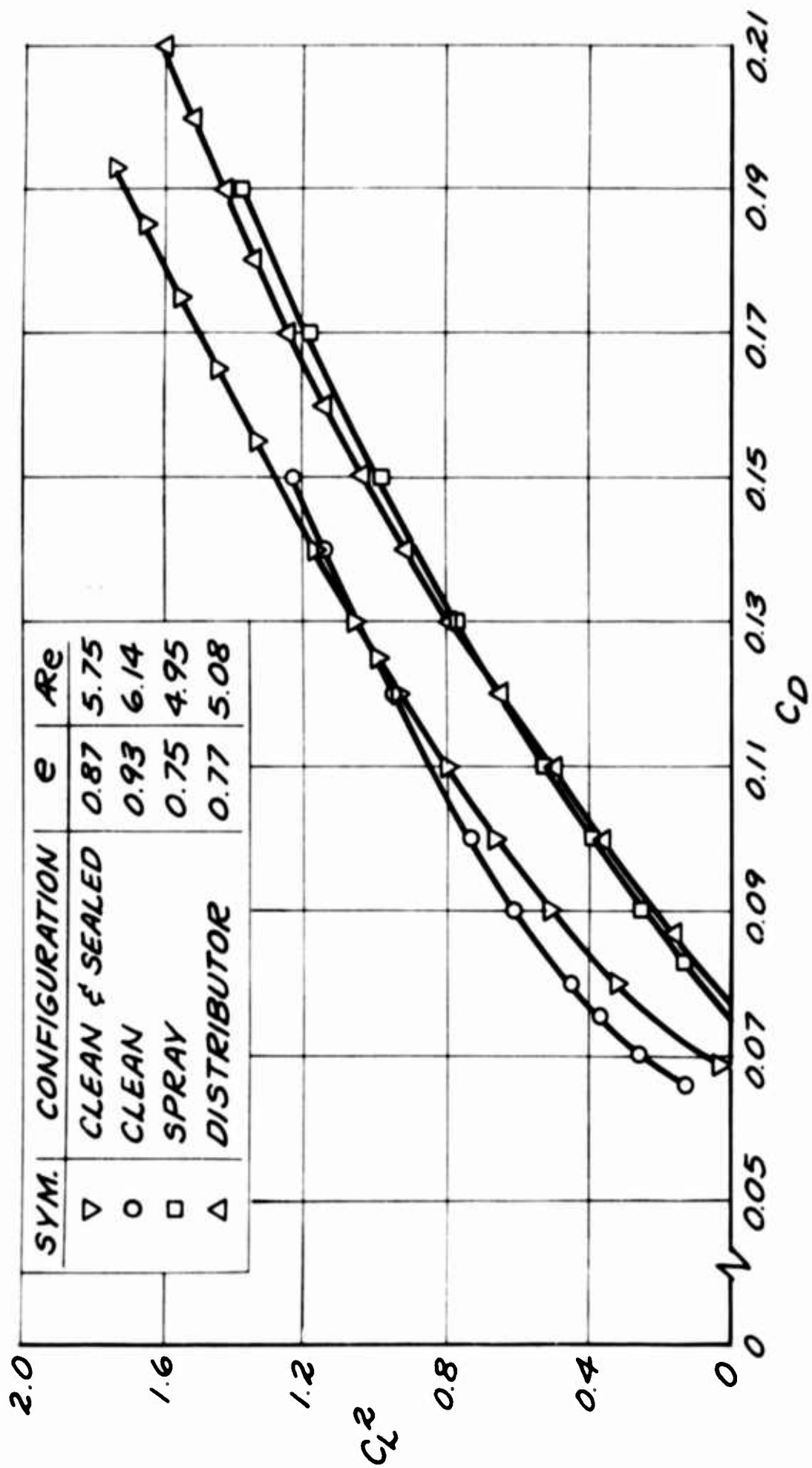


Figure 10. Linearized Drag Polars for CallAir A-9 in Gliding Flight.

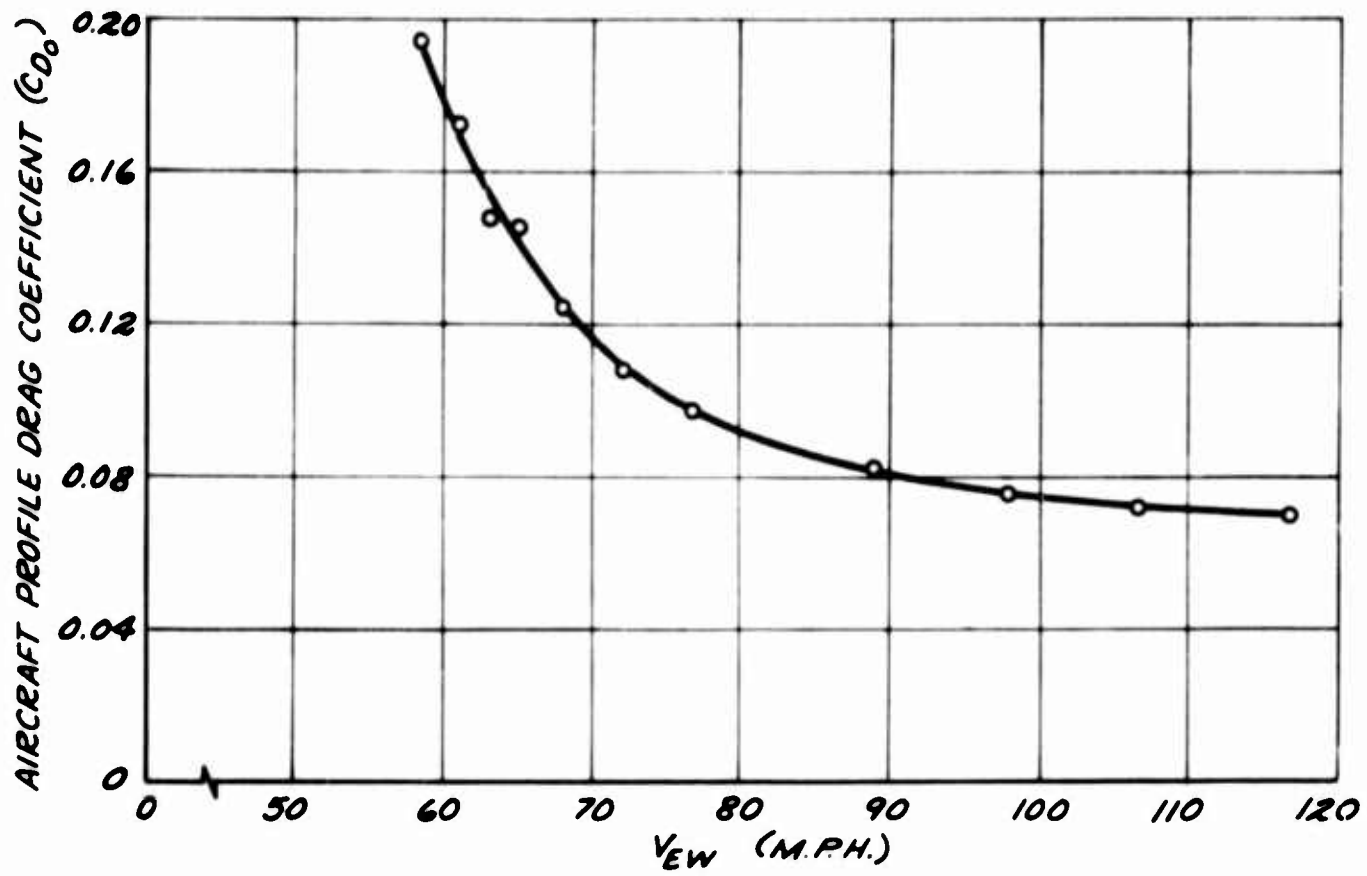


Figure 11. Aircraft Profile Drag Coefficient in Gliding Flight.

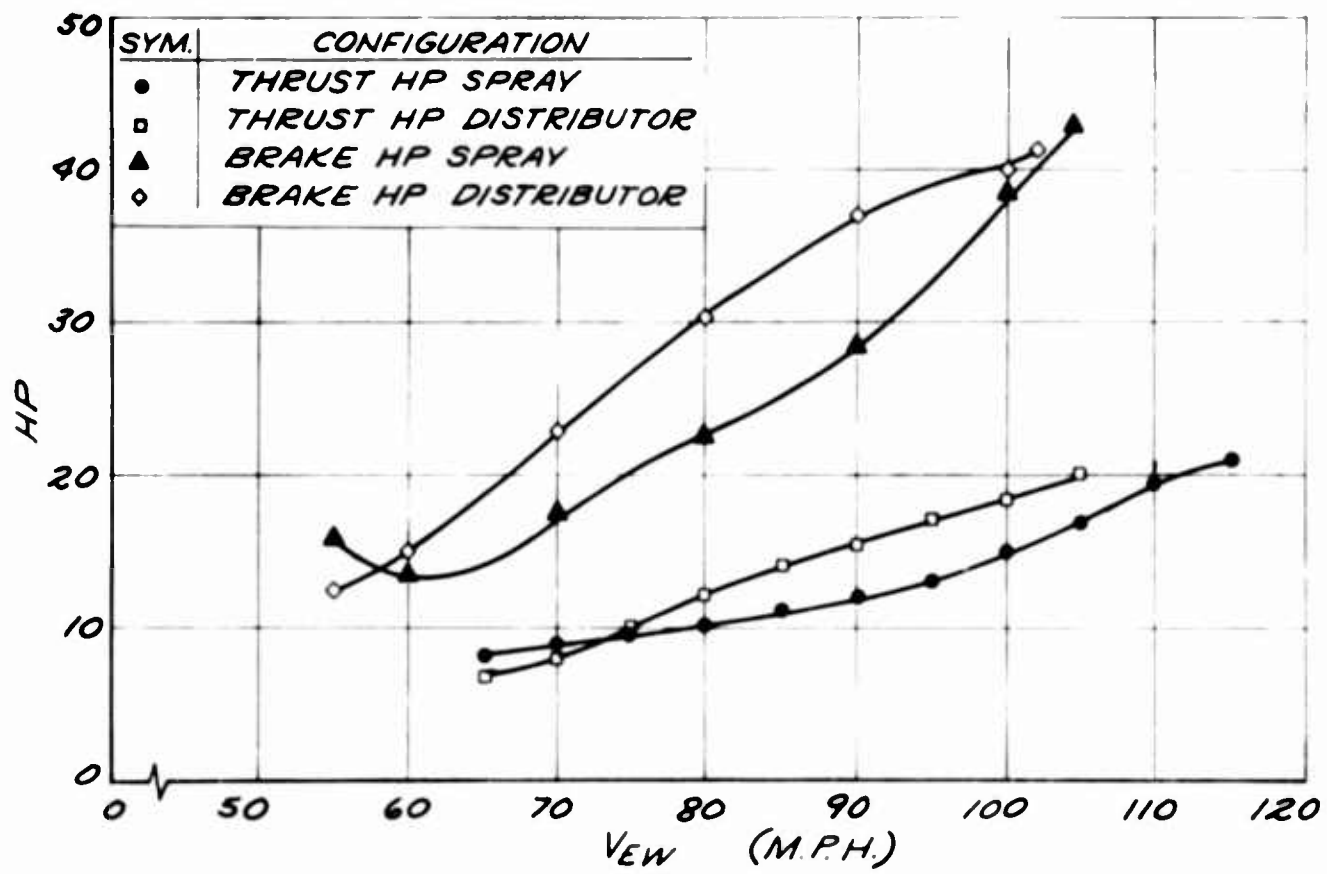


Figure 12. Power Requirements of Dispersal Systems.

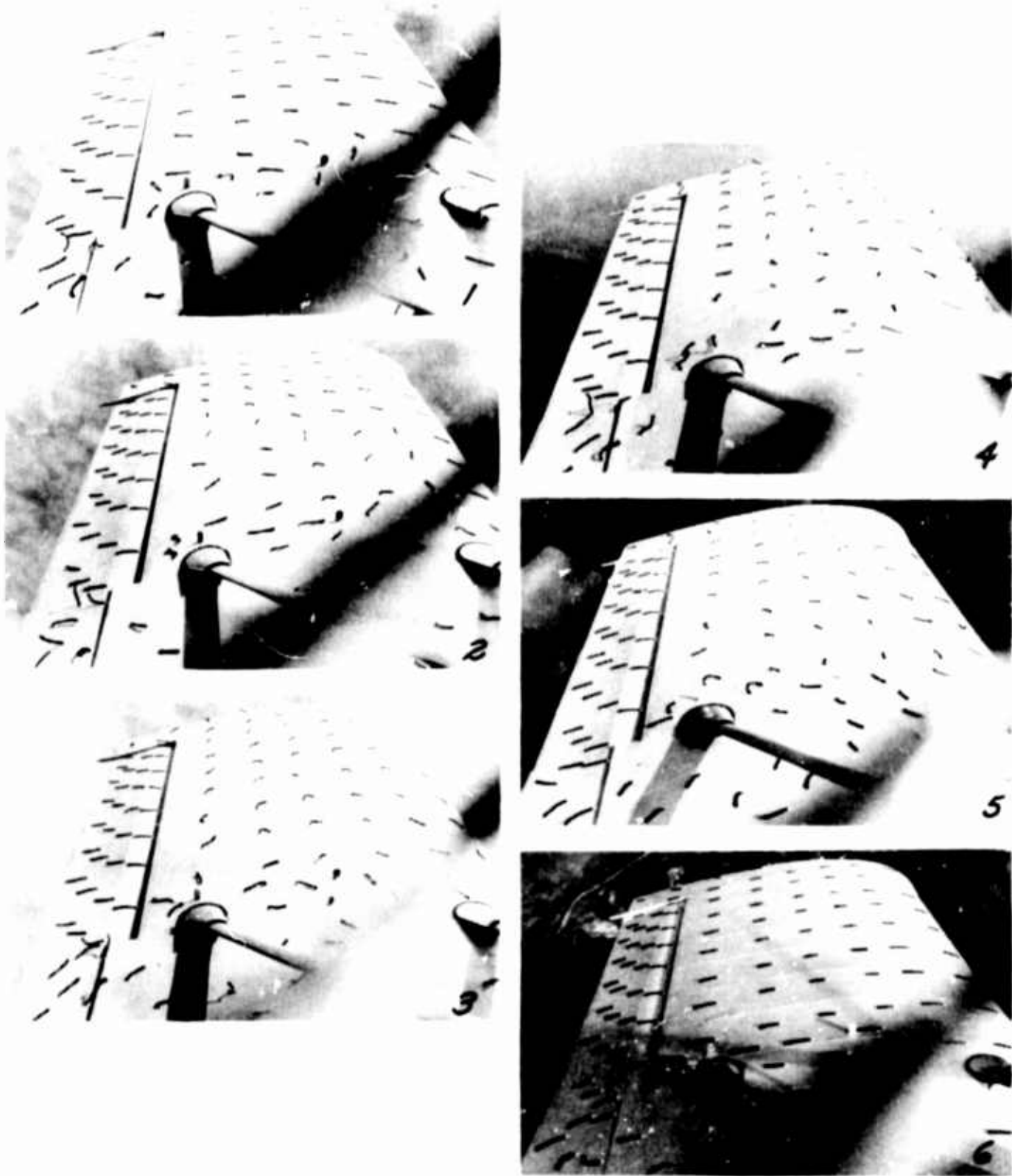
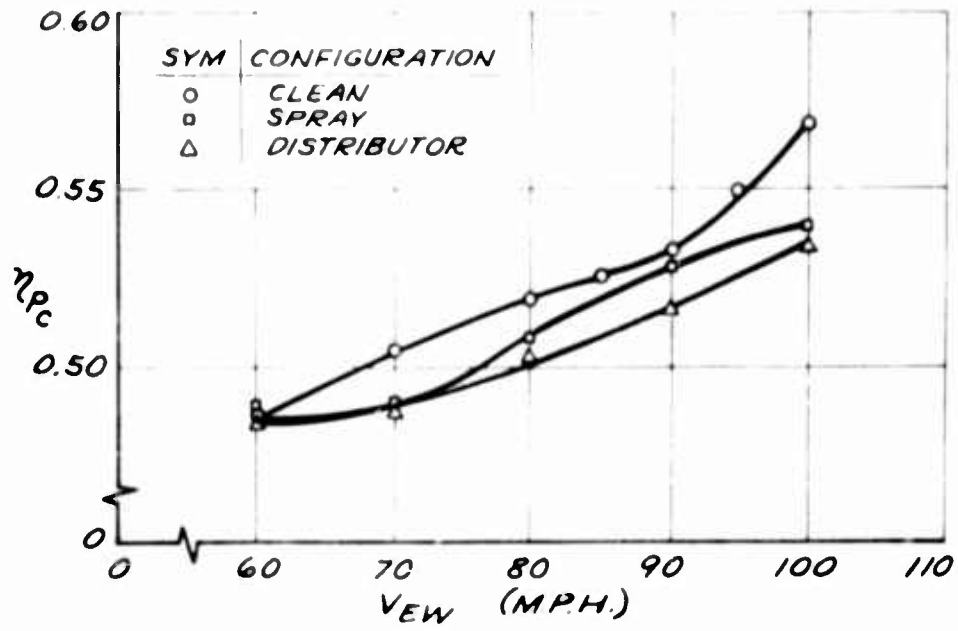
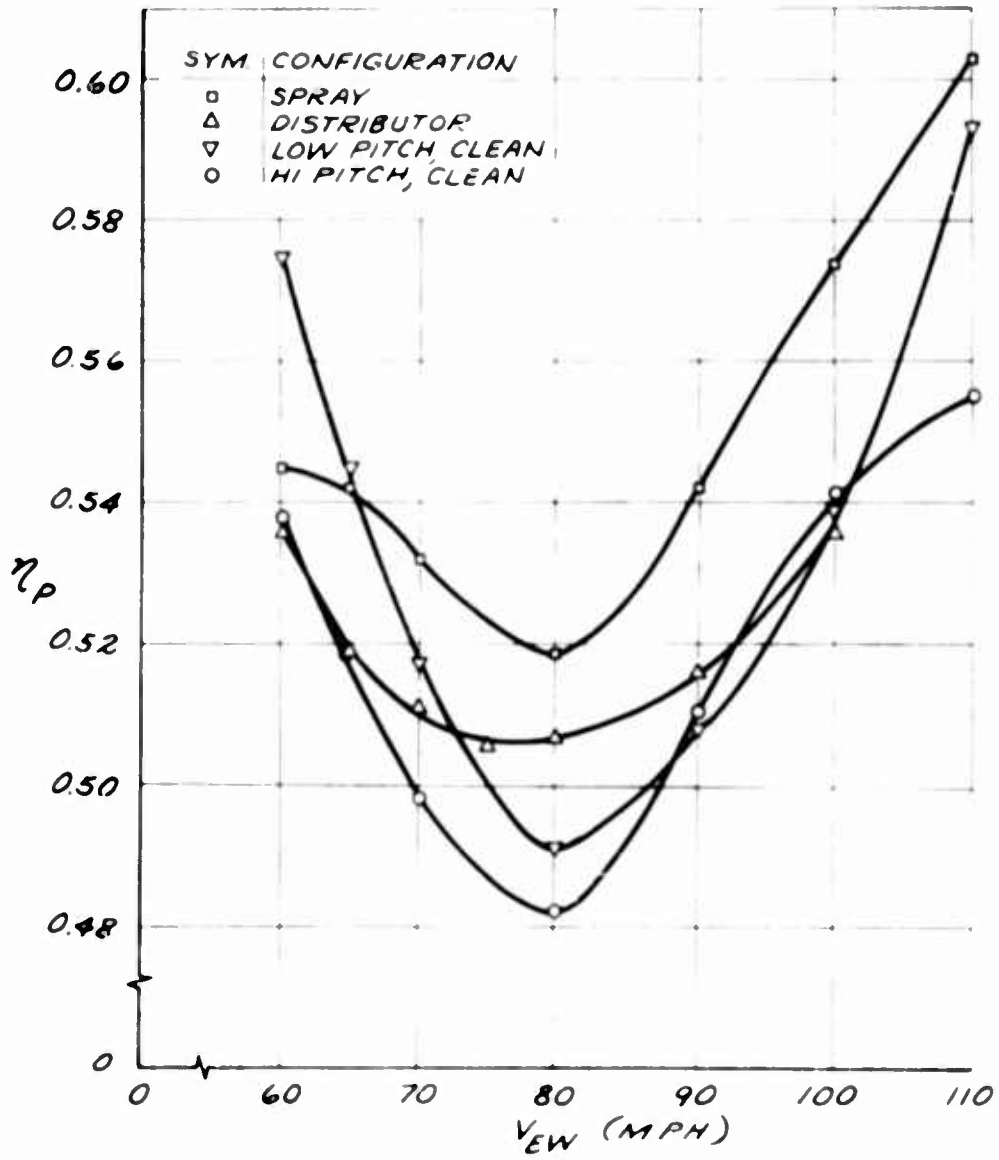


Figure 13. Wing Stall Pattern in a Right Climbing Turn.



(a). Climb.



(b). Level Flight.

Figure 14. Propulsive Efficiency.

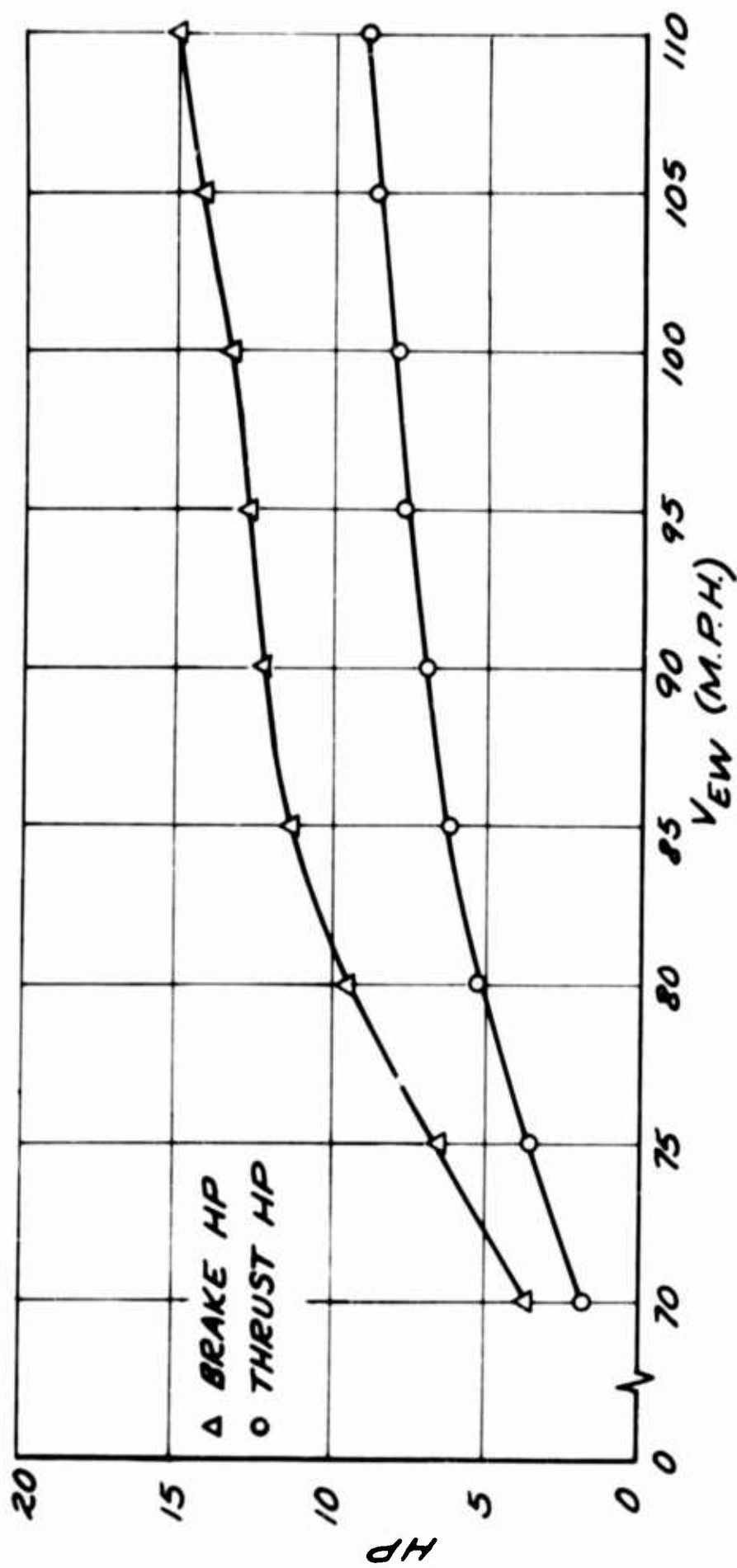
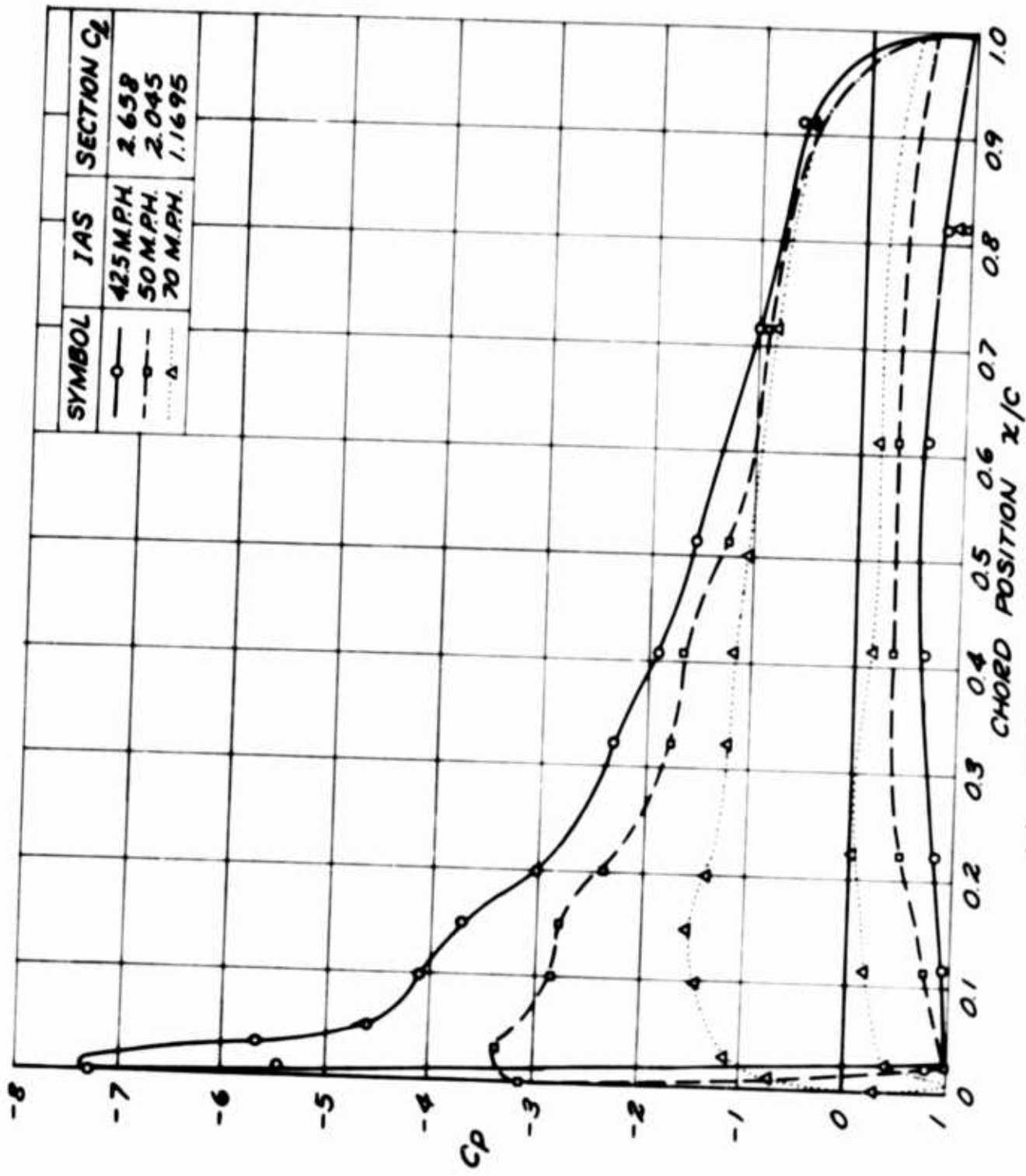
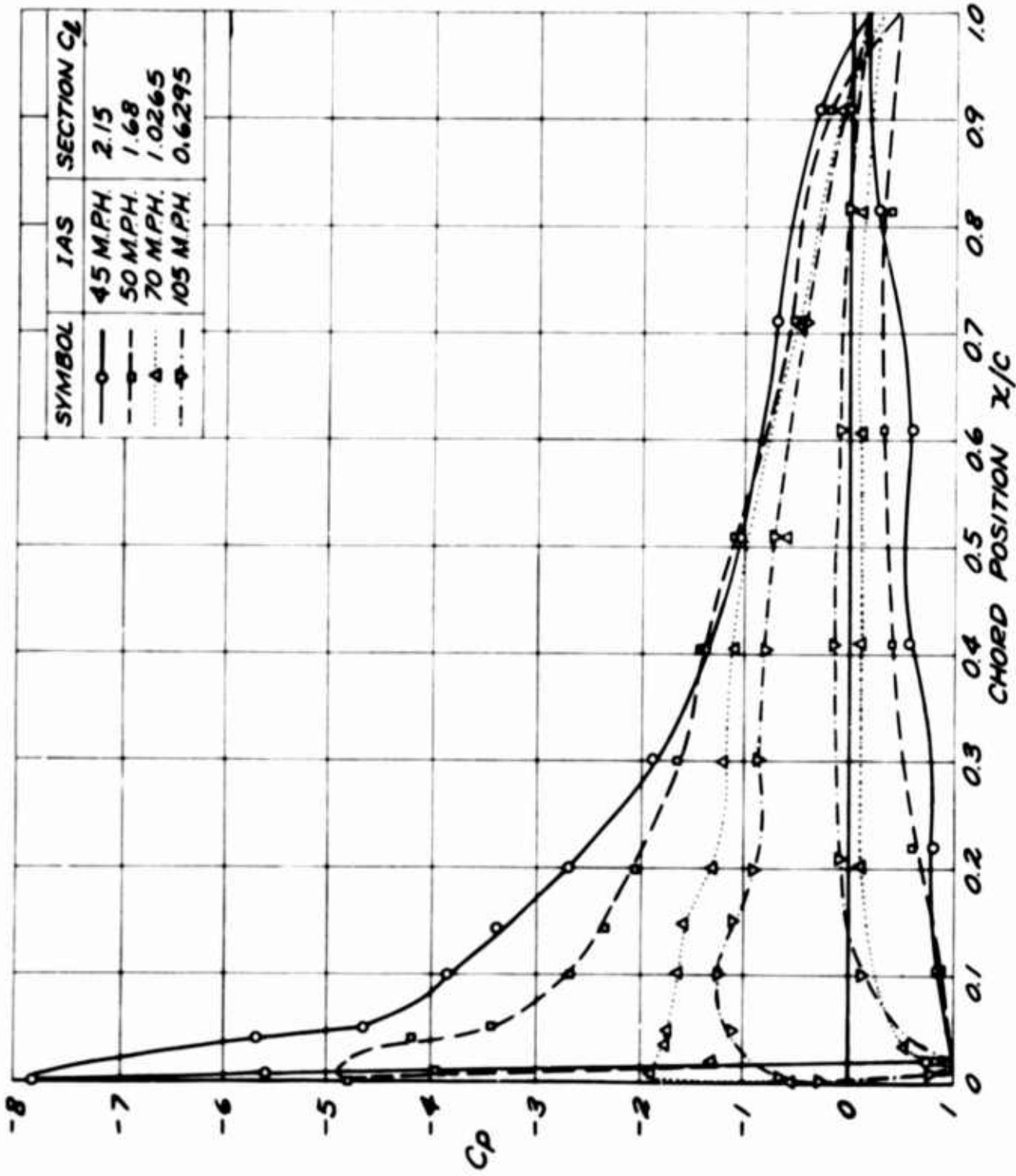


Figure 15. Power Required for Engine Cooling.

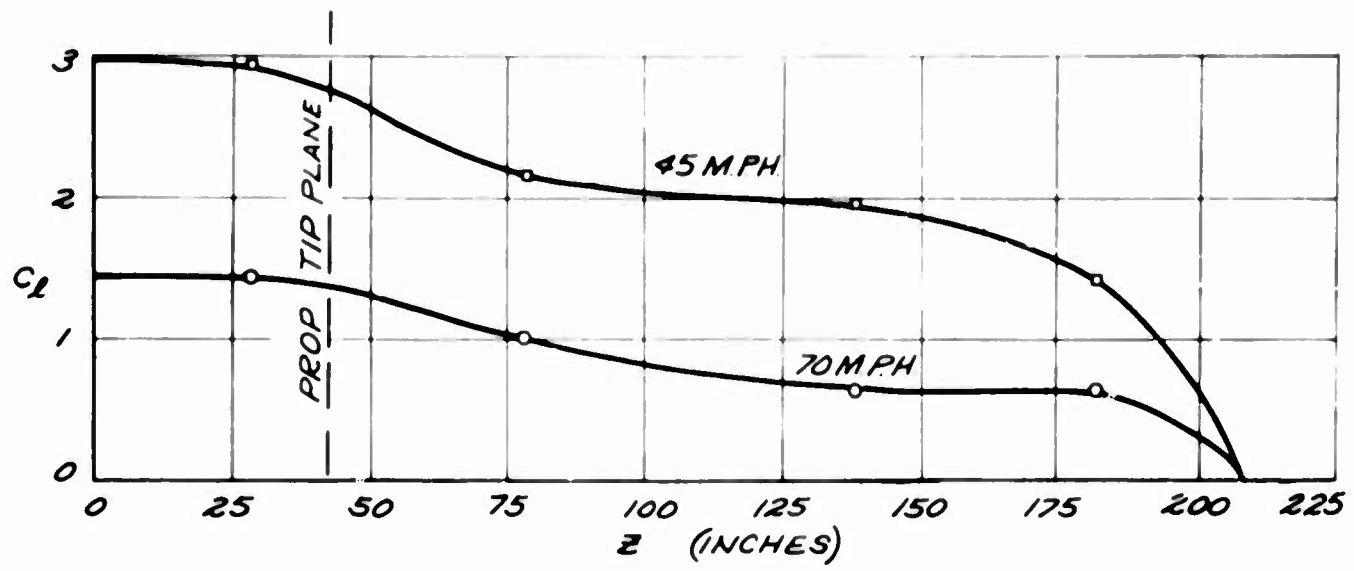


(a). 24° Flaps, $W_s = 2100$ Pounds.
 Figure 16. Wing Pressure Distributions.

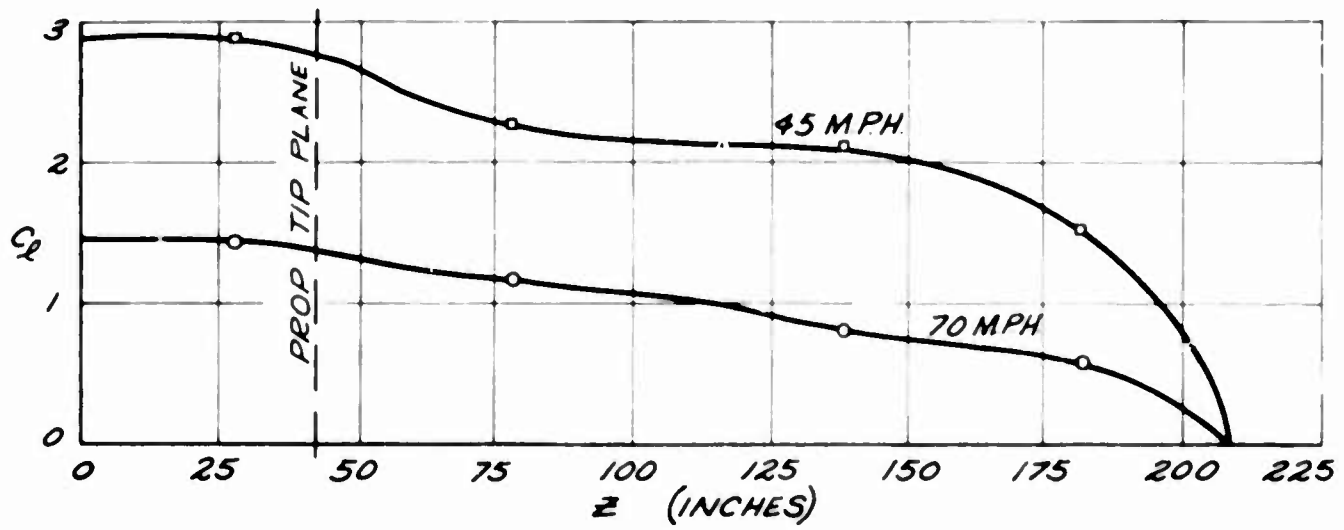


(b). 0° Flaps, $W_s = 2100$ Pounds.

Figure 16 (Cont.). Wing Pressure Distributions.



(a). 24° Flaps, $W_S = 2100$ Pounds.



(b). 0° Flaps, $W_S = 2100$ Pounds.

Figure 17. Spanwise Lift Distributions.

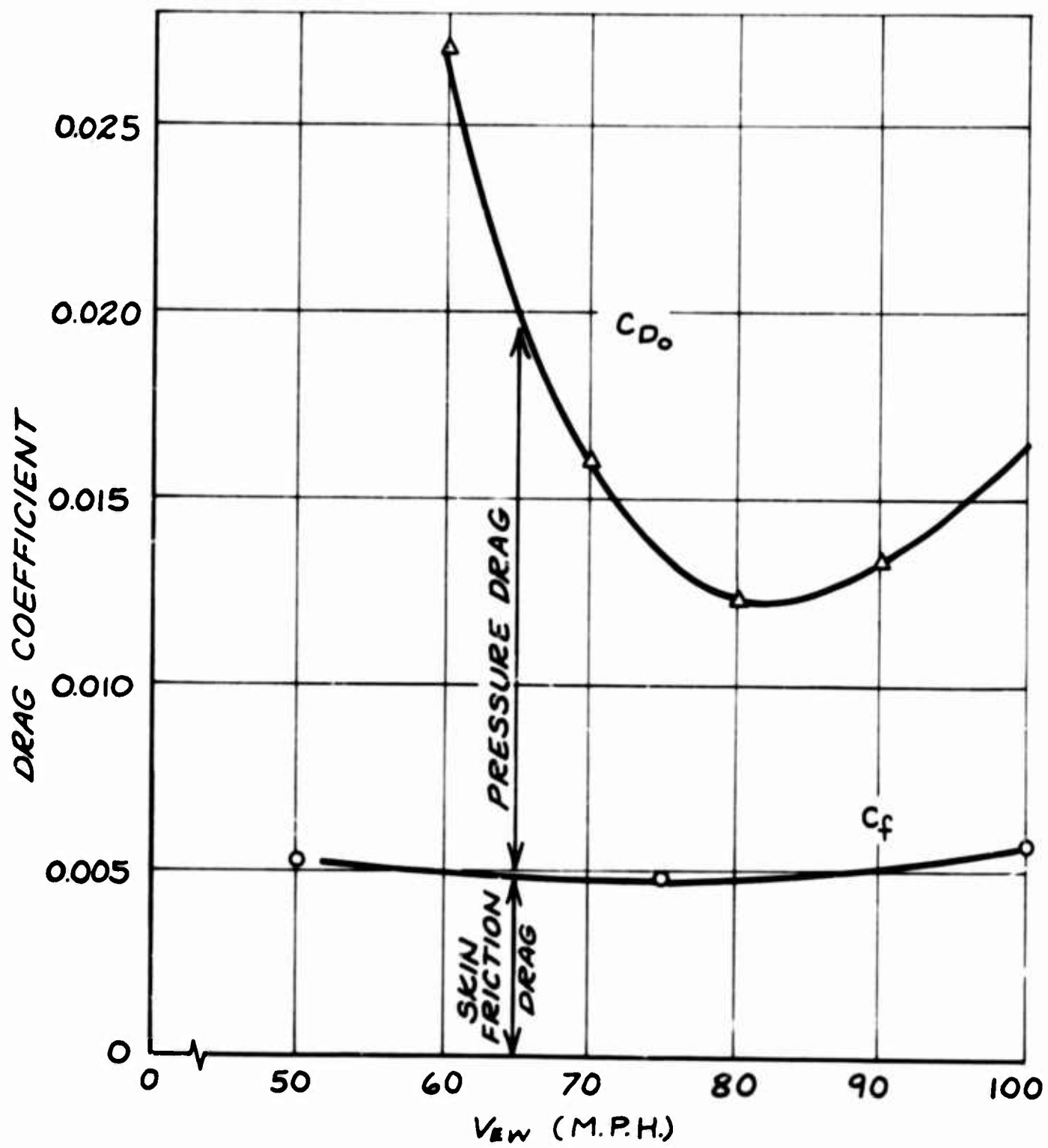


Figure 18. Analysis of Wing Drag.

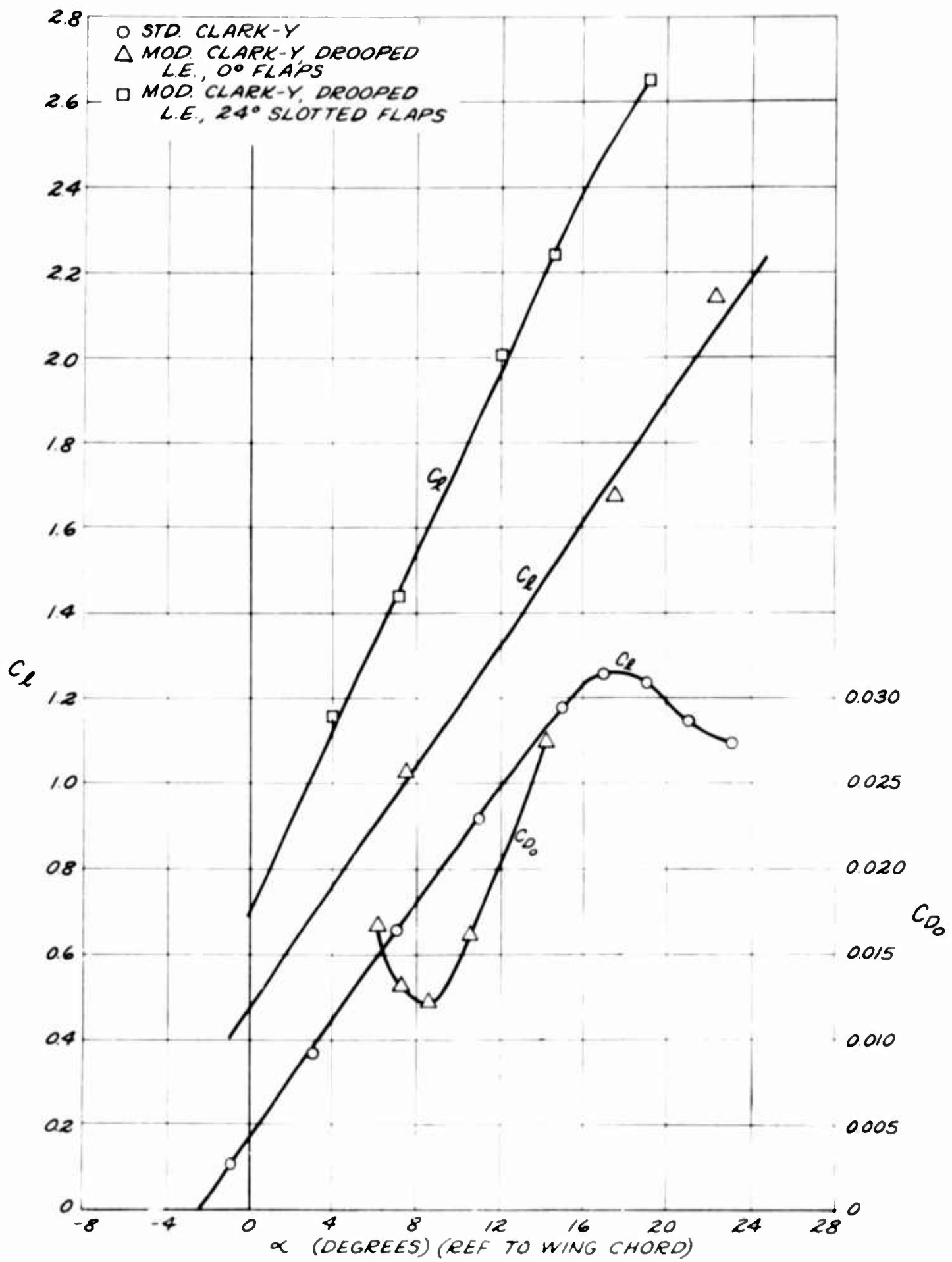


Figure 19. Aerodynamic Wing Data.

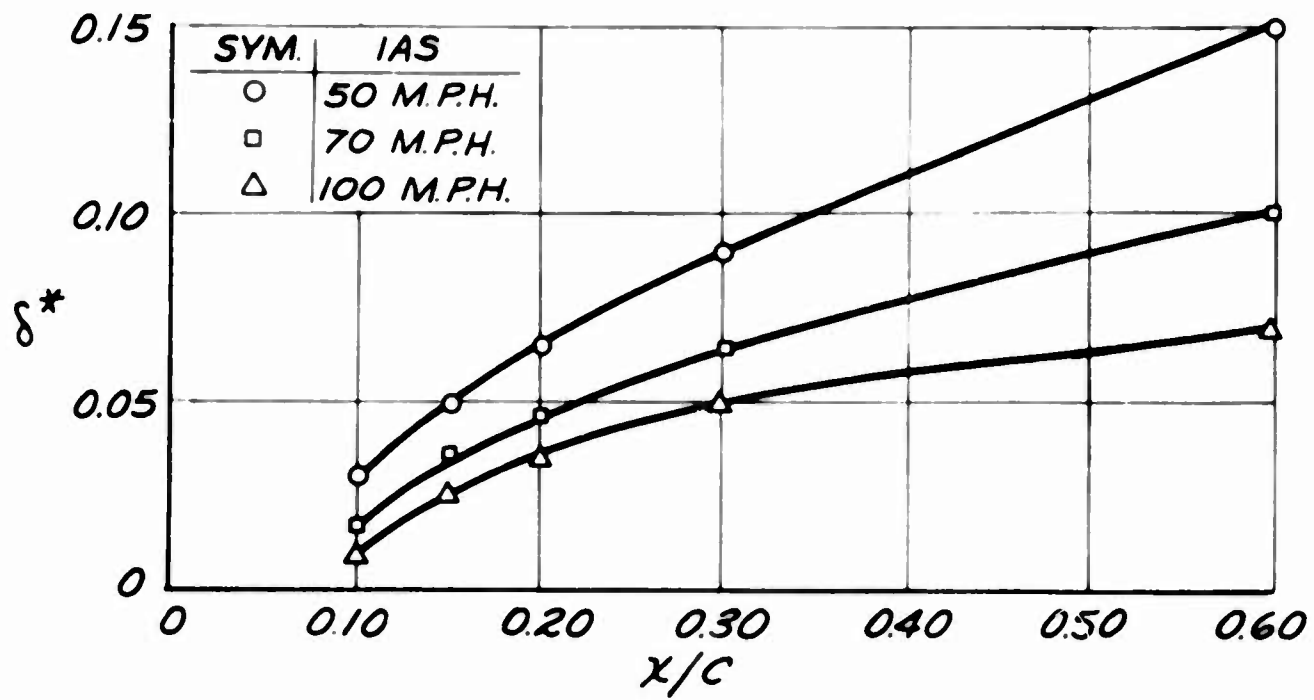
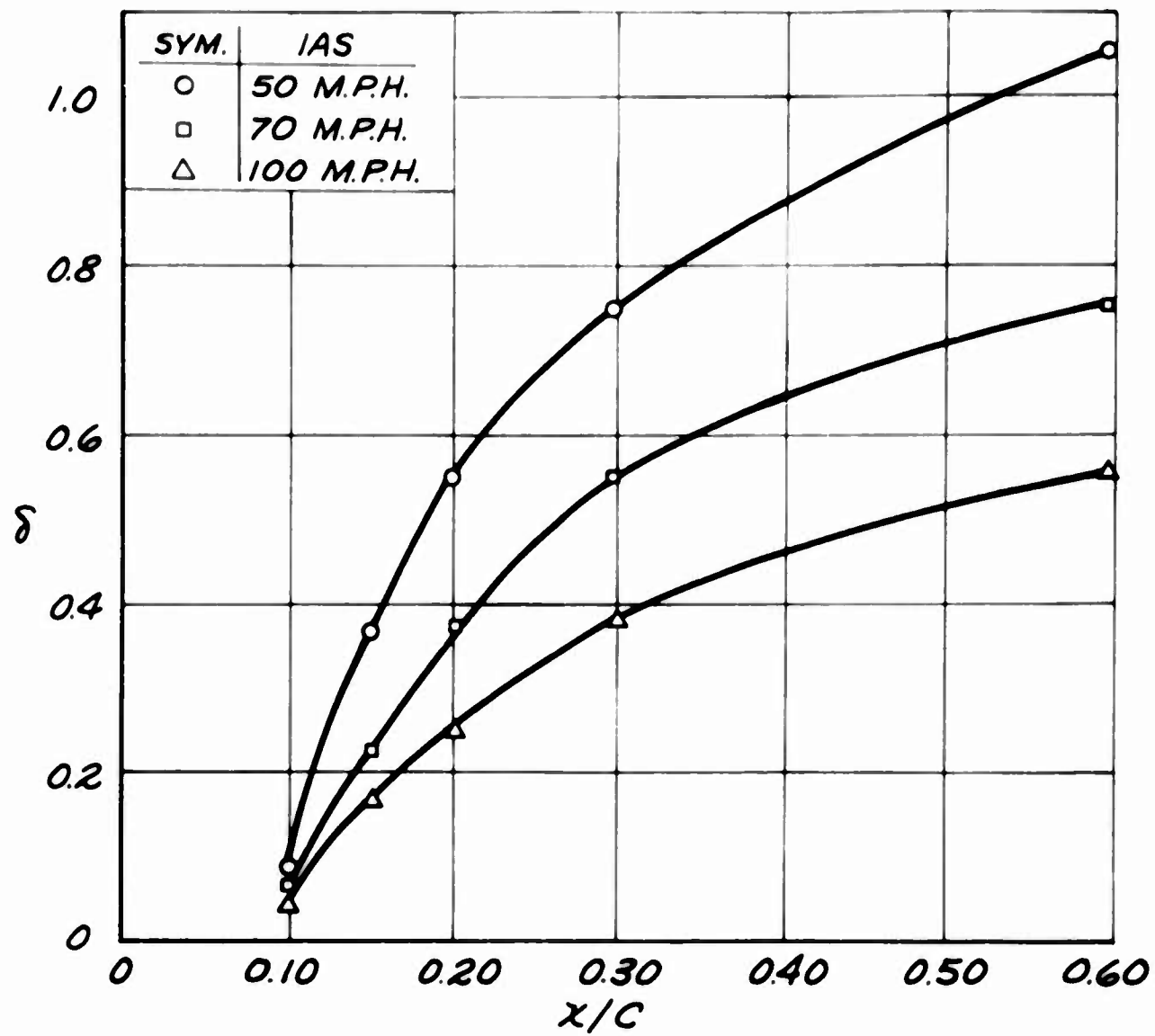


Figure 20a. Boundary Layer Parameters.

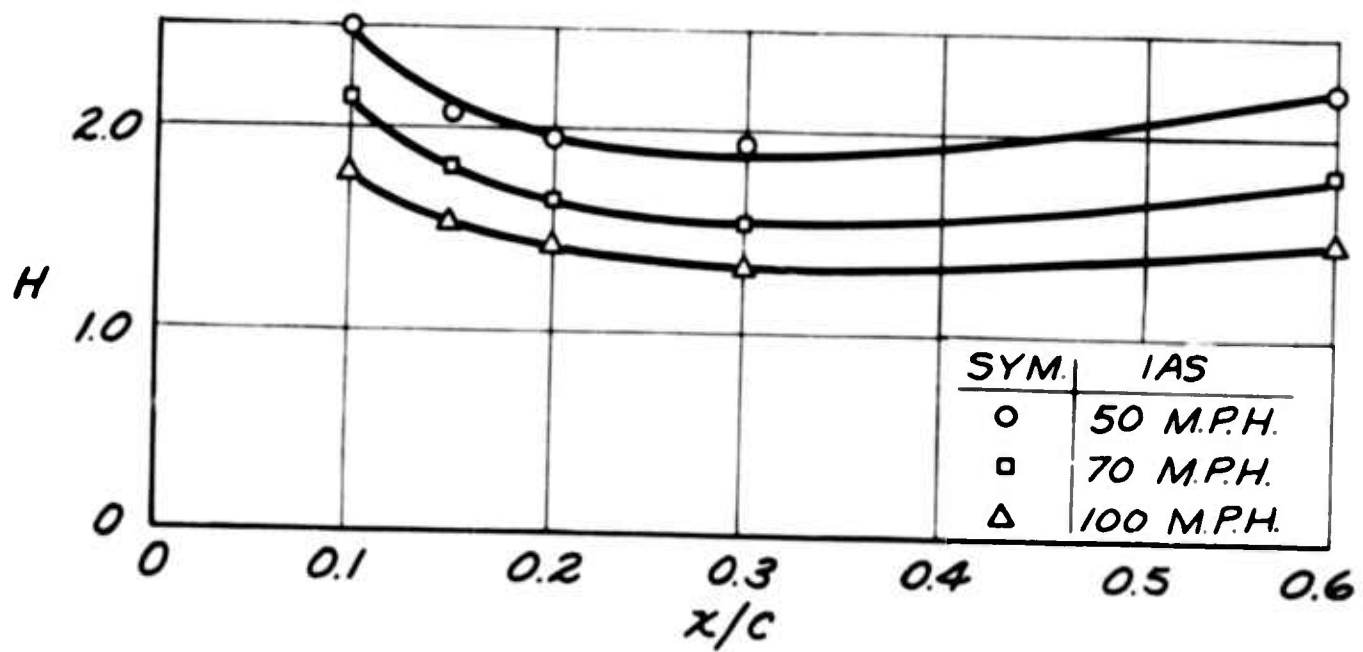
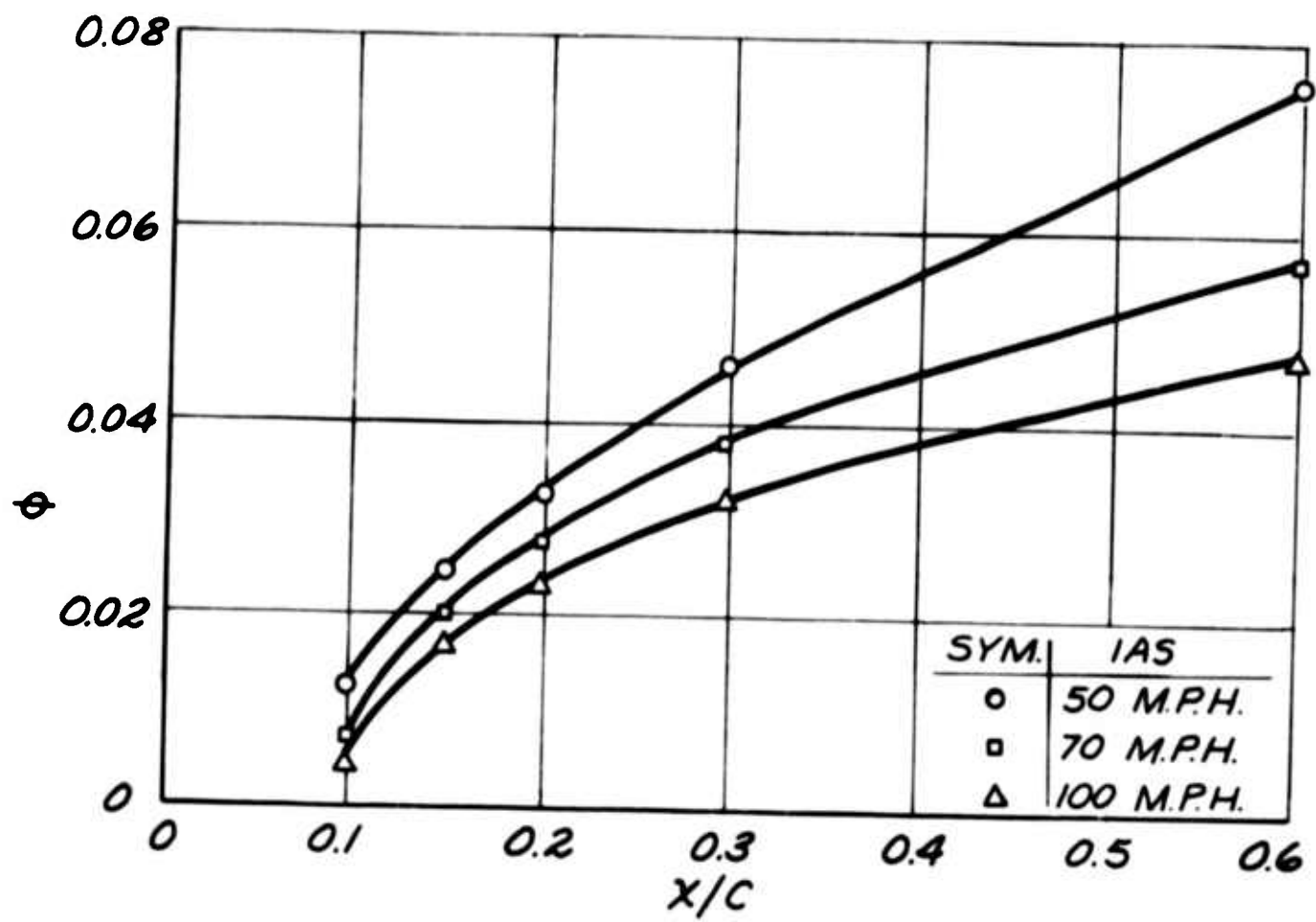


Figure 20b. Boundary Layer Parameters.

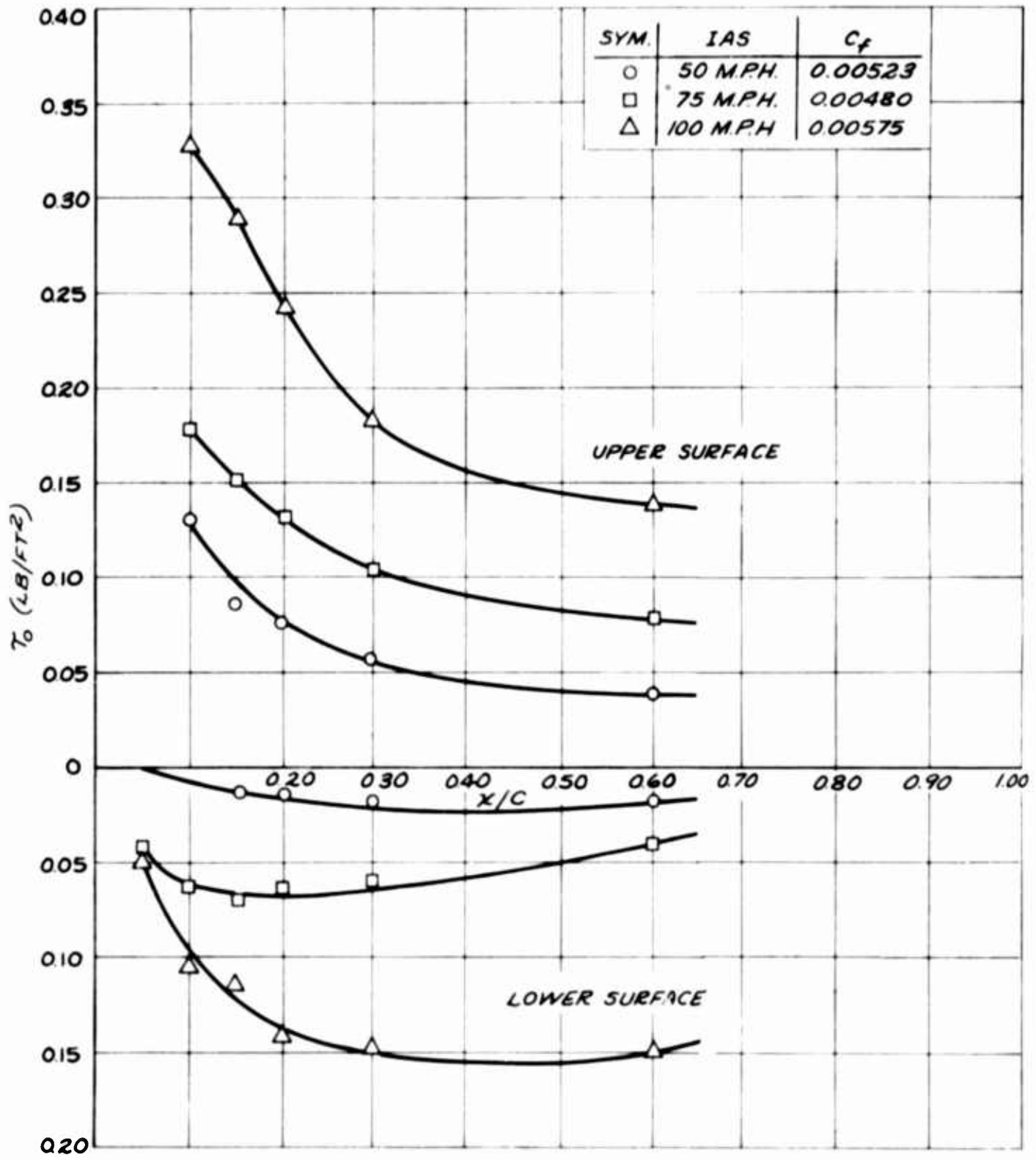
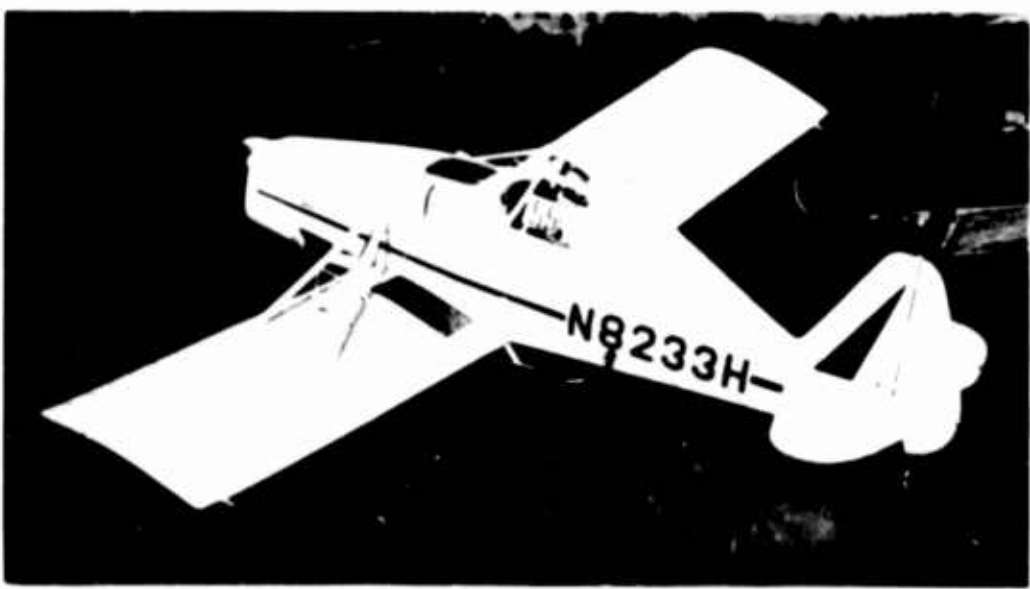
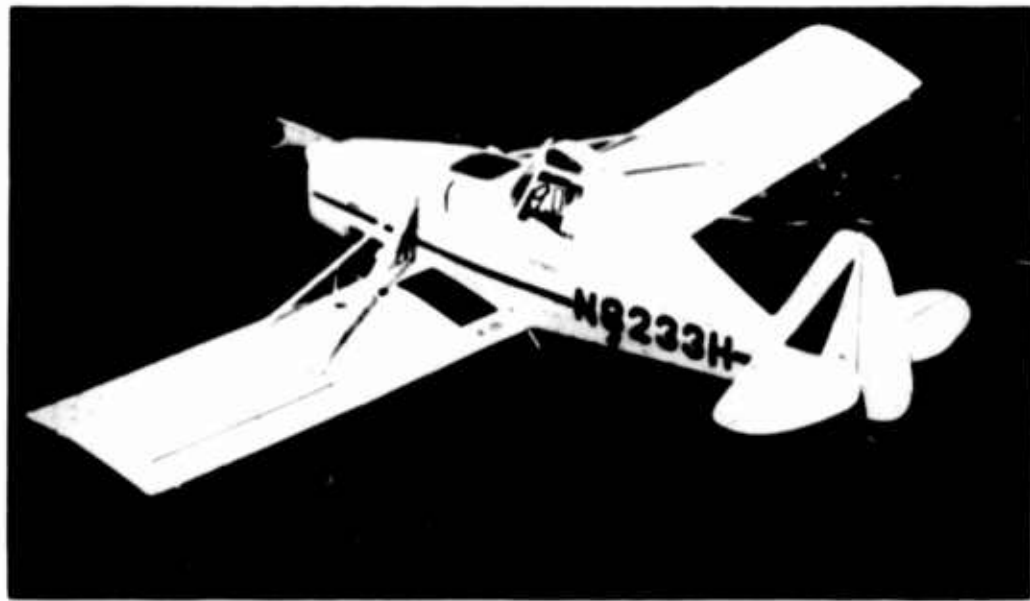
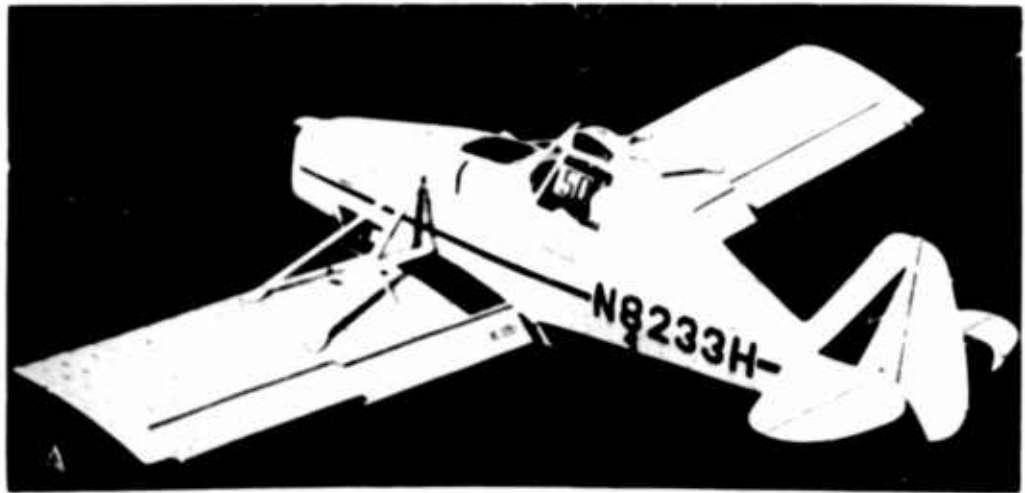
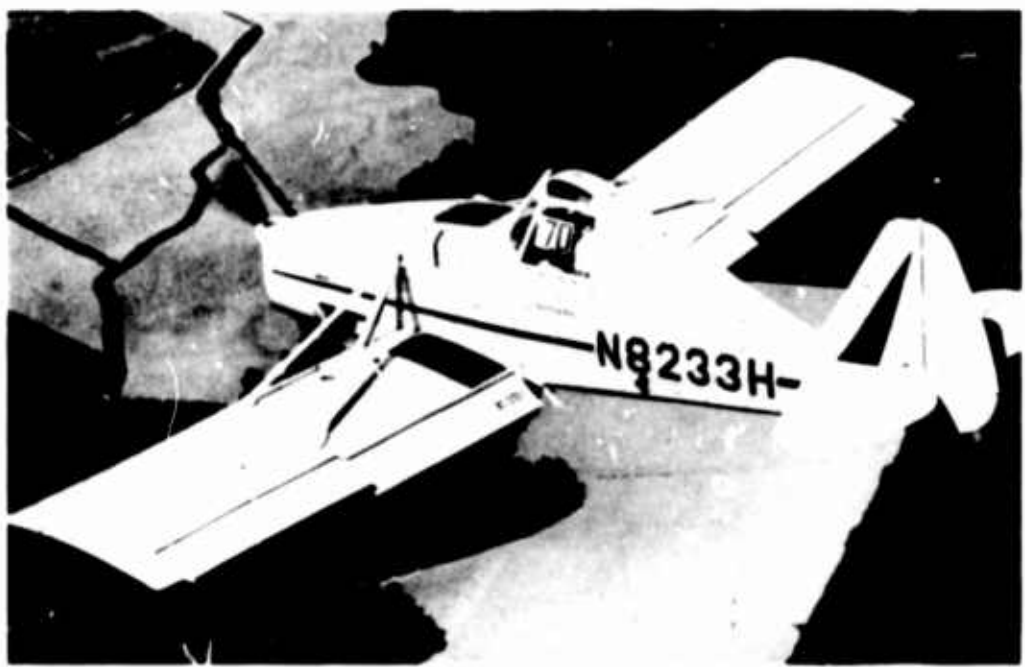


Figure 21. Skin Friction Distribution.



(a). 0° Flaps.

Figure 22. Visualization of Airflow Over the Wing and Fuselage.



(b). 24° Flaps.

Figure 22 (Cont.). Visualization of Airflow Over the Wing and Fuselage.



Figure 23. Visualization of Wing Tip Vortices.

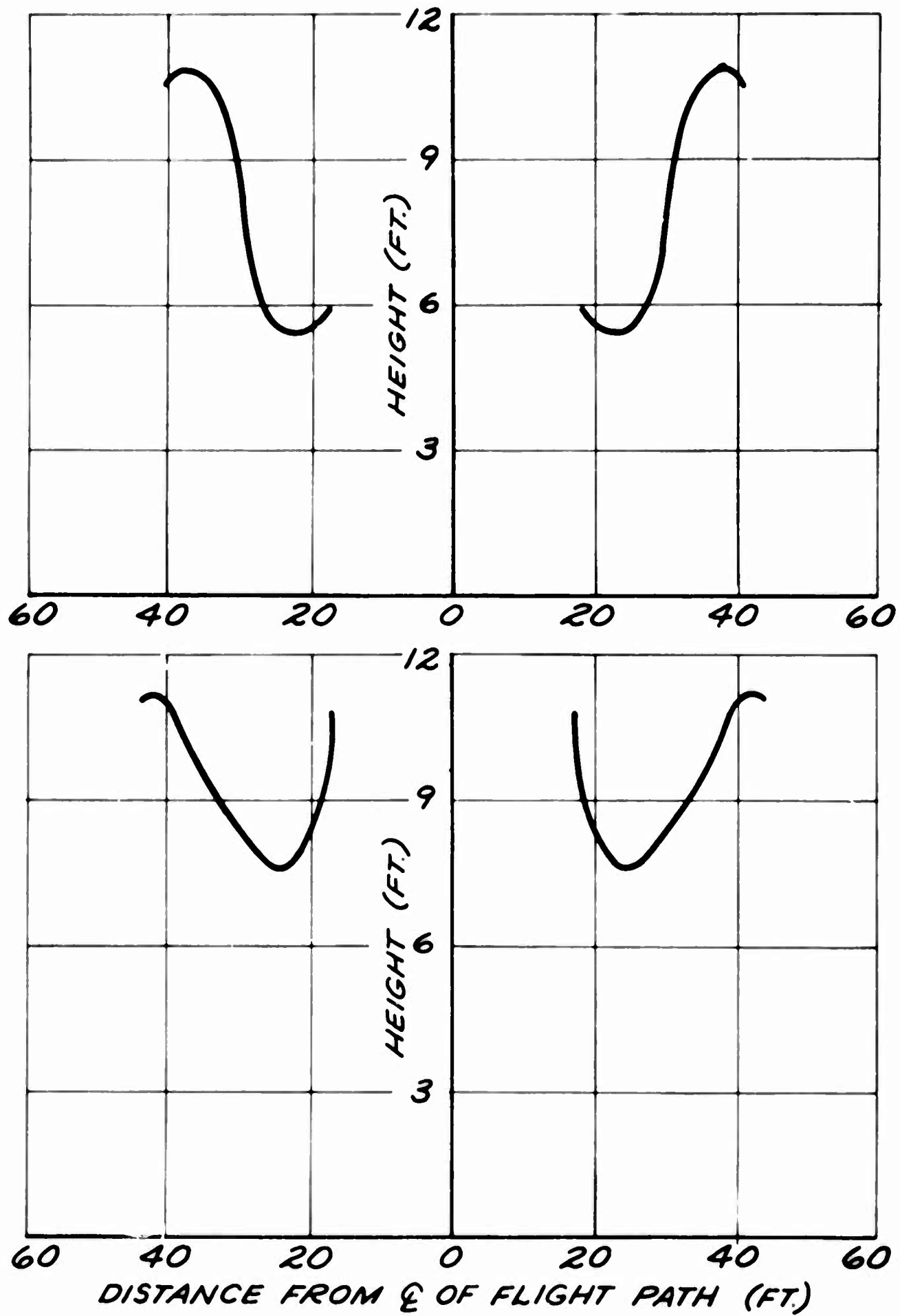


Figure 24. Path of Motion of Wing Tip Vortices for Several Heights of Operation - $C_L = 1.15$, $W_S = 2100$ Pounds.

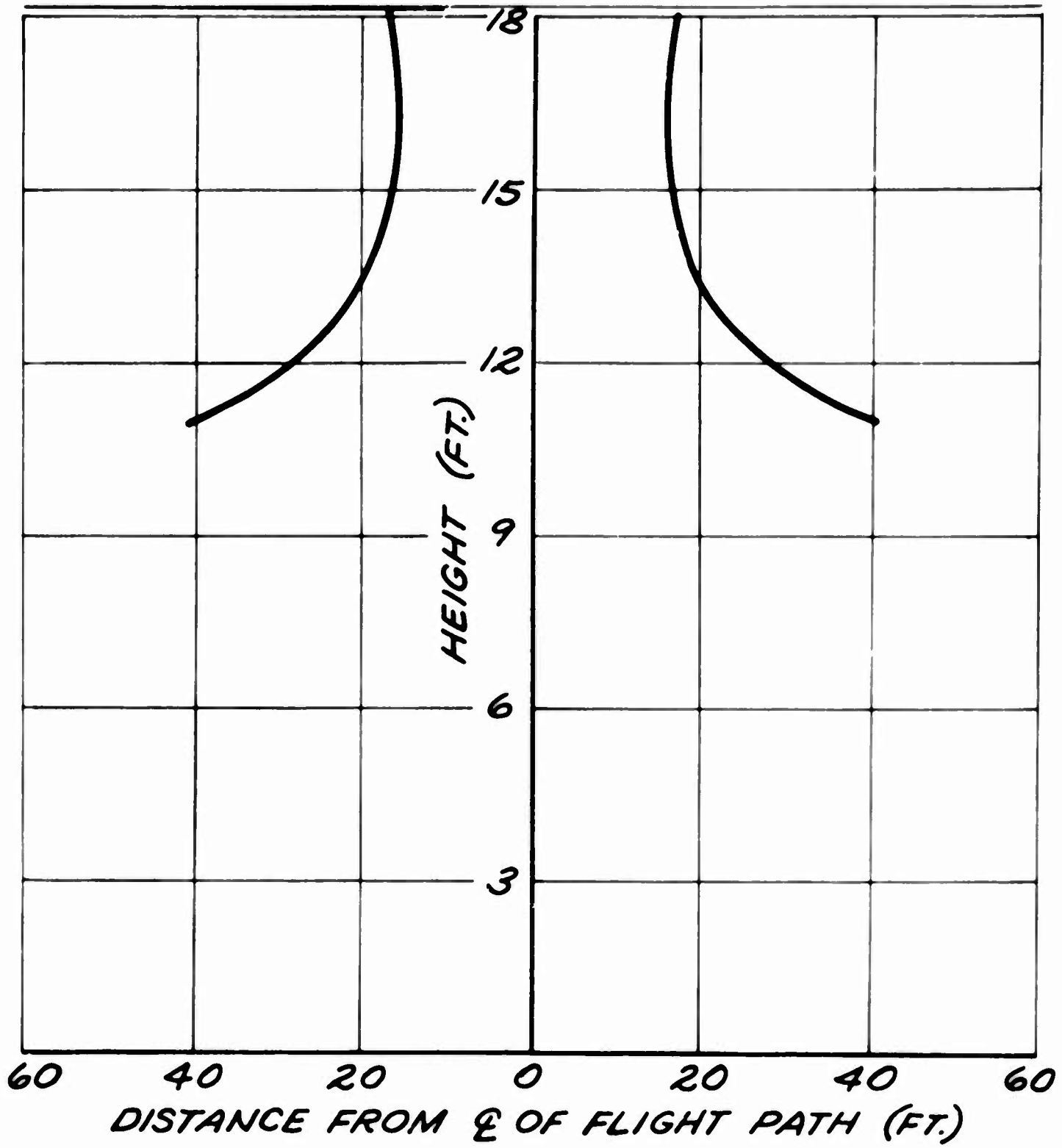


Figure 24 (Cont.). Path of Motion of Wing Tip Vortices for Several Heights of Operation - $C_L = 1.15$, $W_s = 2100$ Pounds.

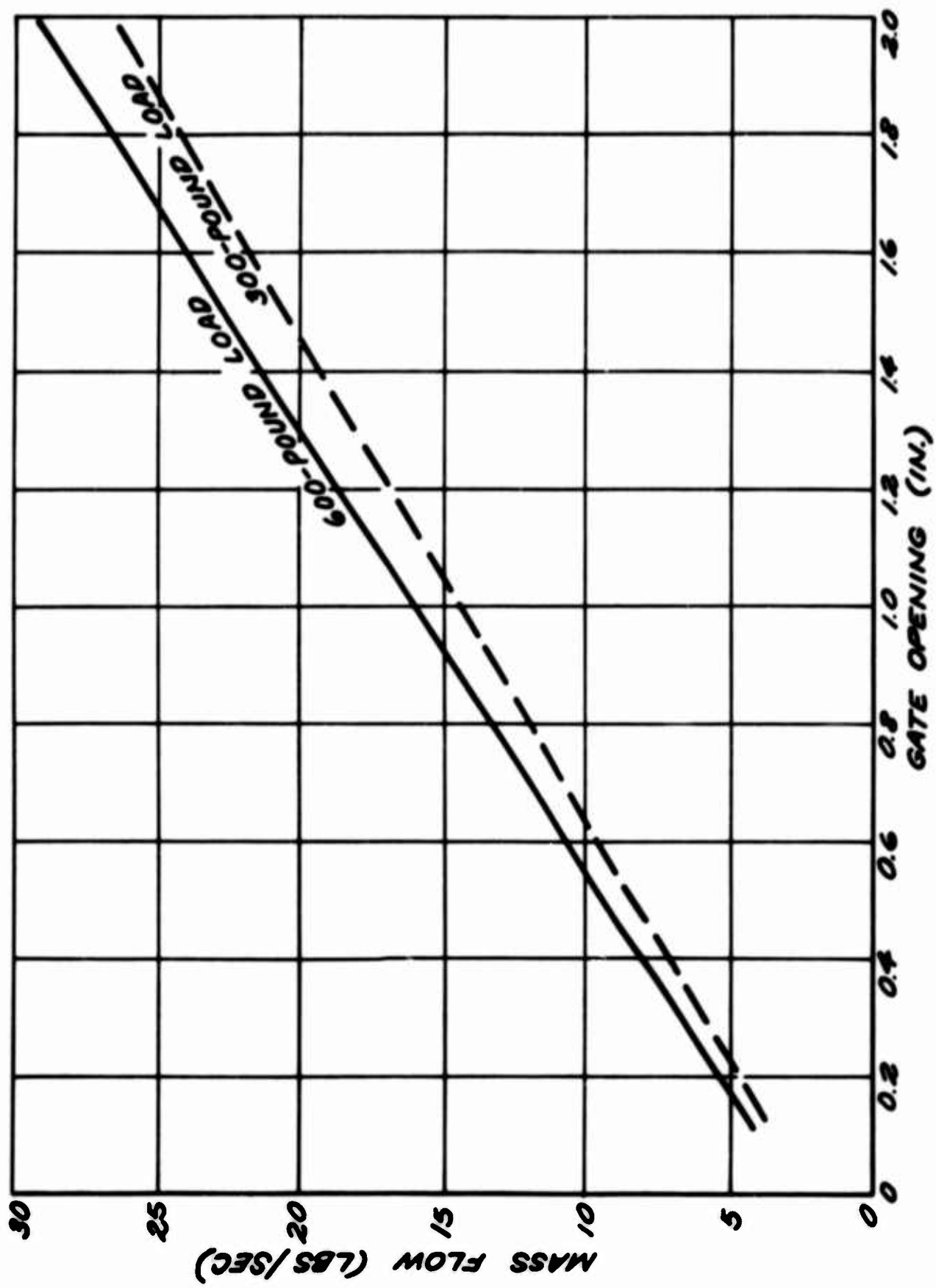
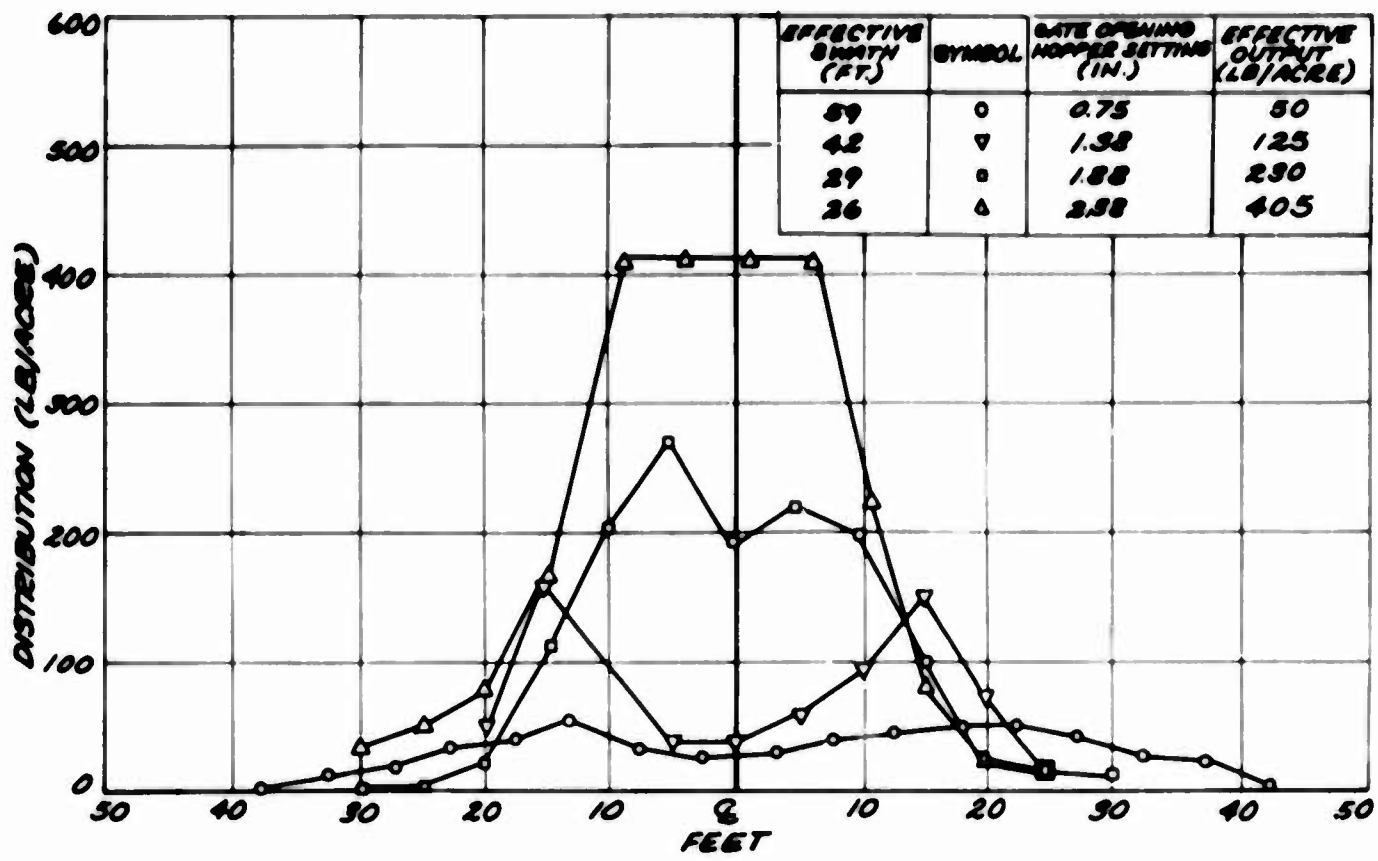
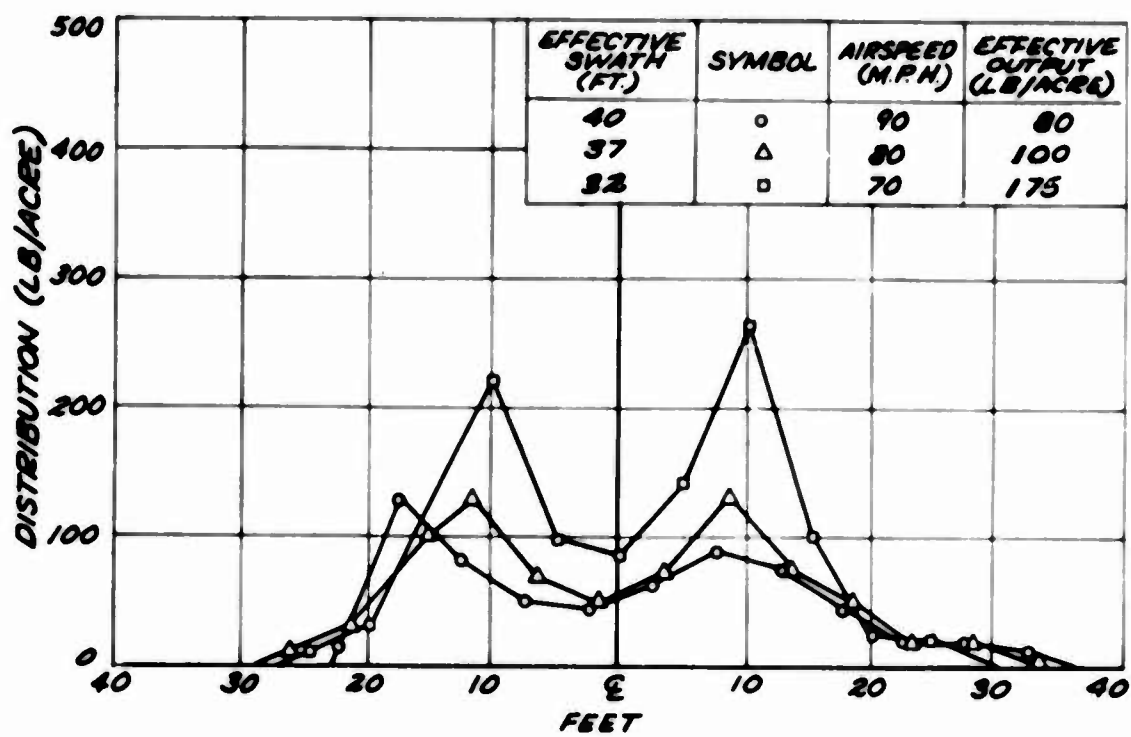


Figure 25. Hopper Calibration Curve.

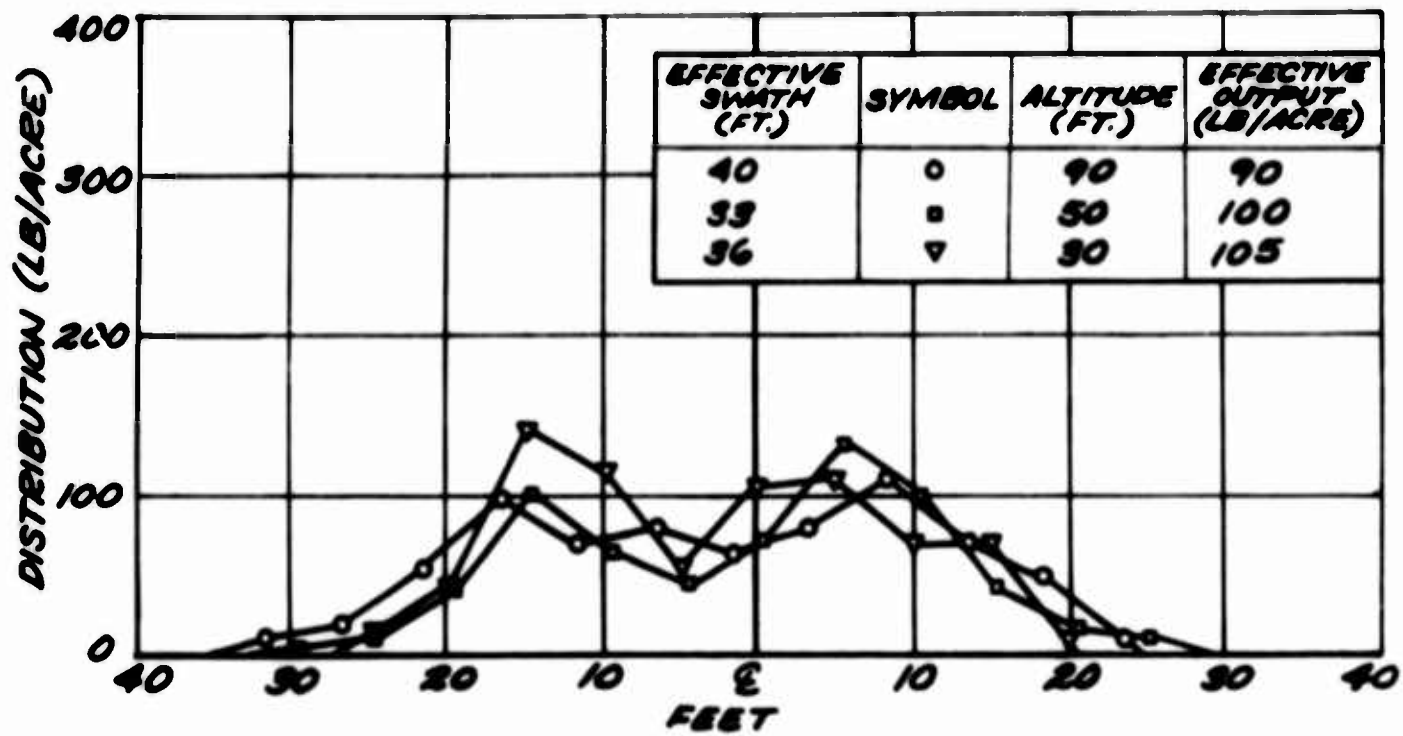


(a). Effect of Rate of Application on Swath Distribution.

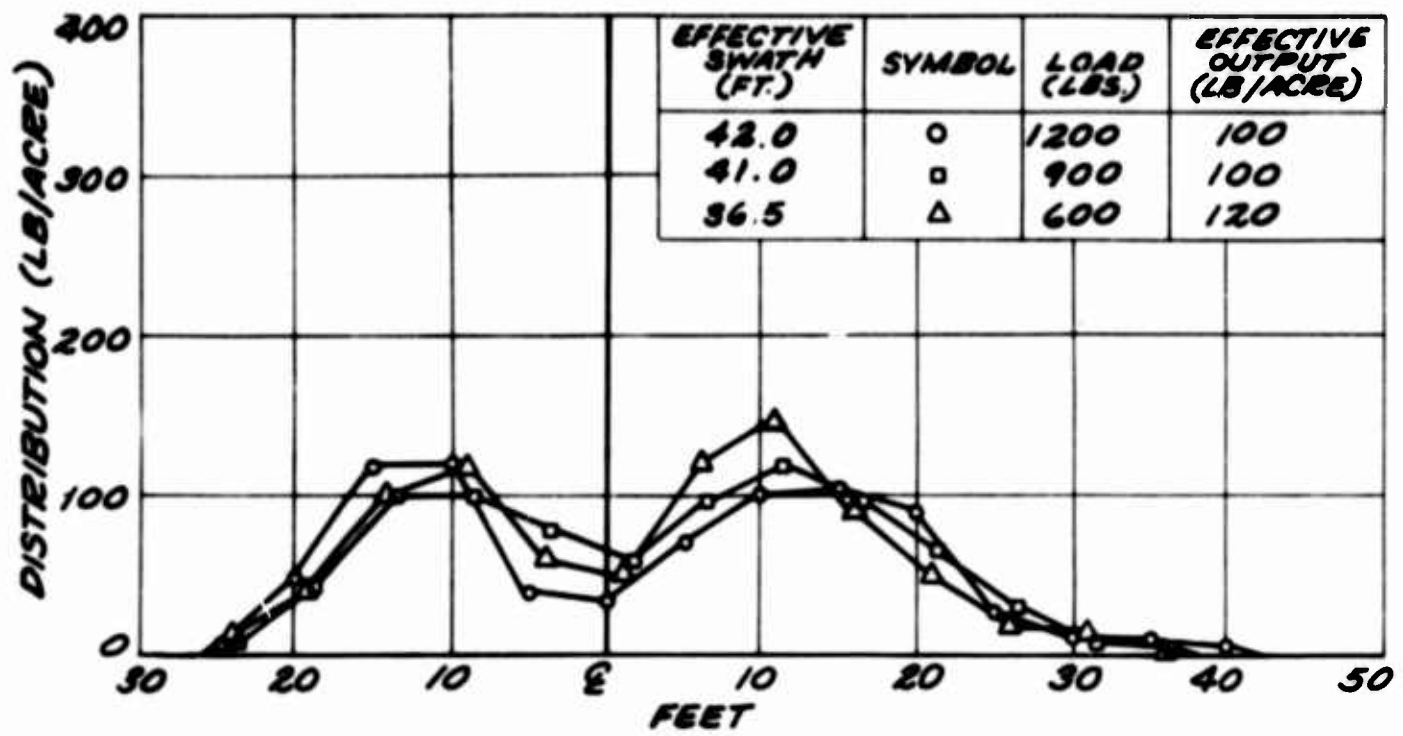


(b). Effect of Airspeed on Swath Distribution.

Figure 26. Granular Swath Distributions.

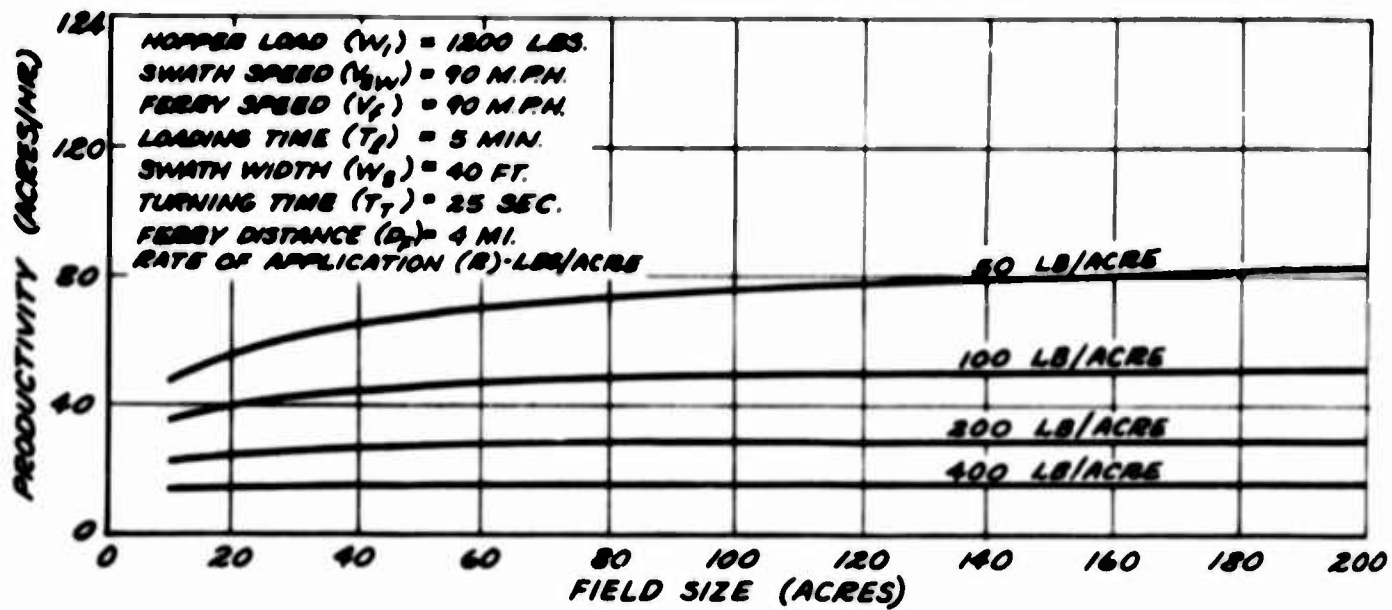


(c). Effect of Altitude on Swath Distribution.

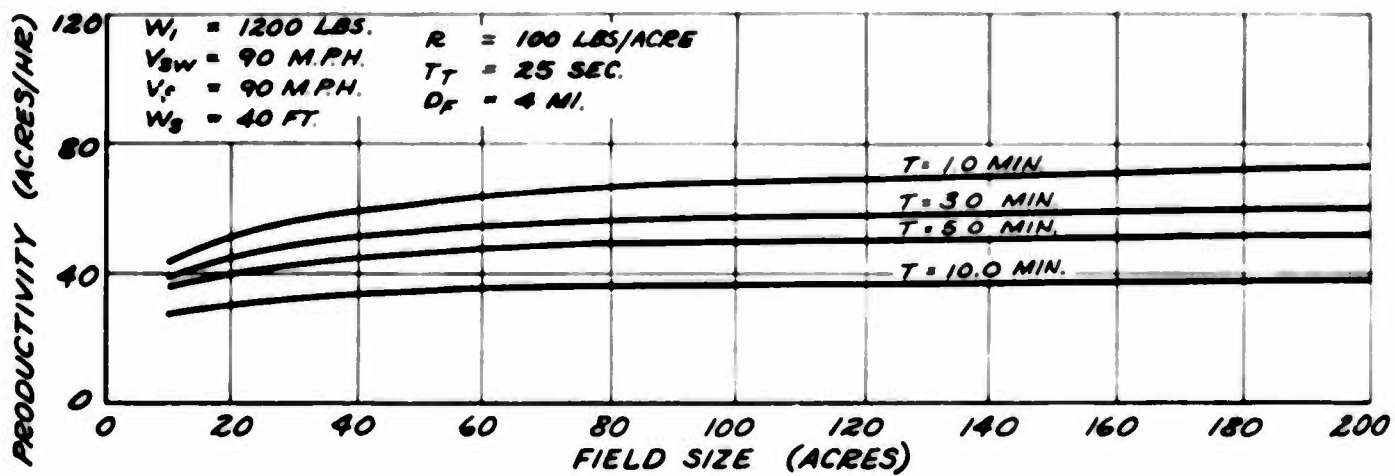


(d). Effect of Load on Swath Distribution.

Figure 26 (Cont.). Granular Swath Distributions.

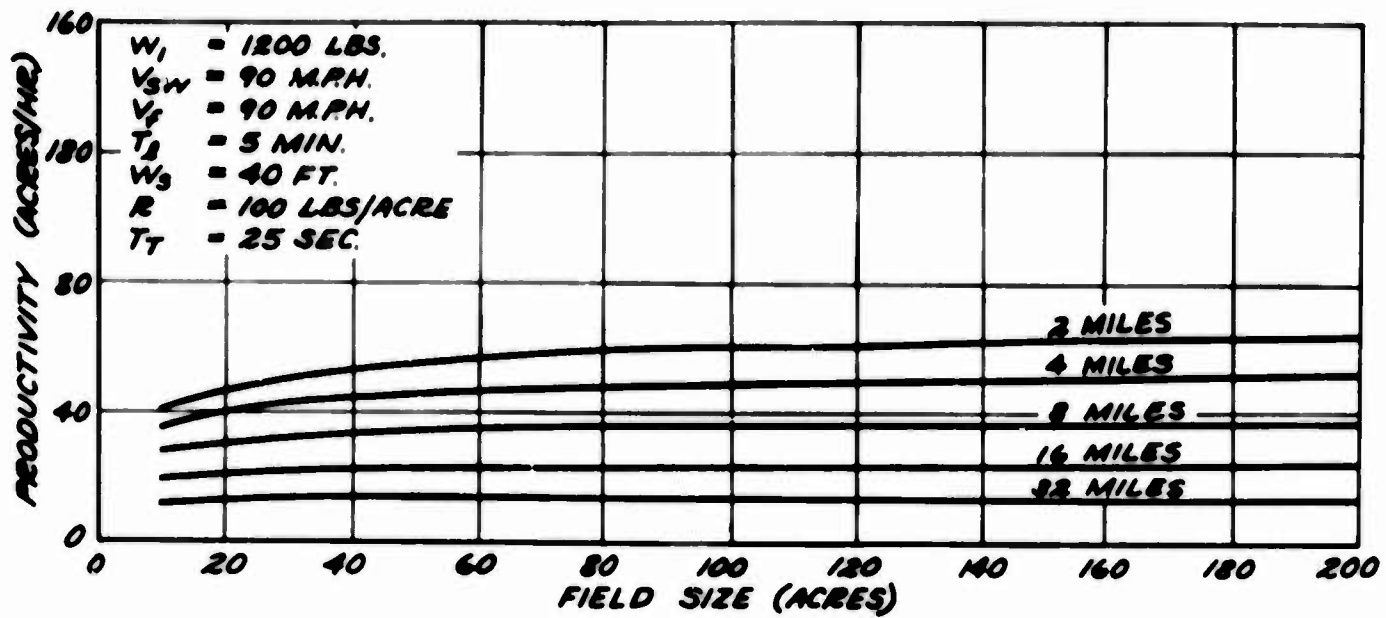


(a). Effect of Rate of Application on Productivity.

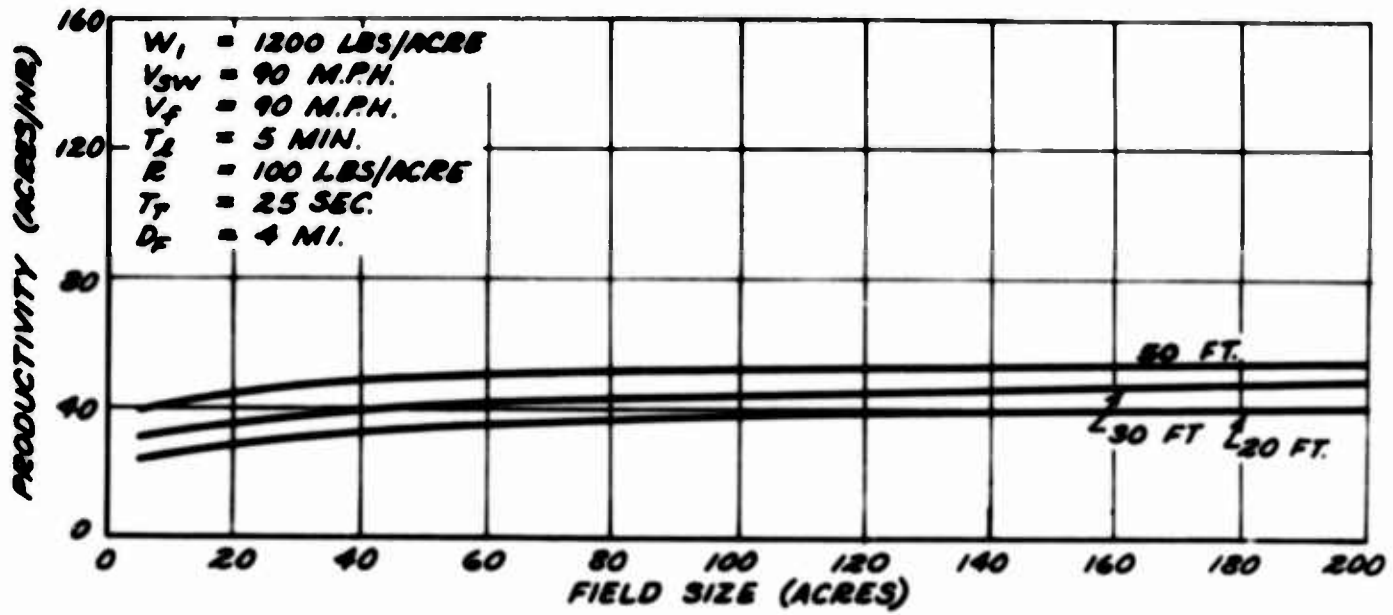


(b). Effect of Loading Time on Productivity.

Figure 27. Operation Analysis for Granular Materials.

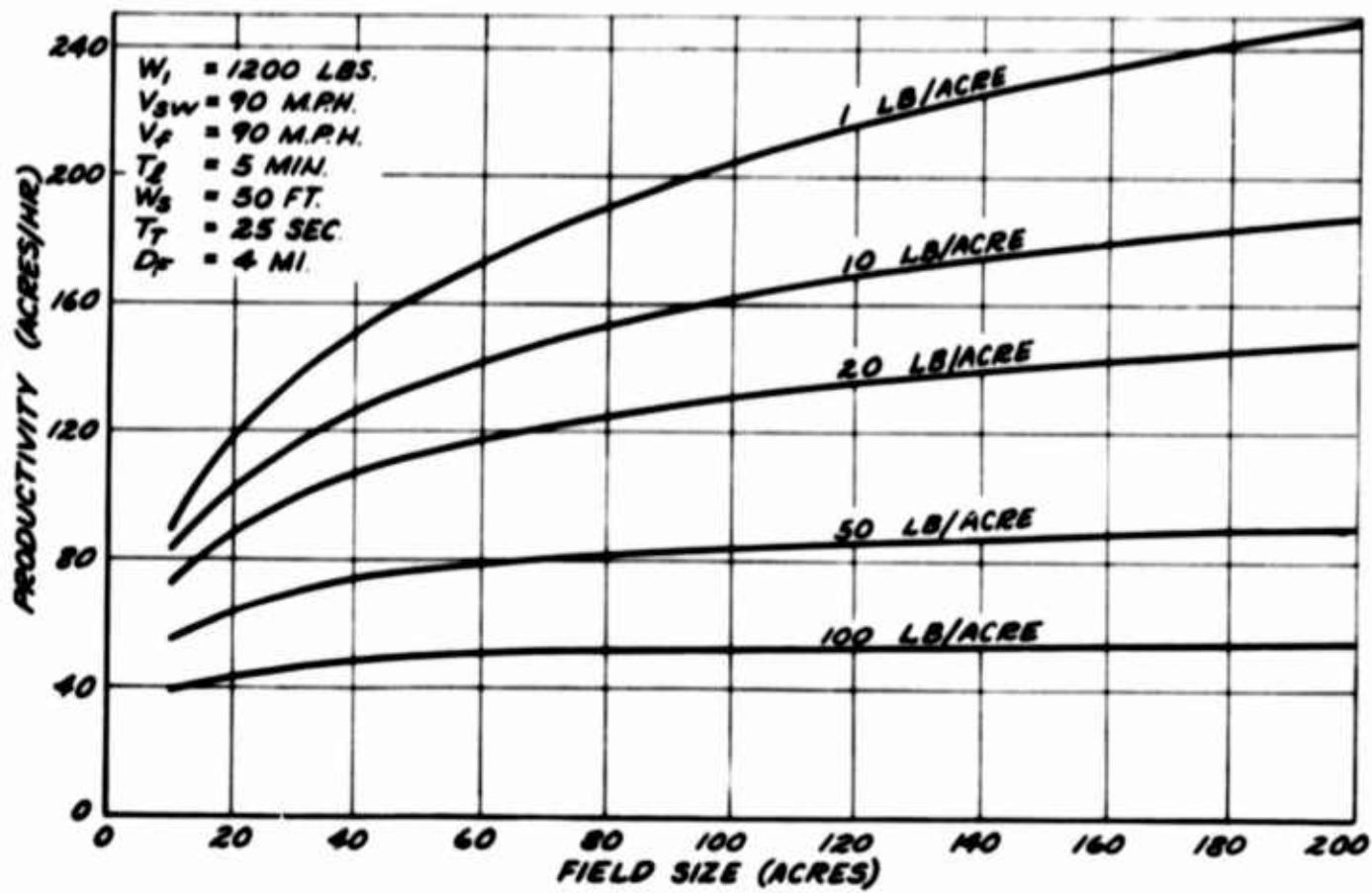


(c). Effect of Ferry Distance on Productivity.

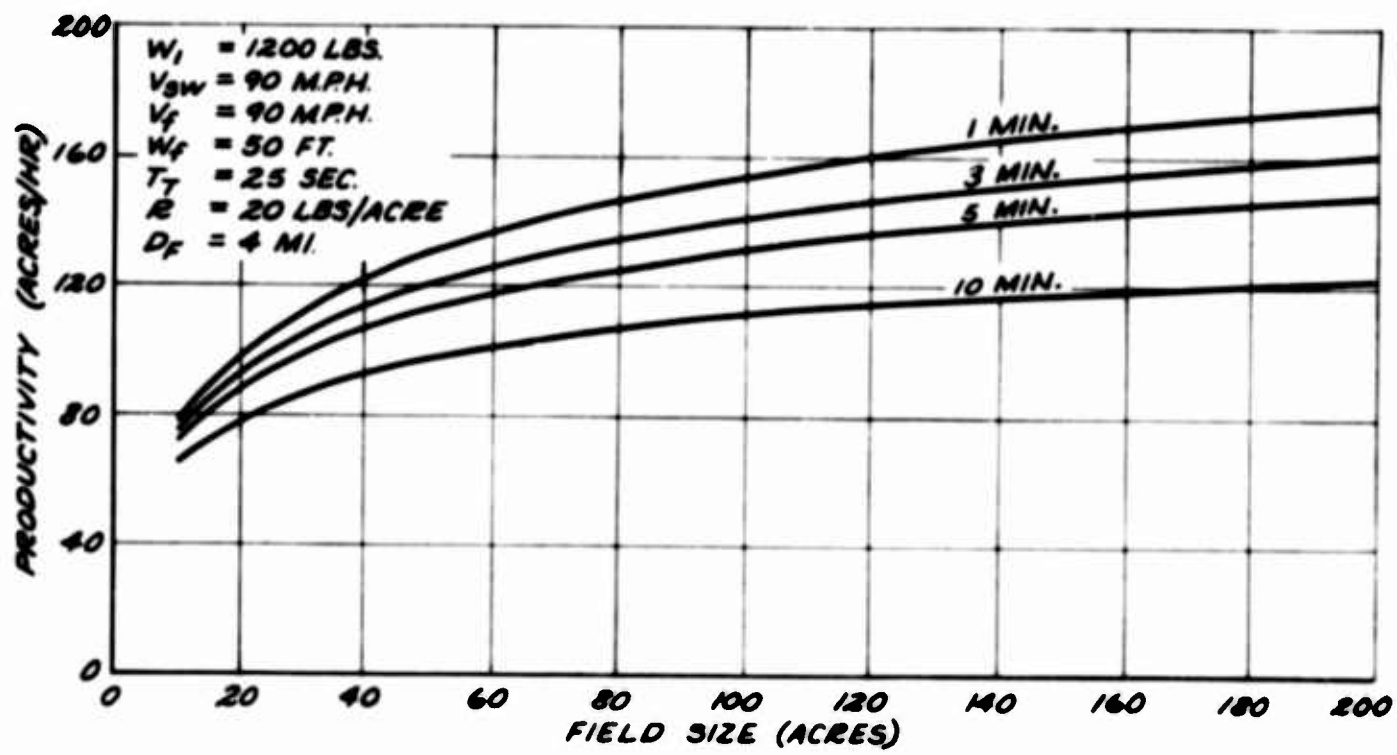


(d). Effect of Swath Width on Productivity.

Figure 27 (Cont.). Operation Analysis for Granular Materials.

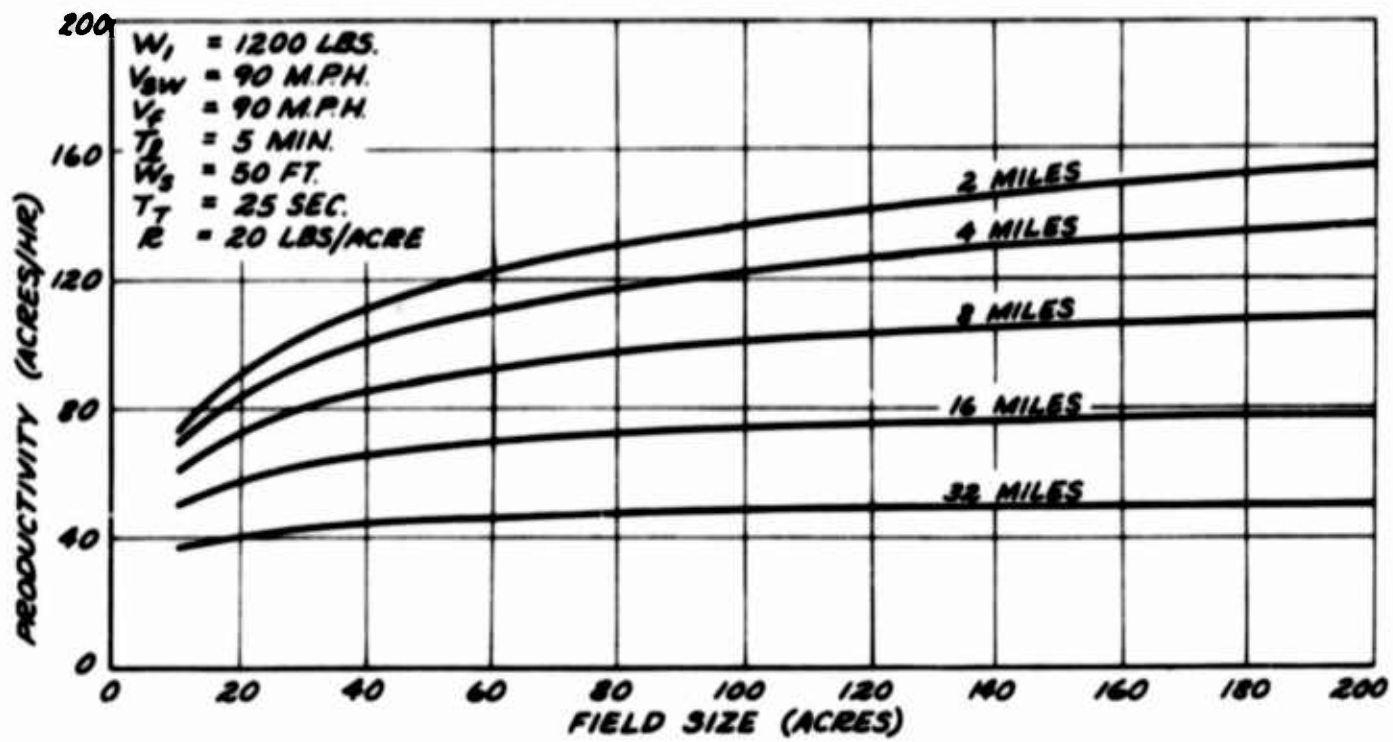


(a). Effect of Rate of Application on Productivity.

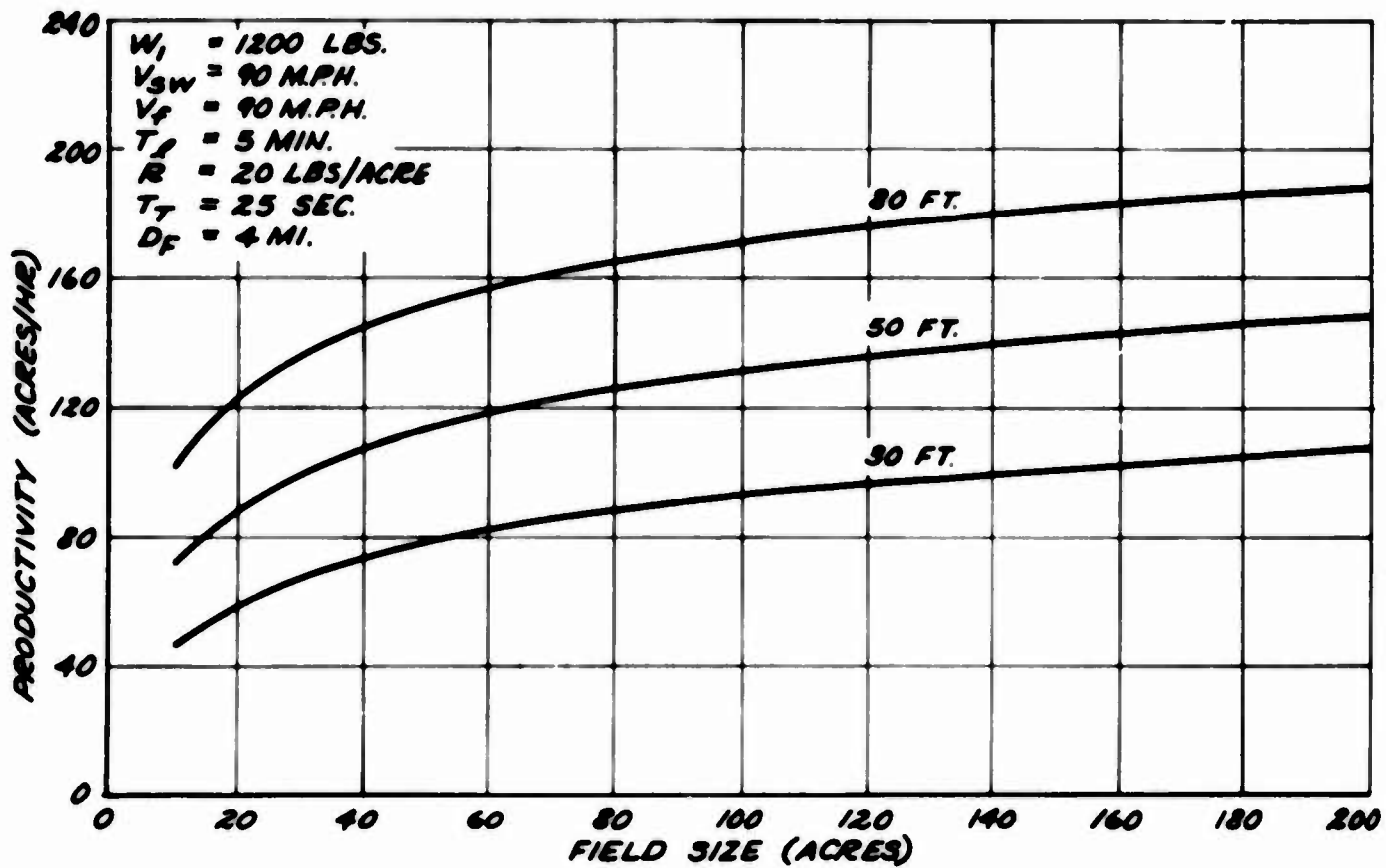


(b). Effect of Loading Time on Productivity.

Figure 28. Operation Analysis for Spray Materials.



(c). Effect of Ferry Distance on Productivity.



(d). Effect of Swath Width on Productivity.

Figure 28 (Cont.). Operation Analysis for Spray Materials.

REFERENCES

1. Roberts, Seán C., and Smith, Michael R., Flow Visualization Techniques Used in Full-Scale Flight Tests, Research Report No. 49, Aerophysics Department, Mississippi State University, State College, Mississippi, April 1964.
2. Roberts, Seán C., and Smith, Michael R., The Evaluation of a Positive Energy Distribution System for the Aerial Application of Solid Materials, Research Note No. 20, Aerophysics Department, Mississippi State University, State College, Mississippi, December 1963.
3. Smith, Michael R., Roberts, Sean C., and Patrick, John D., Evaluation of the Piper PA-18 Agricultural Aircraft, Research Report No. 63, Aerophysics Department, Mississippi State University, State College, Mississippi, September 1965.
4. Roberts, Seán C., Flight Testing of the Marvel and Marvelette Airfoil Section, Research Report No. 38, Aerophysics Department, Mississippi State University, State College, Mississippi, May 1962.

APPENDIX

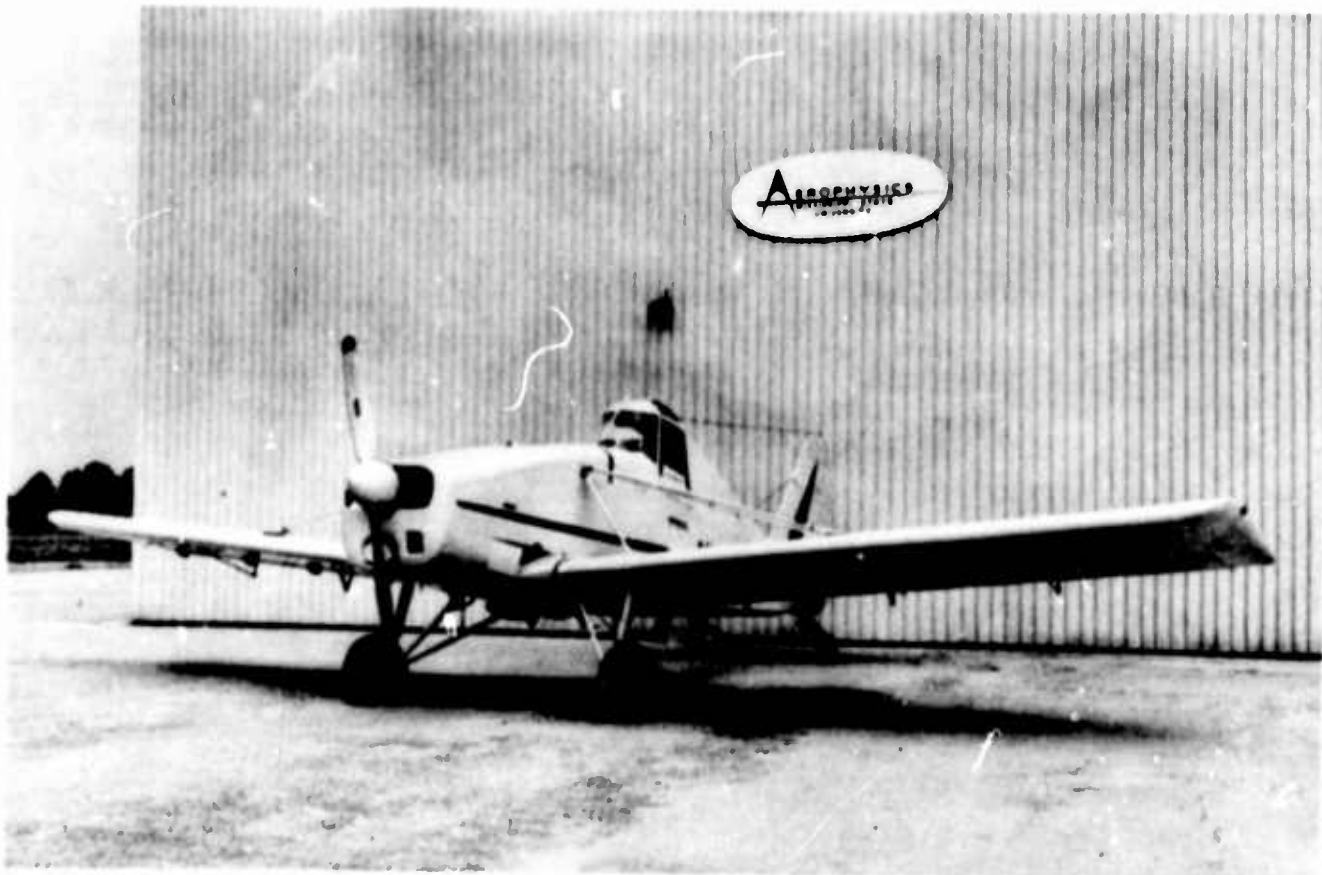


Figure I. Front Quarter View of Test Vehicle in Clean Configuration.



Figure II. Side View of Test Vehicle in Clean Configuration.



Figure III. Rear Quarter View of Test Vehicle in Spray Configuration.

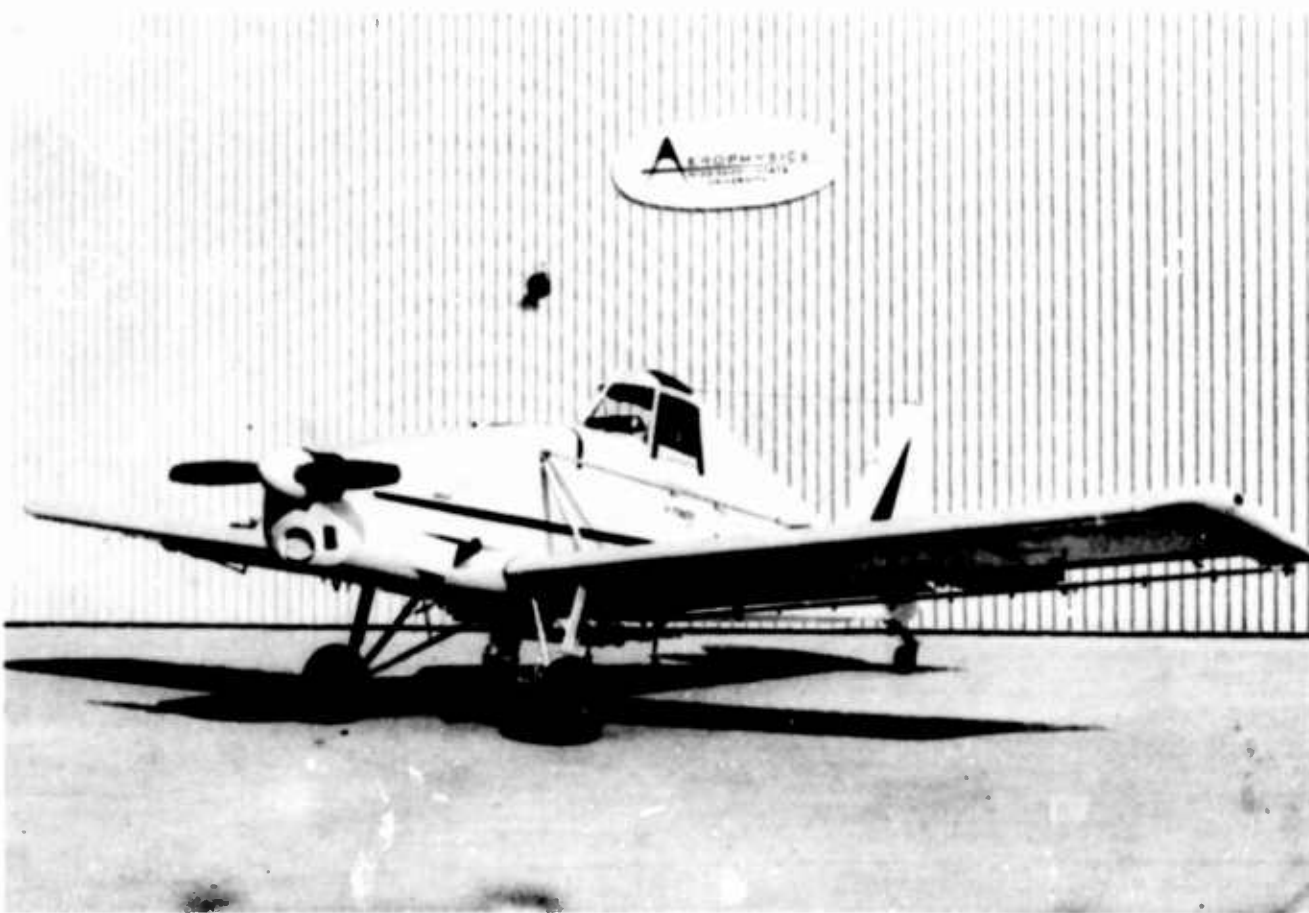


Figure IV. Front Quarter View of Test Vehicle in Spray Configuration.



Figure V. Rear Quarter View of Test Vehicle in Distributor Configuration.



Figure VI. Side View of Test Vehicle in Distributor Configuration.



Figure VII. Controls Operated With the Left Hand.

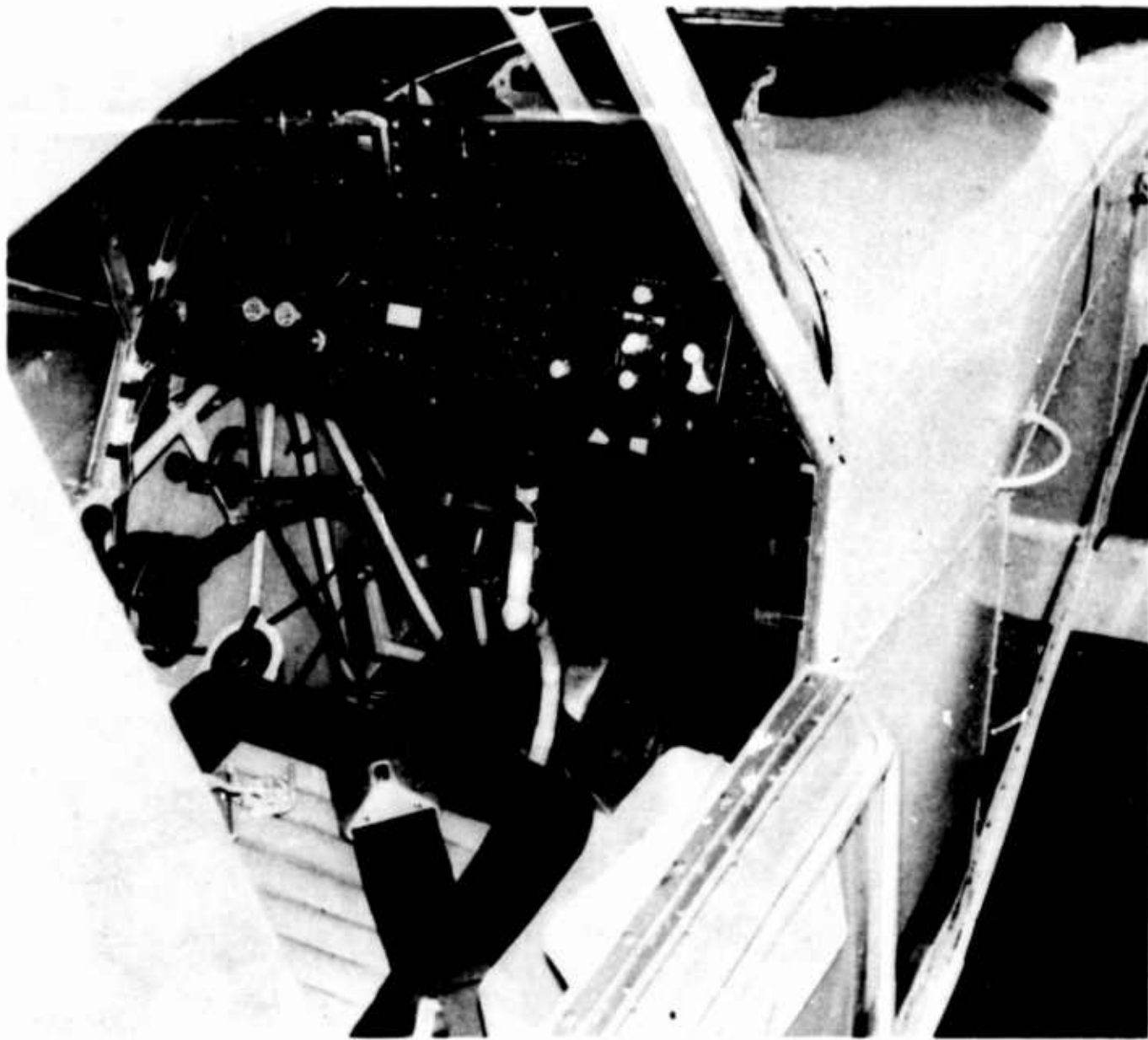
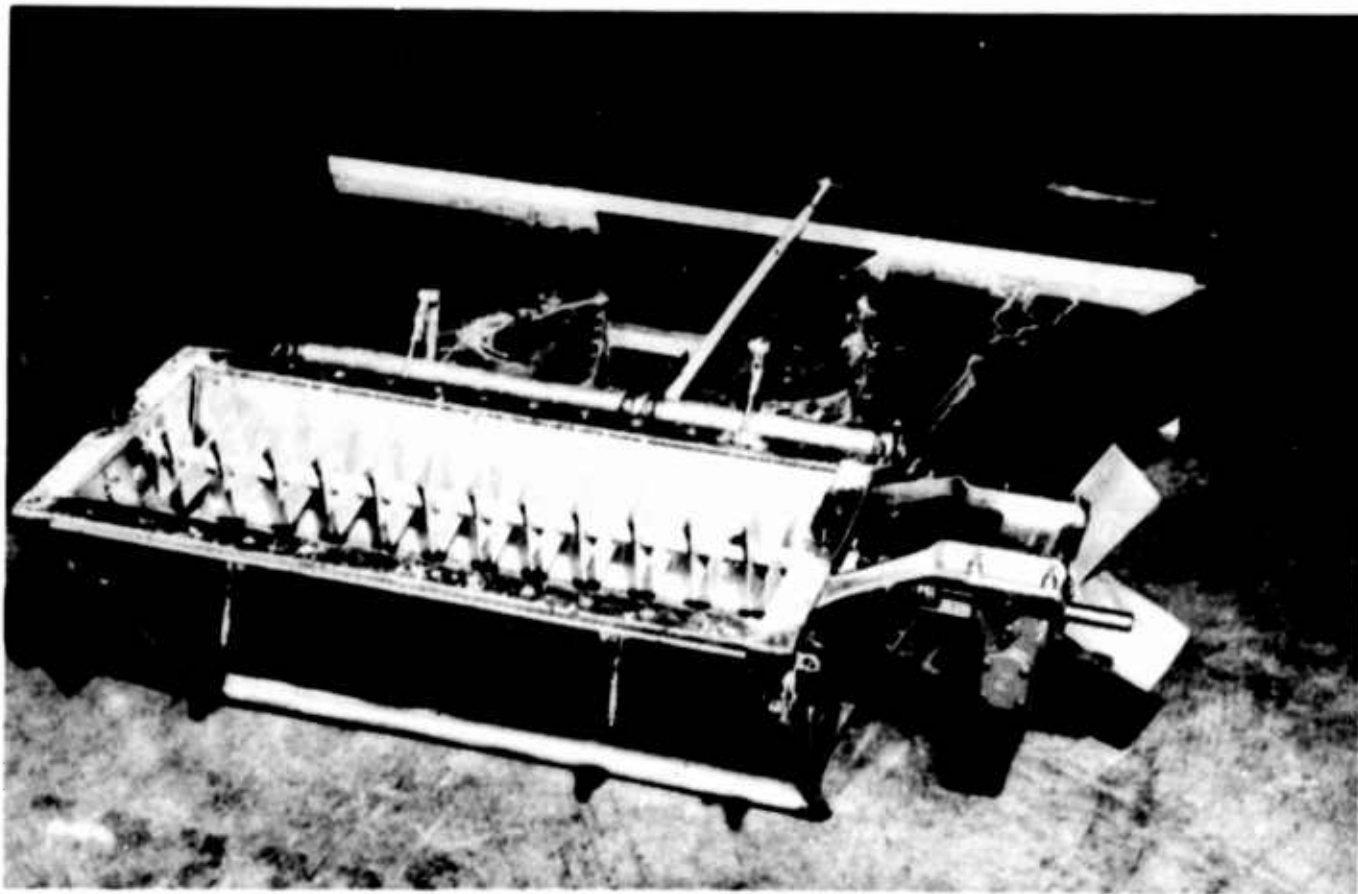
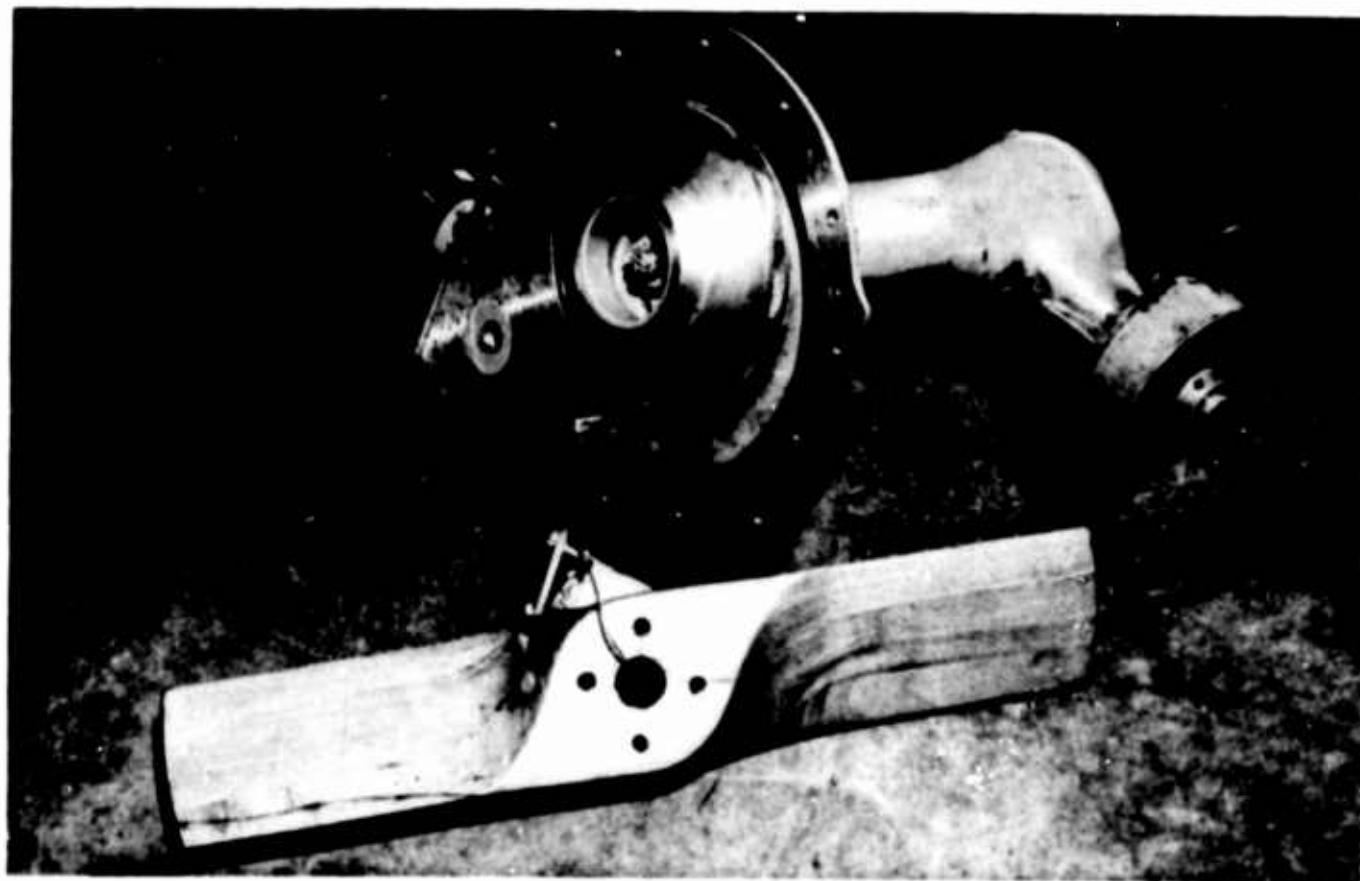


Figure VIII. Cockpit Arrangement - Flight Test Instrument Panel Installed.

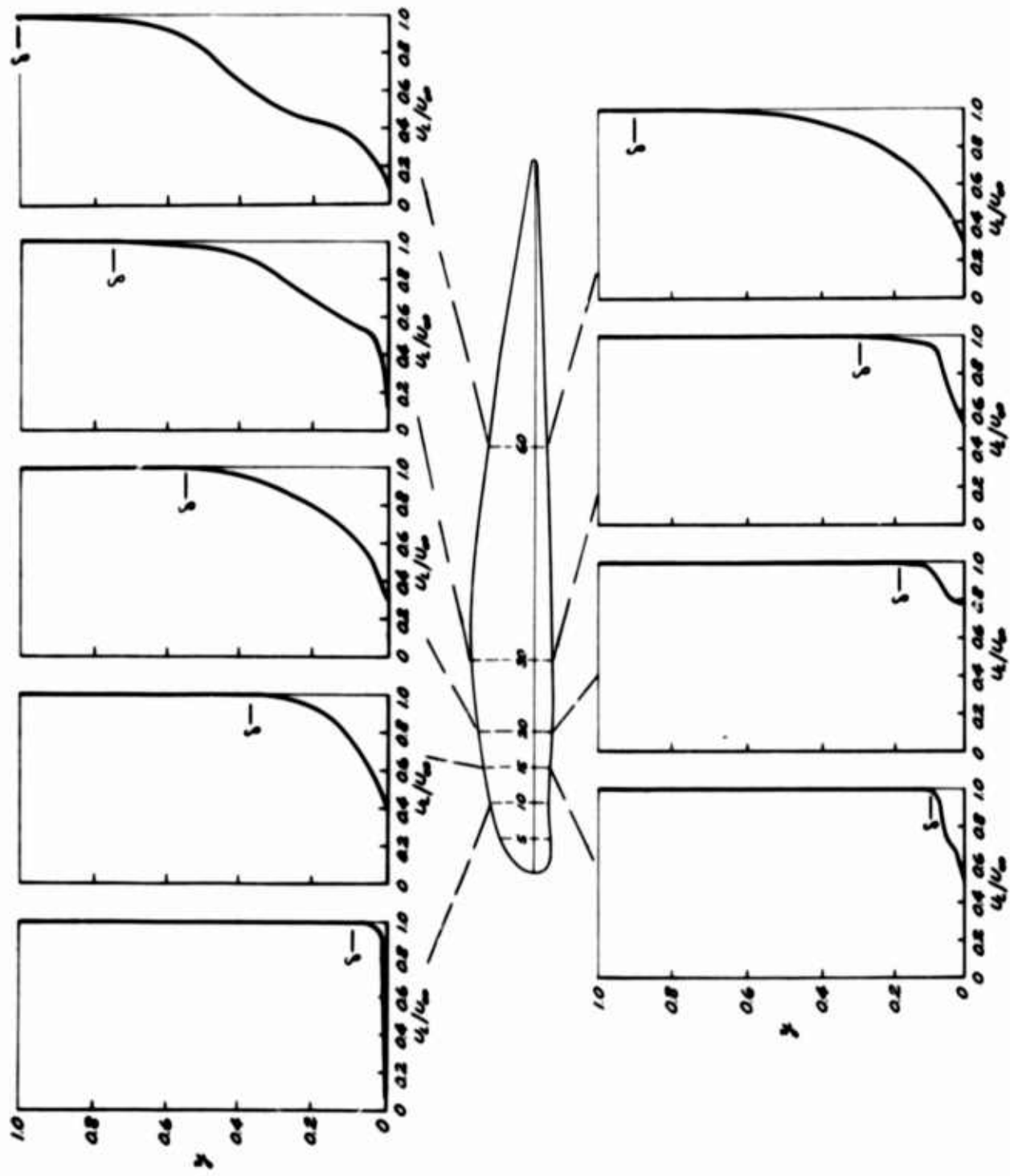


(a). Granular Distributor.



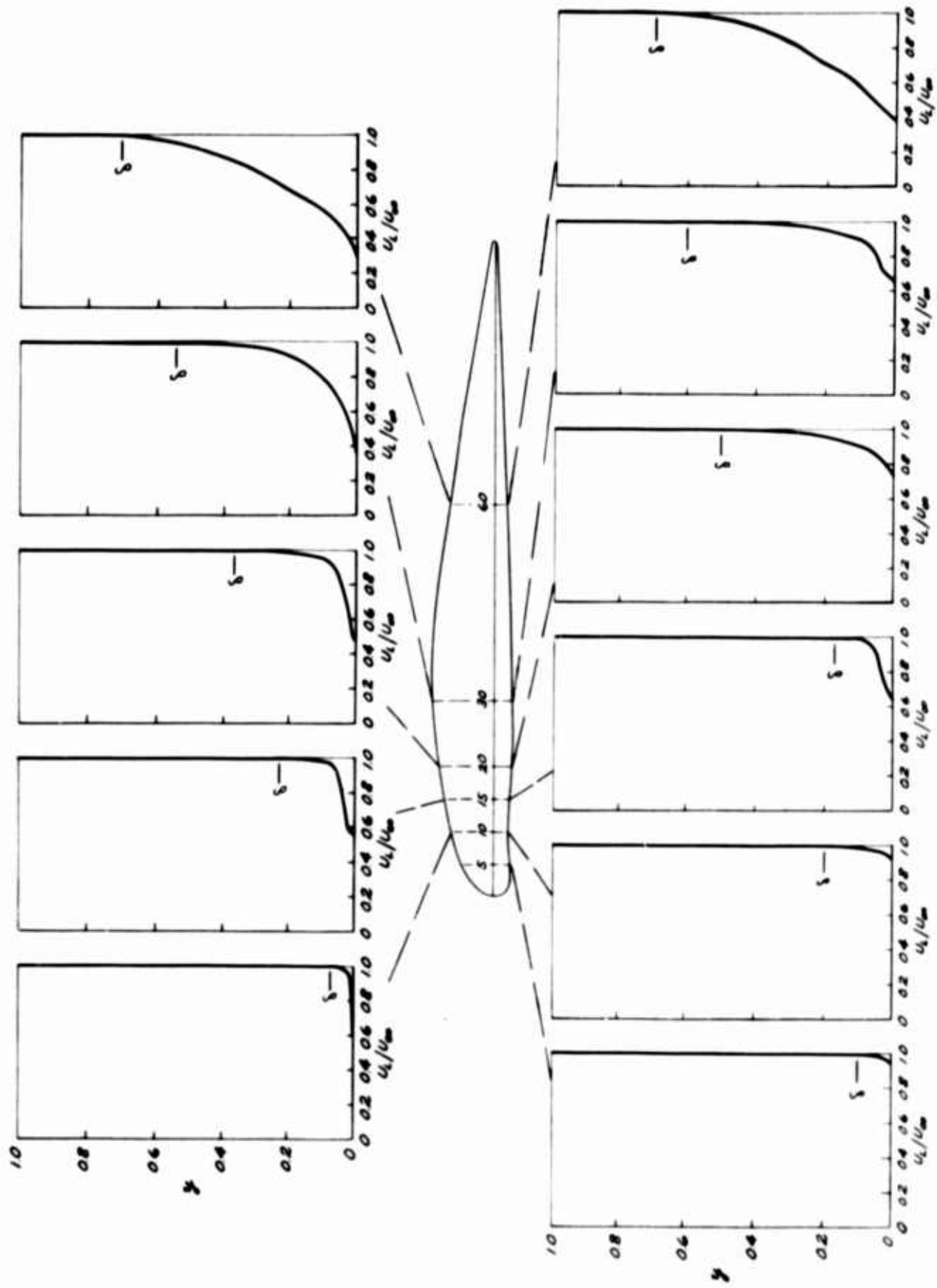
(b). Spray Pump and Windmill Propeller.

Figure IX. Distribution Equipment.



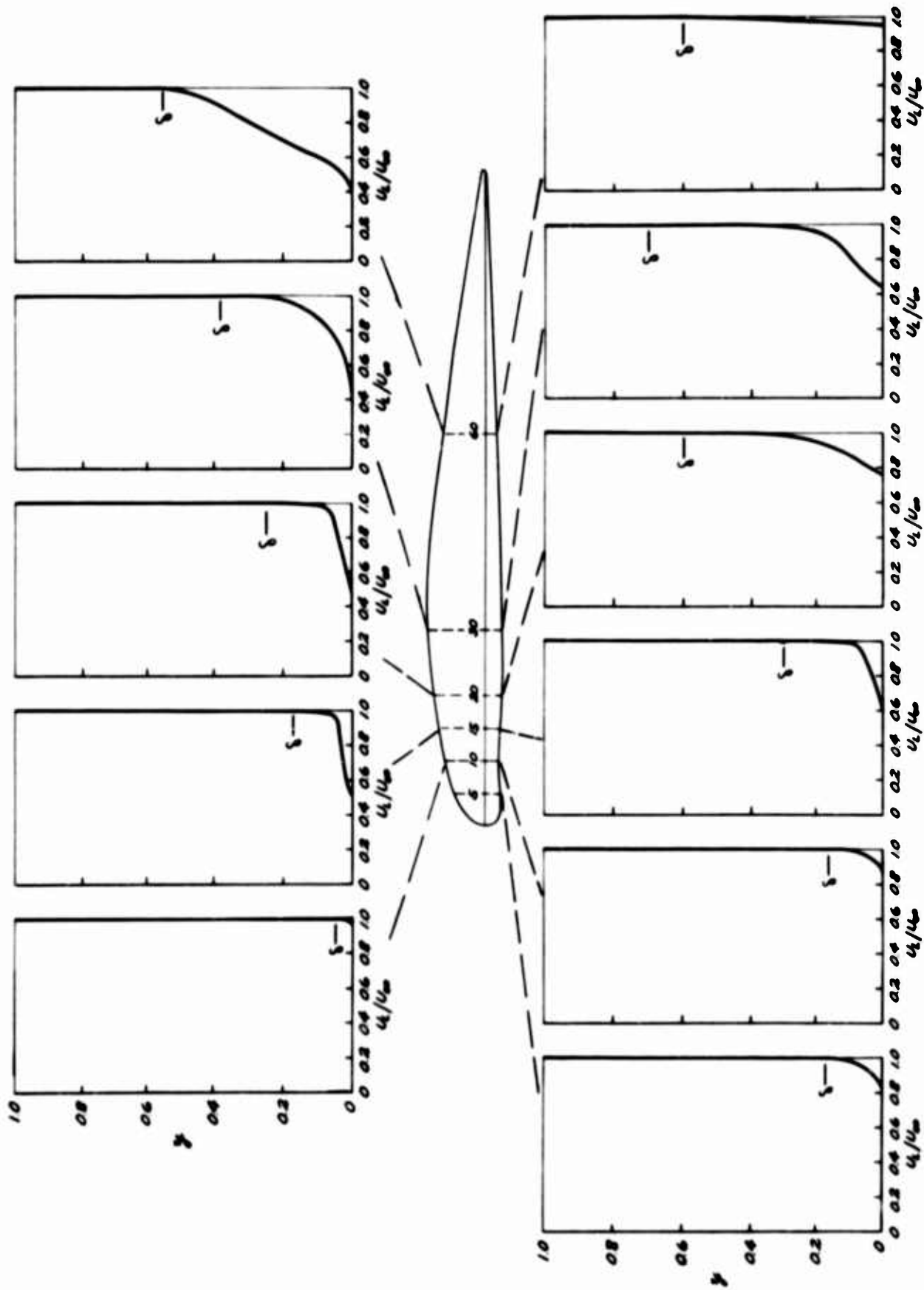
(a). $U_{\infty} = 50$ Miles Per Hour.

Figure X. Boundary Layer Profiles.



(b). $U_{\infty} = 75$ Miles Per Hour.

Figure X (Cont.). Boundary Layer Profiles.



(c). $U_\infty = 100$ Miles Per Hour.

Figure X (Cont.). Boundary Layer Profiles.